

PROCEEDINGS

SIXTH INTERNATIONAL WORKSHOP NANOCARBON PHOTONICS AND OPTOELECTRONICS

19-24 March 2017, Krasnaya Polyana, Sochi, Russia

MOSCOW, RUSSIA 2017

University of Eastern Finland
A.M. Prokhorov General Physics Institute of Russian Academy of Sciences
M.V. Lomonosov Moscow State University
National Research Nuclear University "MEPhI"

Proceedings

Sixth International Workshop Nanocarbon Photonics and Optoelectronics Krasnaya Polyana, Sochi, Russia

Edited by Timofei Eremin

Moscow, Russia
2017

NPO2017 Schedule-at-a-Glance

	Monday, March, 20	Tuesday, March, 21	Wednesday, March, 22	Thursday, March, 23	Friday, March, 24
8.00-9.00	Breakfast	Breakfast	Breakfast	Breakfast	Breakfast
9.00-9.30	Opening	Khlobystov	Bandurin	Young Hee Lee	Okotrub
9.30- 10.00	Usachov	Rybkovskiy	Bel’kov	Luer	Antonova
10.00- 10.15	Krasnikov	Chernov	Obraztsov	Ji-Hee Kim	Kuzhir
10.15-10.30	Coffee Break	Coffee Break	Coffee Break	Coffee Break	
10.30-10.45					Coffee Break
10.45-11.00	Li	Bulusheva	Krstic	Murzina	
11.00- 11.15					
11.15-11.30	He	Nasibulin	Mishina	Purcell	Fedorov
11.30- 11.45					
11.45-12.00	Eliseev	Glazov	Koroteev	Arutyunyan	Closing Awards
12.00-12.15				Kleshch	
12.15-16.30	Discussions	Discussions	Discussions	Discussions	
16.30-18.00	Dinner	Dinner	Dinner	Coffee Break	
18.00-18.30	El’tsov	Gruneis	Tereshchenko	Kuznetsov	
18.30-19.00	Chernozatonskii	Gorshunov	Tarasenko	Liaw	
19.00-19.15	Nebogatikova	Mulbagal	Yashina	Hasan	
19.15-19.30	Coffee Break	Coffee Break			
19.30-19.45				Coffee Break	
19.45-20.00	Smagulova	Konishi	Poster session Young scientist competition for the best posters	Banquet	
20.00-20.15					
20.15-20.30	Pavlova	Bychanok			
20.30-22.00					

Invited talk

oral talk

Workshop Co-Chairs

Elena Obraztsova

A.M. Prokhorov General Physics Institute, RAS, Moscow, Russia

Yury Svirko

University of Eastern Finland, Joensuu, Finland

Alexander Obraztsov

Physics Department of M.V. Lomonosov Moscow State University, Moscow, Russia

Program Committee

Elena Obraztsova

A. M. Prokhorov General Physics Institute RAS, Moscow, Russia

Yury Svirko

University of Eastern Finland, Joensuu, Finland

Alexander Obraztsov

M. V. Lomonosov Moscow State University, Moscow, Russia

Esko Kauppinen

Aalto University, Espoo, Finland

Hiromichi Kataura

AIST, Tsukuba, Japan

Vladimir Kuznetsov

G. K. Boreskov Institute of Catalysis SB RAS, Novosibirsk, Russia

Organizing Committee

Sofia Bokova-Sirosh

A. M. Prokhorov General Physics Institute RAS, Moscow, Russia)

Alexander Osadchy

A. M. Prokhorov General Physics Institute RAS, Moscow, Russia)

Ekaterina Obraztsova

Shemyakin and Ovchinnikov Institute of Bioorganic Chemistry, RAS, Moscow, Russia

Timofei Eremin

Physics Department of M.V. Lomonosov Moscow State University, Moscow, Russia

Valery Savin

Immanuel Kant Baltic Federal University, Kaliningrad, Russia

Dear colleagues,

you are welcome to the Sixth International Workshop on Nanocarbon Photonics and Optoelectronics (NPO2017) which takes place on 19-24 March 2017 at Krasnaya Polyana resort, Sochi, Russia in the hotel "Golden Tulip Rosa Khutor". The NPO workshops were held each two years since 2008 in Finland. This year the workshop is arranged in the first time in Russia in the wonderful ski resort Rosa Khutor.

Both fundamental and application problems related to the photonic and optoelectronic applications of nanocarbon materials have recently attracted the attention of research community worldwide. The NPO2017 is the sixth workshop in a series of meetings devoted to progress in this field. The Workshop will be focused on photonics and optoelectronics of graphene and other two-dimensional materials, topological insulators, carbon nanotubes and nanodiamonds. The NPO2017 are organized on the initiative and with the financial support of the Russian Science Foundation (the project 15-12-30041). The co-founders of the workshop are University of Eastern Finland, A.M. Prokhorov General Physics Institute of Russian Academy of Sciences, M.V. Lomonosov Moscow State University and the National Research Nuclear University "MEPhI".

The Workshop venue is situated in Krasnaya Polyana, the Winter Olympics 2014 snow events cluster located 50 km from Sochi at the Aibga Ridge of the Western Caucasus.

Scope

The workshop includes the invited lectures, oral and poster presentations devoted to different nanocarbon and 2D materials. The presentations will be distributed in modules beginning from synthesis and characterization of structural, optical and electronic properties of these materials to their application in photonic and electronic devices.

Publications

The materials presented at the conference will be published in form of a regular scientific papers in "Physica Status Solidi B" journal (Wiley). The issue Guest editor is Prof. Alexander Obraztsov. The deadline for the paper submission is May, 15, 2017.

We wish you a fruitful and pleasant week in sunny and beautiful Krasnaya Polyana!

The Program Committee of NPO2017

Contents

Monday, March 20

9.30-10.00	Dmitriy Usachov "Synthesis and characterization of single-layer graphene" <i>St.-Petersburg State University, Russia</i>	3
10.00-10.15	Dmitriy Krasnikov "A One-Step In Situ Synthesis of the Carbon Nanotube Aerogels" <i>Boreskov Institute of Catalysis, SB RAS, Novosibirsk, Russia</i>	4
10.45-11.15	Yan Li "Chirality-Specific Synthesis and Spectroscopic Characterization of Single-Walled Carbon Nanotubes" <i>Peking University, China</i>	5
11.15-11.45	Maoshuai He "Key Roles of Carbon Concentration in Nucleating and Growing Single-Walled Carbon Nanotubes" <i>Shandong University of Science and Technology, China</i>	6
10.45-12.15	Andrei Eliseev "Doping of Single-Walled Carbon Nanotubes by Encapsulation of Inorganic Compounds" <i>Depart. of Chemistry, M.V. Lomonosov Moscow State University, Russia</i>	7
18.00-18.30	Konstantin Eltsov "Synthesis of intrinsic and N-doped monocrystalline graphenes on Ni(111)" <i>A.M. Prokhorov General Physics Institute, RAS, Moscow, Russia</i>	8
18.30-19.00	Leonid Chernozatonskii "Graphene in heterostructures: optoelectronic properties and applications" <i>Emmanuel Inst. of Biochemical Physics, RAS, Moscow, Russia</i>	9
19.00-19.15	Nadezhda Nebogatikova "Nanostructured few-layer graphene films for optic and electronic applications" <i>Inst. Of Semiconductor Physics SB RAS, Novosibirsk, Russia</i>	10
19.45-20.15	Svetlana Smagulova "Study of optical, fluorescent and sensing properties of graphene oxide films" <i>North-Eastern Federal University, Yakutsk, Russia</i>	11
20.15-20.30	Tatiana Pavlova "DFT study of gold intercalation under graphene monolayer on Ni(111)" <i>A.M. Prokhorov General Physics Institute, RAS, Moscow, Russia</i>	12

Tuesday, March 21

9.00-9.30	Andrey Khlobystov "Carbon Nanotubes as Nanoreactors: Synthesis & Analysis of Low-Dimensional Materials" <i>School of Chemistry, University of Nottingham, UK</i>	15
9.30-10.00	Dmitrii Rybkovskiy "Phonon contribution to electrical resistance of acceptor-doped single-wall carbon nanotubes assembled into transparent films" <i>Southern Federal University, Rostov-on-Don, Russia</i>	16
10.00-10.15	Alexander Chernov "Modification of single-walled carbon nanotube optical properties by graphene nanoribbon filling" <i>A.M. Prokhorov General Physics Institute, RAS, Moscow, Russia</i>	17
10.45-11.15	Lyubov Bulusheva "Carbon nanotube filling by inorganic compounds" <i>Nikolaev Inst. of Inorganic Chemistry, SB RAS, Novosibirsk, Russia</i>	18
11.15-11.45	Albert Nasibulin "Enhancing the conductivity of single-walled carbon nanotubes films" <i>Skoltech, Moscow, Russia</i>	19
10.45-12.15	Mikhail Glazov "Nonlinear optics of excitons in transition metal dichalcogenides monolayers" <i>Ioffe Institute, St.-Petersburg, Russia</i>	20
18.00-18.30	Alexander Grüneis "Electronic and optical properties of lithium doped graphene nanoribbons" <i>University of Cologne, Köln, North Rhine-Westphalia, Germany</i>	21
18.30-19.00	Boris Gorshunov "Charge Transport in carbon Nanotube Films Studied by Terahertz Spectroscopy" <i>A.M. Prokhorov General Physics Institute RAS, Moscow, Russia</i>	22
19.00-19.15	P. Mulbagal "High quality Carbon Nanotube - Amorphous Silicon Heterojunction solar cells" <i>Skoltech, Moscow, Russia</i>	23
19.45-20.15	Kuniaki Konishi "Circular polarization control with metallic artificial structures" <i>IPST, University of Tokyo, Japan</i>	24
20.15-20.30	Dmitry Bychanok "Carbon nanotube based composites in periodic structures: electromagnetic properties and band structure in microwaves" <i>Research Institute for Nuclear Problems of Belarusian State University, Minsk, Belarussia</i>	25

Wednesday, March 22

9.00-9.30	Denis Bandurin "High Electron Mobility, Quantum Hall Effect and Anomalous Optical Response in Atomically Thin InSe" <i>The University of Manchester, UK</i>	29
9.30-10.00	Vasiliy Bel'kov "Terahertz Radiation Induced Photocurrents in Topological Insulators" <i>Ioffe Institute, St.-Petersburg, Russia</i>	30
10.00-10.15	Petr Obratsov "Terahertz Emission Spectroscopy of 3D Topological Insulators" <i>A.M. Prokhorov General Physics Institute RAS, Moscow, Russia</i>	31
10.45-11.15	Voislav Krstic "Interplay of Raman response and electrical properties in covalent graphene derivatives" <i>Friedrich-Alexander-University, Erlangen-Nürnberg, Germany</i>	32
11.15-11.45	Elena Mishina "Optical characterization and kinetics of photoinduced carriers of 2D transition metal dichalcogenides" <i>Moscow Technological University (MIREA), Russia</i>	33
10.45-12.00	Victor Koroteev "Molybdenum disulphide composite materials for energy applications". <i>Nikolaev Inst. of Inorganic Chemistry SB RAS, Novosibirsk, Russia</i>	34
18.00-18.30	Oleg Tereshchenko "Electronic and spin structure of Bi-graphene-like system" <i>Rzhanov Inst. of Semiconductor Physics, SB RAS, Novosibirsk, Russia</i>	35
18.30-19.00	Sergey Tarasenko "Structure and Spin Dynamics of Si-Vacancies in SiC" <i>Ioffe Institute, St.-Petersburg, St.-Petersburg, Russia</i>	36
19.00-19.30	Lada Yashina "Surface modification, stability and spin polarization of excited electrons in tetradymite topological insulators" <i>Depart. of Chemistry, M.V. Lomonosov Moscow State University, Russia</i>	37
20.00 – 22.00	Poster session. Competition for the best posters of young scientists	39

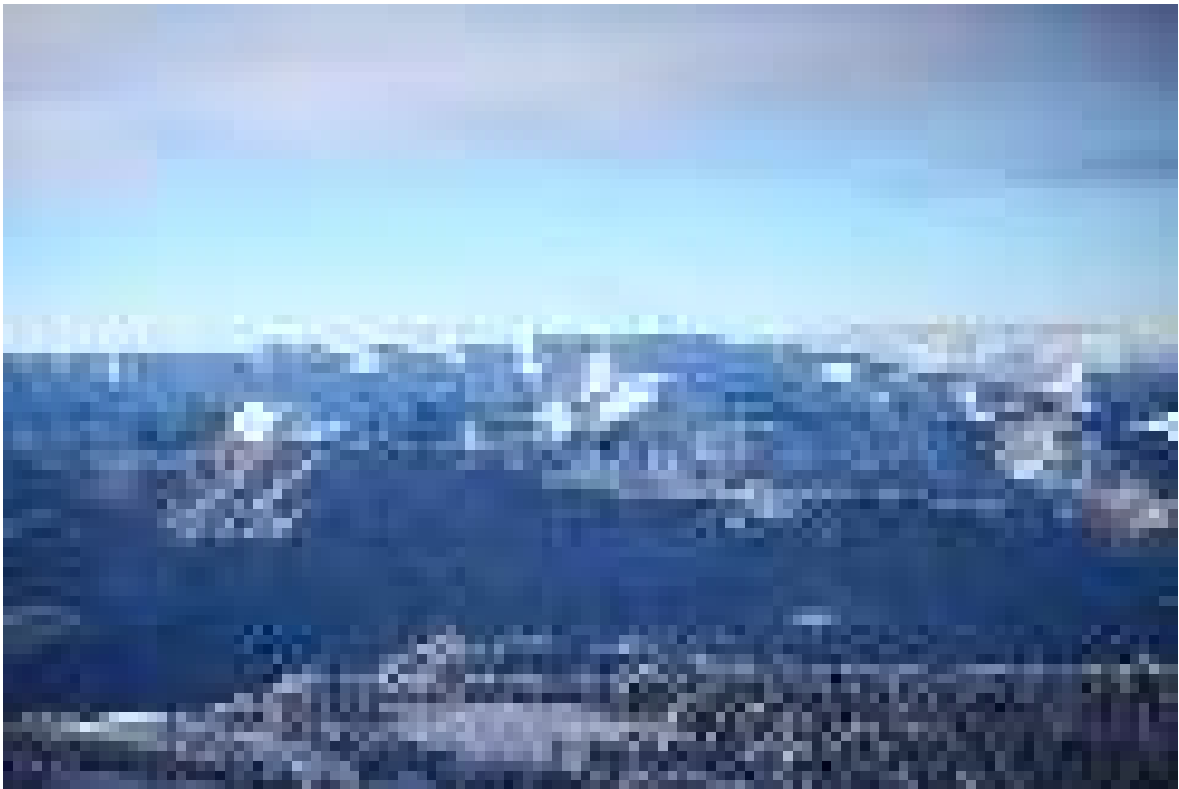
Thursday, March 23

9.00-9.30	Young Hee Lee "Exciton dynamics in van der Waals materials" <i>Sungkyunkwan University, Suwon, South Korea</i>	75
9.30-10.00	Larry Luer "Charge dynamics in SWNT-polymer blends for photovoltaics: from charge generation to extraction" <i>Instituto Madrileño de Estudios Avanzados, Madrid, Spain</i>	76
10.00-10.15	Ji-Hee Kim "Ultrafast Exciton and Phonon Dynamics in Two-dimensional van der Waals Materials" <i>Sungkyunkwan University, Suwon, South Korea</i>	77
10.45-11.15	Tatiana Murzina "Nonlinear optical effects in organic microstructures" <i>Depart.t of Physics, M.V. Lomonosov Moscow State University, Russia</i>	78
11.15-11.45	Stephen Purcell "Optical Excitation of Semiconducting Field Emission Cathodes" <i>Inst. Lumière Matière, Univ.Claude Bernard, Lyon, UMR CNRS, France</i>	79
11.45-12.00	Natalia Arutyunyan "SERS of linear carbon chains synthesized by laser ablation in liquids" <i>A.M. Prokhorov General Physics Institute RAS, Moscow, Russia</i>	80
12.00-12.15	Victor Kleshch "Electron Energy Spectroscopy of Field-Emission Coulomb Blockade from Carbon Nanostructures" <i>Physics Dep. of M.V. Lomonosov Moscow State University, Russia</i>	81
18.00-18.30	Vladimir Kuznetsov "Oxide matrix composites containing carbon nanotubes" <i>Borisevsk Institute of Catalysis SB RAS, Novosibirsk, Russia</i>	82
18.30-19.00	Der-Jang Liaw "Carbon Related Polymeric Nanomaterials for Photonics and Optoelectronics Applications" <i>National Taiwan University of Science and Technology, Taipei, Taiwan</i>	83
19.00-19.30	Tawfique Hasan "Using solvents for composites, functional inks and soft lithography patterns of 2D materials for optoelectronics and photonics" <i>The University of Cambridge, UK</i>	84

Friday, March 24

9.30-10.00	Irina Antonova "Graphene-based field effect transistors for various applications: approaches for engineering" <i>Rzhanov Inst. of Semiconductor Physics SB RAS, Novosibirsk, Russia</i>	87
9.00-9.30	Alexander Okotrub "Gas sensors and micro-supercapacitors based on fluorinated graphene films" <i>Nikolaev Inst. of Inorganic Chemistry, SB RAS, Novosibirsk, Russia</i>	88
10.00-10.30	Polina Kuzhir "Fully carbon microwave absorbers: thin vs light" <i>Research Institute for Nuclear Problems of Belarusian State University</i>	89
11.00-11.30	Huaping Liu "Production and Application of Multifunctional Carbon Nanotube Electronic Ink" <i>Beijing National Laboratory for Condensed Matter Physics, China</i>	90
11.30-12.00	Georgy Fedorov "Graphene-based nanostructures for detecting terahertz radiation" <i>National Research Center "Kurchatov Institute", Moscow, Russia</i>	81
	Author index	92

Monday, March 20



©M.Rybin

Synthesis and Characterization of Single-Layer Graphene

Dmitry Yu. Usachov

*St. Petersburg State University, 7/9 Universitetskaya nab, St. Petersburg, 199034, Russia
dmitry.usachov@spbu.ru*

It is already well-established that graphene is a promising material for the development of novel electronic devices, including transistors, memory, solar cells, fuel cells, biosensors, catalysts, batteries, flexible displays, capacitors, spin filters, etc., and the range of possible applications continues to expand. However, the mass production of graphene devices remains a matter for the future due to a problem of synthesis of graphene-based systems with predefined structure and physico-chemical properties. Practical use of graphene requires further improvement of synthesis methods, controlling its electronic structure and a systematic study of its properties, depending on the substrate material and synthesis procedure.

This work is focused at the synthesis of single-layer graphene and its characterization with an efficient combination of methods, including angle-resolved and spin-resolved photoemission spectroscopy, atomically-resolved scanning tunneling microscopy and spectroscopy, electron and photoelectron diffraction and microscopy, X-ray absorption spectroscopy, Raman spectroscopy and DFT simulations. These methods provide deep insight into the structural and electronic properties, which can be efficiently tuned due to purposefully designed interface of graphene with different magnetic and nonmagnetic materials [1-3]. In particular, a promising approach for the graphene band gap engineering is to introduce a sublattice asymmetry by means of selective incorporation of impurities into only one of the two carbon sublattices. It is shown that boron impurities embedded in graphene on the Co(0001) surface preferably occupy one sublattice due to a site-specific interaction with the substrate [1,2]. Such B-graphene possesses a band gap that can be controlled by the dopant concentration.

Another intriguing property of graphene-Co interface is a possibility for graphene recrystallization during thermal annealing. It is demonstrated that recrystallization may lead to reorientation of graphene domains and their alignment in one direction, thus providing a route for the formation of single-crystalline graphene from a polycrystalline layer due to a driving force of self-organization.

An important characteristic of single-layer graphene is its high sensitivity to the environment. Here we show that this property strongly complicates graphene diagnostics on metal surfaces. Once exposed to air conditions graphene-metal interface may undergo severe structural transformations accompanied by oxygen intercalation under graphene. This may lead to erroneous interpretation of spectroscopic data. A systematic study of the influence of air on the graphene-metal contact allowed to understand the role of oxygen in the graphene diagnostics with photoemission and Raman spectroscopies.

This work was supported by RFBR grant No 17-02-00427 and SPbU grant No 11.65.42.2017.

[1] D. Usachov et al., *Large-Scale Sublattice Asymmetry in Pure and Boron-Doped Graphene*. Nano Lett. **16**, 4535 (2016).

[2] D. Usachov et al., *Epitaxial B-Graphene: Large-Scale Growth and Atomic Structure*. ACS Nano **9**, 7314 (2015).

[3] D. Usachov et al., *Observation of Single-Spin Dirac Fermions at the Graphene/Ferromagnet Interface*. Nano Lett. **15**, 2396 (2015).

A One-Step *In Situ* Synthesis of the Carbon Nanotube Aerogels

D.V. Krasnikov^{1,2,*}, V.L. Kuznetsov^{1,2,3}, M.A. Kazakova^{1,2}, S.I. Moseenkov¹, T.E. Smirnova³,
V.I. Suslyayev³, I.O. Dorofeev³, G.I. Kovalenko^{1,2}

¹ Borekov Institute of Catalysis, Novosibirsk, 630090 Russia

² Novosibirsk State University, Novosibirsk, 630090 Russia

³ National Tomsk State University, Tomsk, 634050 Russia

*dk@catalysis.ru

1. Introduction

Aerogels of multi-walled carbon nanotubes (MWCNTs) combine unique mechanical, thermal and electrical properties of nanotubes with specific characteristics of aerogels. This material as well as MWCNT forests can be more promising than conventional MWCNT powder for such applications as EMI and acoustic shielding, gas sensors and substrates for biological objects. Usually MWCNT aerogel synthesis includes MWCNT-based gel formation supplied by specific cross-linking agents and following supercritical drying. However, one-step MWCNT aerogel production during the synthesis of nanotubes is to be more cost-efficient. Catalyst sputtering during MWCNT growth and additional reactive ion etching of catalyst during synthesis of MWCNT forest led to aerogel formation. In the present work, we report one-step MWCNT aerogel production via catalytic CVD technique under conditions close to industrial nanotube synthesis ($\sim 700^\circ\text{C}$, ~ 1 atm).

2. Results and discussion

The catalysts used consist of nanosized mixed metal oxides of Fe, Co, Ca or Mg. Fe-Co alloy is an active component of this catalysts. An activation of preformed catalyst was carried out in the same conditions as following MWCNT growth (670°C , $\text{C}_2\text{H}_4/\text{Ar}$ 1:1, 400 sccm). Ethylene decomposition on the catalyst surface led to Fe, Co species reduction followed by alloy formation with subsequent nanotube nucleation and growth. Catalyst structural changes and MWCNT aerogel morphology were observed with HRTEM (JEM-2010) and SEM (JSM6460LV). N_2 adsorption isotherms (77 K) were determined with ASAP-2400 (Micromeritics). Electric and magnetic polarizabilities of MWCNT aerogels were measured by open microwave resonator with a measuring hole in one of the mirrors (8-12 GHz).

In situ activation of the preformed catalyst results in the formation of multiple nanosized active centers on the surface support particle (fig. 1B). This self-assembling system provides multi-center growth of MWCNTs. Following tangling of the MWCNTs results in the formation sponge-like and rigid structure of aerogel (fig. 1 C,D). Due to intensive MWCNT growth, a volume of resulting material significantly increases in comparison with the initial catalysts. This leads to the formation of aerogels with density of $0.03\text{--}0.08\text{ g/cm}^3$. Any shape of MWCNT aerogels is possible to obtain by using different geometry of preformed catalyst (balls, cylinders etc.). Pores of size $>120\text{ nm}$ occupy $>95\%$ of MWCNT aerogel volume whereas smaller pores take up $<2\%$. MWCNT aerogels showed polarizability intermediate to that of metal conductors and dielectrics with values close to metals while having a substantially lower weight.

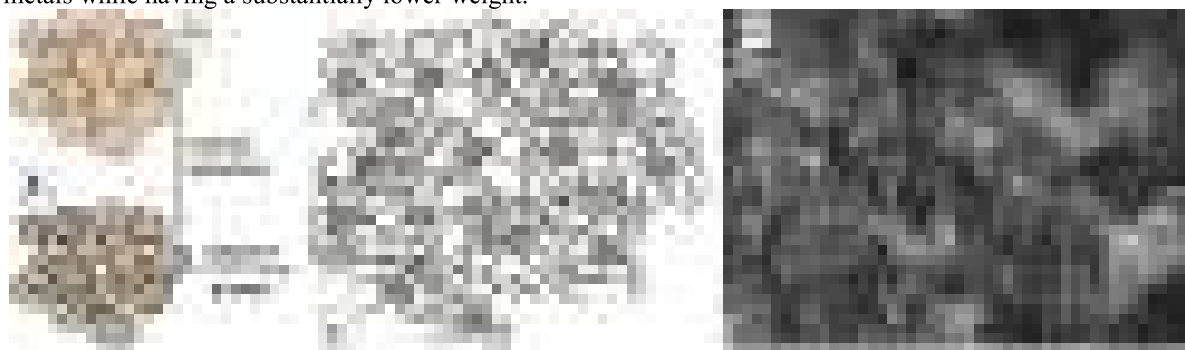


Fig. 1. A-C: A scheme for the formation of the MWCNT aerogel structure; D: Typical SEM microphotography of the aerogel structure.

3. Conclusions

A new cost-efficient technique for one-step *in situ* MWCNT aerogel production under conditions close to industrial nanotube synthesis was developed. Such properties of the aerogels as S_{BET} , pore size distribution, density, conductivity and shape can be varied in a wide range. *In situ* produced MWCNT aerogels demonstrate high electrical conductivity (several S/cm), remain stable in different solvents and hold more than 2500 their weight. Due to high polarizability, MWCNT can be employed as low weight reflecting coatings. It was shown that macroporous and rigid structure combined with high surface area allow MWCNT aerogel to be promising support material for a different compounds including biological and supramolecular species.

This research was partially supported by grant of RFBR Bel_a 16-53-00146.

Chirality-Specific Synthesis and Spectroscopic Characterization of Single-Walled Carbon Nanotubes

Feng Yang, Daqi Zhang, Juan Yang, Yan Li*

Key Laboratory for the Physics and Chemistry of Nanodevices, BNLM, State Key Laboratory of Rare Earth Materials Chemistry and Applications, College of Chemistry and Molecular Engineering, Peking University, Beijing 100871, China
yanli@pku.edu.cn

Single-walled carbon nanotubes (SWNTs) have shown great application potentials attributed to their unique structure-dependent properties. Therefore the controlled preparation and accurate characterization of the chemically and structurally pristine SWNTs is a crucial issue for their advanced applications (e.g. nanoelectronics). Recently, we developed a new family of catalysts, tungsten-based intermetallic compounds, which have high melting point and very special crystal structure, to synthesize SWNTs with designed chirality [1,2]. The chirality-specific growth of SWNTs is realized by the cooperation of two factors: the structural match between SWNTs and the catalysts makes the growth of SWNTs with specific chirality thermodynamically favourable; further manipulation of CVD conditions obtains optimized growth kinetics for SWNTs with this designed chirality. This idea has been proved to be valid for several chiralities such as metallic (12,6) [1], semiconducting (14,4) [3] and zigzag (16,0) [4].

We developed a Raman spectra based SWNT (n,m) characterization and quantification methods. For SWNTs on silicon substrate, we used the “sparse region” in Kataura plot to obtain the relation between RBM frequency (ω_{RBM}) and tube diameter (d_t) [1,5,6]. An RBM counting based quantification method considering the tube density calibration and ω_{RBM} variation is developed to obtain the content of the single-chirality samples on substrate [1,6]. For metallic SWNTs, we observed two electronic Raman scattering (ERS) features centered at M_{11}^+ and M_{11}^- , respectively [7]. The M_{11}^+ and M_{11}^- values are thus determined with high accuracy and (n,m) are accurately assigned accordingly [8]. The environmental effects including bundling and laser heating on the SWNT Raman spectra are also discussed [7,8].

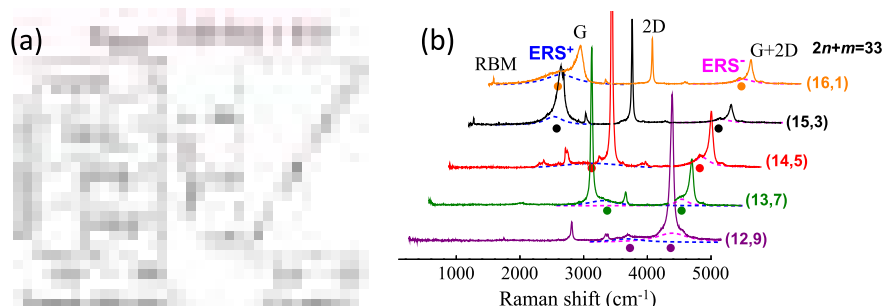


Fig 1. (a) Typical Raman spectra of SWNTs on silicon substrate and the $\omega_{\text{RBM}} - d_t$ relation [6]. (b) ERS⁺ and ERS⁻ features in metallic SWNTs [8].

Acknowledgement

This research is financially supported by Ministry of Science and Technology of China (2016YFA0201904), National Natural Science Foundation of China (grant 21631002, U1632119, and 91333105).

References

- [1] F. Yang, X. Wang, D.Q. Zhang, J. Yang, D. Luo, Z.W. Xu, J.K. Wei, J.-Q. Wang, Z. Xu, F. Peng, X.M. Li, R.M. Li, Y.L. Li, M.H. Li, X.D. Bai, F. Ding, and Y. Li*. *Nature*, **510**, 522 (2014).
- [2] F. Yang, X. Wang, M.H. Li, X.Y. Liu, X.L. Zhao, D.Q. Zhang, Y. Zhang, J. Yang, and Y. Li*. *Acc. Chem. Res.*, **49**, 606 (2016).
- [3] F. Yang, X. Wang, J. Si, X.L. Zhao, K. Qi, C.H. Jin, Z.Y. Zhang, M.H. Li, D.Q. Zhang, J. Yang, Z.Y. Zhang, Z. Xu, L.-M. Peng, X.D. Bai, and Y. Li*. *ACS Nano*, DOI:10.1021/acsnano.6b06890, (2016).
- [4] F. Yang, X. Wang, D.Q. Zhang, K. Qi, J. Yang, Z. Xu, M.H. Li, X.L. Zhao, X.D. Bai, and Y. Li*. *J. Am. Chem. Soc.*, **137**, 8688 (2015).
- [5] D.Q. Zhang, J. Yang*, and Y. Li*. *Small*, **9**, 1284 (2013).
- [6] D.Q. Zhang, J. Yang*, F. Yang, R.M. Li, M.H. Li, D. Ji, and Y. Li*. *Nanoscale*, **7**, 10719 (2015).
- [7] D.Q. Zhang, J. Yang*, E. H. Hasdeo, C. Liu, K.H. Liu, R. Saito, and Y. Li*. *Phys. Rev. B*, **93**, 245428 (2016).
- [8] D.Q. Zhang, J. Yang*, M.H. Li, and Y. Li*. *ACS Nano*, DOI: 10.1021/acsnano.6b04453, (2016).

Key Roles of Carbon Concentration in Nucleating and Growing Single-Walled Carbon Nanotubes

Maoshuai He^a, Yann Magnin^b, Hakim Amara^c, Hua Jiang^d, Esko Kauppinen^d, Annick Loiseau^c, Christophe Bichara^b

^a School of Materials Science and Engineering, Shandong University of Science and Technology, 266590 Qingdao, P. R.China

^b Aix-Marseille University and CNRS, CINaM UMR 7325, 13288 Marseille, France

^c Laboratoire d'Étude des Microstructures, ONERA-CNRS, BP 72, 92322 Châtillon CEDEX, France

^d Department of Applied Physics, Aalto University School of Science, P.O. Box 15100, FI-00076 Aalto, Finland
maoshuai.he@sdust.edu.cn

Searching for chirality-controlled growth of single-walled carbon nanotubes (SWNTs) during the chemical vapor deposition (CVD) process is a much coveted goal that has been partially reached in a number of experiments [1,2]. However, the rationale behind these successful achievements has never been fully understood, precluding coherent synthesis strategies.

In this talk, we will highlight that controlling the level of dissolved carbon inside a metal particle is of key importance to enable SWNT nucleation and growth. First of all, both experimental and simulation approaches emphasize that the presence of subsurface carbon in the nanoparticles is necessary to enable the cap lift-off [3,4], initiating the possible nucleation of SWNTs. Secondly, we demonstrate experimentally that the SWNT length is related with the tube growth mode, depending on the carbon content of metal particles: low (or high) carbon concentration in the nanoparticle leads to tangential (or perpendicular) growth [5]. Finally, the carburization degree of metal particle is proven to be sensitive to the environmental carbon potential, determined by the carbon precursor and the reaction pressure.



Fig. 1. UV-vis-NIR adsorption spectra of SWCNTs grown on catalysts with different active components. All growth experiments are performed at 873K using CO as the carbon precursor.

On the basis of the above understandings, we could not only control the formation of intramolecular junctions by tuning the SWNT growth mode *via* modulating the CVD reaction parameters, but also interpret diverse experimental results by the growth mode (Fig. 1). Our work thus provides a rational understanding of the key factor that determines SWNT lengths and diameters, shedding more light on chirality-controlled synthesis of SWNTs.

[1] M. He, A.I. Chernov, P.V. Fedotov, E.D. Obraztsova, J. Sainio, E. Rikkinen, H. Jiang, Z. Zhu, Y. Tian, E.I. Kauppinen, M. Niemela and A.O. Krause, J. Am. Chem. Soc., **132**, 13994 (2010).

[2] M. He, H. Jiang, B. Liu, P.V. Fedotov, A.I. Chernov, E.D. Obraztsova, F. Cavalca, J.B. Wagner, T.W. Hansen, I.V. Anoshkin, E.A. Obraztsova, A.V. Belkin, E. Sairanen, A.G. Nasibulin, J. Lehtonen and E.I. Kauppinen, Sci. Rep., **3**, 1460 (2013).

[3] M. He, H. Amara, H. Jiang, J. Hassinen, C. Bichara, R.H. Ras, J. Lehtonen, E.I. Kauppinen and A. Loiseau, Nanoscale, **7**, 20284 (2015).

[4] M. He, H. Jin, L. Zhang, H. Jiang, T. Yang, H. Cui, F. Fossard, J.B. Wagner, M. Karpinen and E.I. Kauppinen, Carbon, **110**, 243 (2016).

[5] M. He, Y. Magnin, H. Amara, H. Jiang, H. Cui, F. Fossard, A. Castan, E. Kauppinen, A. Loiseau and C. Bichara, Carbon, **113**, 231 (2017).

Doping of Single-Walled Carbon Nanotubes by Encapsulation of Inorganic Compounds

A.A. Eliseev^{1,2}, N.S. Falaleev¹, N.I. Verbitskiy³, I.I. Verbitskiy², M.M. Brzhezinskaya⁴, A.A. Volykhov², A.S. Kumskov⁵, V.G. Zhigalina⁵, L.V. Yashina², J. Sloan⁶, N.A. Kiselev⁵

¹Department of Materials Science, Moscow State University, 119991, Moscow, Russia

²Department of Chemistry, Moscow State University, 119991, Moscow, Russia

³University of Vienna, 1090 Vienna, Austria

⁴Institute for Nanometre Optics and Technology, Helmholtz-Zentrum Berlin für Materialien und Energie GmbH, Albert-Einstein-Straße 15, 12489 Berlin, Germany

⁵Shubnikov Institute of Crystallography RAS, 119333, Moscow, Russia

⁶Department of Physics, University of Warwick, Coventry, Warwickshire CV47AL, UK

General methodology for the synthesis of one-dimensional crystals inside the inner channels of single-wall carbon nanotubes is reviewed. Size dependent nanocrystal structure relations to SWCNT diameters in the range of 1,2 – 2,5 nm are revealed indicating gradual thinning of nanocrystal with decrease of SWNT diameter to a certain limit (~1,3 nm), then the uncharged crystal cannot be fit to the nanotube. Necessity for in-tube charge compensation introduces serious modifications to 1D crystals structure resulting in certain cases in nanometer-scale dipole chains formation. Fundamental relations governing the atomic and the electronic structure of SWNTs infilled with inorganic compounds are extensively examined using statistical analysis. The data on X-ray absorption, XPS, optical absorption and Raman spectroscopy, HRTEM, local EELS and EDX is provided and analyzed for over 50 binary capsules $AX_n@SWNT$ (where A = 3d, 4d or 4f – metal, X = halogen or chalcogen). Interparameter correlations are reported and discussed. The relationship between the degree of crystallinity of guest 1D crystals, lengths of interatomic bonds 1D crystals and ionic radius was established. It is shown that the structure and crystallinity of the guest compounds in the internal channels of nanotubes is dictated by inconsistency between the parameters of the unit cell of the crystal and an inner diameter of the tube. SWNT loading correlates with the diameter of encapsulated nanocrystal, attaining 100% when nanocrystal fully fills the internal nanotube volume. Electronic structure of composites depends strongly on the nanocrystal/SWNT diameter ratio and an effective charge on nanotube walls. The latter is mostly governed by work function and stoichiometry deviation of the nanocrystal. Filling leads to both localized and delocalized effects of charge redistribution. Partial coordination of intercalated compounds by SWNT walls was also established by NEXAFS and the high angle angular dark field (HAADF) HRTEM data. Moreover the stoichiometry of nanocrystals established by local microanalysis can deviate from that of bulk materials, which indicates possible chemical bonding of the embedded nanocrystals with the walls of the nanotube. Consequently, localized binding states appear in the energy spectrum of nanotubes and overall Fermi energy shift occurs. The crystal charge leads to strong variation of carbon p_z -orbital overlap, manifesting itself in van Hove singularities energy separation changes. Provided results represent a comprehensive picture of modifications in SWNT electronic structure upon doping and allow suggesting fast and easy approach for quick determination of doping levels from Raman spectroscopy and optical absorption.

Synthesis of intrinsic and N-doped monocrystalline graphenes on Ni(111)

K.N. Eltsov

*A.M. Prokhorov General Physical Institute RAS, 119991 Moscow, ulitsa Vavilova 38, Russia
e-mail: eltsov@kapella.gpi.ru*

1. *Synthesis of pristine single-crystalline quasi-freestanding graphene on Ni (111).* Method for synthesis of pristine graphene by epitaxial growth of the propylene molecules on Ni(111) is proposed and implemented, allowing to create single crystal of target-size graphene. Synthesis of such single crystalline graphene monolayer on Ni(111) includes the following steps.

- C₃H₆ adsorption at room temperature causes dehydrogenation of hydrocarbon molecules (C₃H₆) on atomic terraces or complete dissociation of the molecules at atomic steps; then formation of carbon chains on atomic terraces or diffusion of carbon atoms under the nickel surface through the edge of atomic steps and their accumulation between atomic layers in subsurface of nickel (mainly under the first layer of nickel).
- Annealing of carbon dosed Ni(111) at 500 °C causes segregation of carbon atoms on the surface of the nickel, surface carbide (Ni₂C) formation, and its transformation into graphene.
- Intercalation of gold under graphene layer causes formation of gold monolayer and “separation” graphene layer from nickel substrate. As a result, electron dispersion of graphene in a K-point of Brillouin zone shows a linear behavior (Dirac cone) close to the dispersion of freestanding graphene monolayer sheet.

2. *Synthesis of monocrystalline monolayer N-graphene on Ni (111).* The monolayer of N-doped graphene (N-graphene) is obtained by temperature programmed synthesis of acetonitrile (C₂H₃N): adsorption acetonitrile (10⁻⁶ Torr) of Ni(111) at 600 °C for 20 min and then annealing at 480 °C during one hour in ultrahigh vacuum. As a result, we have synthesized monolayer of N-graphene with ~1% nitrogen concentration and found that the nitrogen atoms are introduced into the lattice by replacing graphene carbon atoms in graphene lattice. To identify the defects in Gr/Ni(111) containing nitrogen atoms, DFT simulations were performed. The main types of defects were: a nitrogen atom instead of carbon atom and a nitrogen near the carbon vacancy (so-called pyridine defect). Each type of defect was simulated with two different arrangements of carbon atoms in graphene on Ni(111): above (on top) Ni atom and above fcc position in Ni(111). In both types of substitutional nitrogen atoms is energetically favorable one located at fcc position. From our calculations, we have also found that the introduction of nitrogen as a substitutional impurity is more preferable in comparison of pyridine defect creation. The criterion for introducing of gold into the interface of N-graphene/Ni(111) is the appearance (under a layer of graphene) of dislocation network characteristic for binary system Au/Ni(111): Ni(111)- 9.5x9.5-Au.

Acknowledgement

This work was supported by Russian Science Foundation (grant 16-12-00050).

Graphene in heterostructures: optoelectronic properties and applications

L.A. Chernozatonskii

*Emanuel Institute of Biochemical Physics of Russian Academy of Science, Kosygin st, 4, Moscow-119334, Russia.
cherno@sky.chph.ras.ru*

Graphene is the first extensively studied two-dimensional (2D) material [1]. Owing to its unique band structure with linear dispersion near the Dirac point and various forms of light–matter interaction, graphene offers a highly sensitive response to optical signals in a broad spectral range, from far infrared (IR) to ultraviolet (UV). In the mid- and far-IR range (more than 5 μm wavelength), the light–graphene interaction can be further enhanced through the excitation of propagating plasmons or localized plasmon resonances [2].

Combining graphene with other quasi-2D materials such as transition metal dichalcogenides (TMD), h-BN, and black phosphorous, the bandgap can cover a wide spectral range, from visible to mid-IR. The fabrication of graphene contained heterostructures can utilize both top-down and bottom-up approaches. Such interest is often paid to the Van der Waals heterostructures [3]. The possibility to build material with new properties just by placing one material on another opens a new wave of synthesis of 2D materials of different compounds [4]. Between them semiconducting TMDs with the considerable bandgap of ~ 2 eV, especially monolayer MoS₂, have attracted significant attention due to their novel optical dichroic and coupled spin-valley physics.

Here we consider some last results of graphene contained heterostructures in the optoelectronics area:

Graphene/TMD (mainly molybdenum and tungsten disulfides, diselenides) and graphene/h-BN hybrids: synthesis, properties and devices [5,6].

Graphene/h-BN bi-layers with folded holes: formation, structure and optoelectronic properties [7,8].

Perforated bi-layered graphene with folded holes: formation, structure and properties [9].

New heterostructures based on graphene and MoS₂ layers with molecular covered ZnO layer [10] or decorated by C₆₀ fullerenes [11] and their optic and electronic properties.

This work is supported by the Russian Scientific Foundation. All our quantum-chemical calculations in [7-11] were made by using the 'Chebishev' and 'Lomonosov' cluster computers of the Moscow State University and supercomputer of the JS Center of the Russian Academy of Sciences.

- [1] K. S. Novoselov, V. I. Fal'ko, L. Colombo,; P. R. Gellert, M. G. Schwab,; K. Kim, *Nature* **490**, 192 (2012).
- [2] M. Freitag, T. Low, F. N. Xia, P. Avouris, *Nat. Photon.* **7**, 53 (2013).
- [3] A. K. Geim and I. V. Grigorieva, *Nature* **499**, 419 (2013).
- [4] A. N. Grigorenko, M. Polini, K. S. Novoselov, *Nat. Photon.* **6**, 749 (2012).
- [5] K. S. Novoselov, A. Mishchenko, A. Carvalho, and A. H. Castro Neto, *Science* **353**, 9439 (2016).
- [6] N. A. Kumar, M. A. Dar, R. Gul, J. B. Baek, *Materials Today* **18**, 286 (2015).
- [7] L. A. Chernozatonskii, V. A. Demin, S. Bellucci, *Scientific reports*, **6**, 38029 (2016).
- [8] L. A. Chernozatonskii, O. A. Sedelnikova, V. A. Demin, C. P. Ewels, (in preparing).
- [9] L. A. Chernozatonskii, V. A. Demin, , Ph. Lambin, *Phys. Chem. Chem. Phys.* **18**, 27432 (2016).
- [10] L. A. Chernozatonskii, A. G. Kvashnin, (in press).
- [11] A. G. Kvashnin, L. A. Chernozatonskii, P. B. Sorokin, *Nanotechnology* **27**, 365201 (2016).

Nanostructured few-layer graphene films for optic and electronic applications

N. A. Nebogatikova, I. V. Antonova

*Rzhanov Institute of Semiconductor Physics SB RAS, 630090, Lavrentjev av., 13, Novosibirsk, Russia
nadonebo@gmail.com*

Zero bandgap in graphene electronic structure limits its optic and electronic application significantly. To solve this problem one has to investigate new pathways for opening the bandgap in graphene layers and materials, such as nanolithography, functionalization and 2D-inkjet printing [1, 2]. There is a dramatic decrease in carrier mobility due to chemically active dangling bonds near the formed edges. So, one of the most important task for the graphene nanostructuring is to save its excellent properties.

The stability of graphene-based nanostructures without edge atoms has been investigated recently. One can create such materials by embedding graphene islands into a stable matrix. Such approach was realized in our previous studies of graphene suspensions fluorination [1]. We obtained partially fluorinated graphene suspensions with nanosized flakes (20-200 nm in diameter and 0.5-1.5 nm in height) due to peculiarities of the fluorination process. Pristine graphene has no photoluminescence (PL), but studied suspensions demonstrated photoluminescence with three energy levels (2.63, 2.81 and 2.93 eV) [3]. Moreover, studying printed graphene films [2] we obtained self-formed nanoscale graphene-based columns with unexpected optic properties. The excitation of these nanostructures in the range of wavelength of ~ 320 -360 nm causes the appearance of the PL peak with a maximum emission at ~ 515 nm. Self-formation and PL processes for nanoscale graphene-based structures are of considerable interest both for fundamental science and applications. Moreover, the development of graphene-based inkjet printing technology will significantly widen the range of applications for the printing technology in the nearest future.



Fig. 1. Different types of graphene nanostructures

New promising decision how to modificate graphene films properties was suggested by L.A. Chernozatonskii [4]. His main idea is to cut holes in neighboring graphene layers and to bond the chemically active atoms from different layers forming a closed structure of sp^2 -hybridized carbon atoms. We used high energy ions (26 – 167 MeV) to create perforated few-layer graphene films. Both scanning electron microscopy and atomic force microscopy both demonstrate nanosized holes (20-40 nm in diameter) formed by ions irradiation.

The initial ions energy determines the amount of electronic loss and the value of a sharp local temperature rise in the films. As a consequence, the type of the holes edge may be reconstructed in

the range from the dangling bonds to connected edges. We observed the bandgap and electric active traps appearance, dependently on ions energy. We found the conditions for tuning the film electronic and structural properties.

The formation of a continuous graphene surface between two perforated layers are very attractive as well as for nanoelectronic devices because of the bandgap appearance in its electronic band structure, opportunity to save the carrier mobility and capability to transmit high electric currents in contrast to nanostructured graphene and semiconducting graphene nanoribbons. Moreover, such nanostructures are promising for sensors and molecule filters.

Acknowledgement.

This study was supported in part by the Russian Science Foundation (grant No. 15-12-00008).

References

- [1] N. A. Nebogatikova, I. V. Antonova, V. Y. Prinz, I. I. Kurkina, V. I. Vdovin, G. N. Aleksandrov, V. B. Timofeev, S. A. Smagulova, E. R. Zakirov, V. G. Kesler. Fluorinated graphene dielectric films obtained from functionalized graphene suspension: preparation and properties. *Physical Chemistry Chemical Physics*, **17**(20), 13257-13266 (2015).
- [2] N.A. Nebogatikova, P. V. Fedotov, I. I. Kotin, I. V. Antonova, E. D. Obratzova. Properties of self-assembled graphene-based columns formed by 2D inkjet printing. Young scientists summer school "Nanocarbon for optics and electronics", 24-29 July 2016, Russia, Kaliningrad. Book of Abstracts, p. 98.
- [3] N. A. Nebogatikova, P. V. Fedotov, A. I. Komonov, I. V. Antonova, E. D. Obratzova. Optical and electronic properties of the partially fluorinated graphene suspensions and films. *Journal of Colloidal & Interface Science*. In press.
- [4] L. A. Chernozatonskii, V. A. Demin, A. A. Artyukh, Bigraphene nanomeshes: Structure, properties, and formation. *JETP Letters*, **99** (5), 309-314 (2014).

Study of optical, fluorescent, sensing properties of graphene oxide films

Smagulova S.A.

*North-Eastern Federal University, 677000, Belinskogo str., Yakutsk, Republic of Sakha (Yakutia), Russia
smagulova@mail.ru*

The advantages of graphene oxide to create the elements of electronic and optoelectronic devices caused by the simplicity and cheapness of preparing stable aqueous dispersions of graphene oxide. Graphene in an oxidized state can be synthesized from graphite by chemical cleavage. In this case the resulting material is the dispersion with individual monolayer graphene oxide sheets, from which by removing the solvent create graphene oxide film.

High-resistive (10^{12} Ohm/ \square) oxide-graphene films with thickness varying from 9 nm to several micrometers were produced and studied. Films of 9–150 nm on glass had a transparency of 93–98% for wavelengths of 400–700 nm. Also, absorption spectra of graphene oxide films and reduced graphene oxide were investigated in the ultraviolet and infrared ranges. A comparative analysis of the properties of graphene oxide films reduced by different methods: thermal, chemical, laser irradiation (wavelength of laser was 450 nm, 788 nm) was made.

The luminescence properties of graphene oxide by hydrothermal synthesis, which is a thermal reduction of graphene oxide, followed by oxidation in a mixture of sulfuric and nitric acids were investigated.

In this work we study the influence of humidity on the electrical conductivity of graphene oxide and reduced graphene oxide graphene films. The different character of GO films electrical conductivity dependence of humidity was found, it can be attributed with different mechanisms of adsorption of water molecules. In this work we discussed possible mechanisms of interaction of water molecules with the surfaces of the films.

DFT study of gold intercalation under graphene monolayer on Ni(111)

T. V. Pavlova, S. L. Kovalenko, K. N. Eltsov

A.M. Prokhorov General Physics Institute, RAS, Moscow, Russia
pavlova@kapella.gpi.ru

Recently [1], monocrystalline graphene monolayer of size 6x6 mm has been synthesized on Ni(111) by propene adsorption at 25° C and annealing at 500° C (temperature programmed method). The method allows to grow epitaxial graphene without rotated domains, and the only defects are point defects, which we attribute to Ni atom in C vacancy (or bivacancy). As a result of gold intercalation at 450° C, graphene monolayer is detached from nickel without any damage and point defects disappeared. After intercalation by gold atoms, angle resolved photoemission spectroscopy (ARPES) measurements show perfect Dirac cone in electron dispersion corresponding to quasi free-standing graphene.

The density functional theory (DFT) calculations were performed to understand the mechanism of gold intercalation at the interface graphene/Ni(111). All calculations have been done using VASP code [2] with PAW potentials [3] (400 eV cut-off) and GGA PBE exchange-correlation functional [4] as the basis for the DFT-D2 (Grimme) correction [5]. The reaction barriers were evaluated using the nudged elastic band (NEB) method [6] implemented into VASP.

Different scenarios of intercalation process have been tested. The pathway for gold atoms penetration underneath a perfect graphene monolayer on Ni(111) has very high activation energy due to strong C-C bounds in graphene, in agreement with other calculations for Pd intercalation at the interface graphene/Ru(0001) [7]. According to our calculations, C-C bond breaking in graphene near C vacancy is easier than that in the absence of defect. It means that collective mechanism of Au atoms penetration can be through C atoms dissolution in nickel and re-grown of graphene after all Au atoms reach Ni surface. Also, we discuss intercalation process when one metal atom penetrates through single atom vacancy (or bivacancy) in graphene on Ni(111). Theoretically investigated mechanisms of gold atoms penetration through graphene via vacancies are consistent with our STM experiments. According to STM images, most of intercalated islands are located close to chains of point defects.

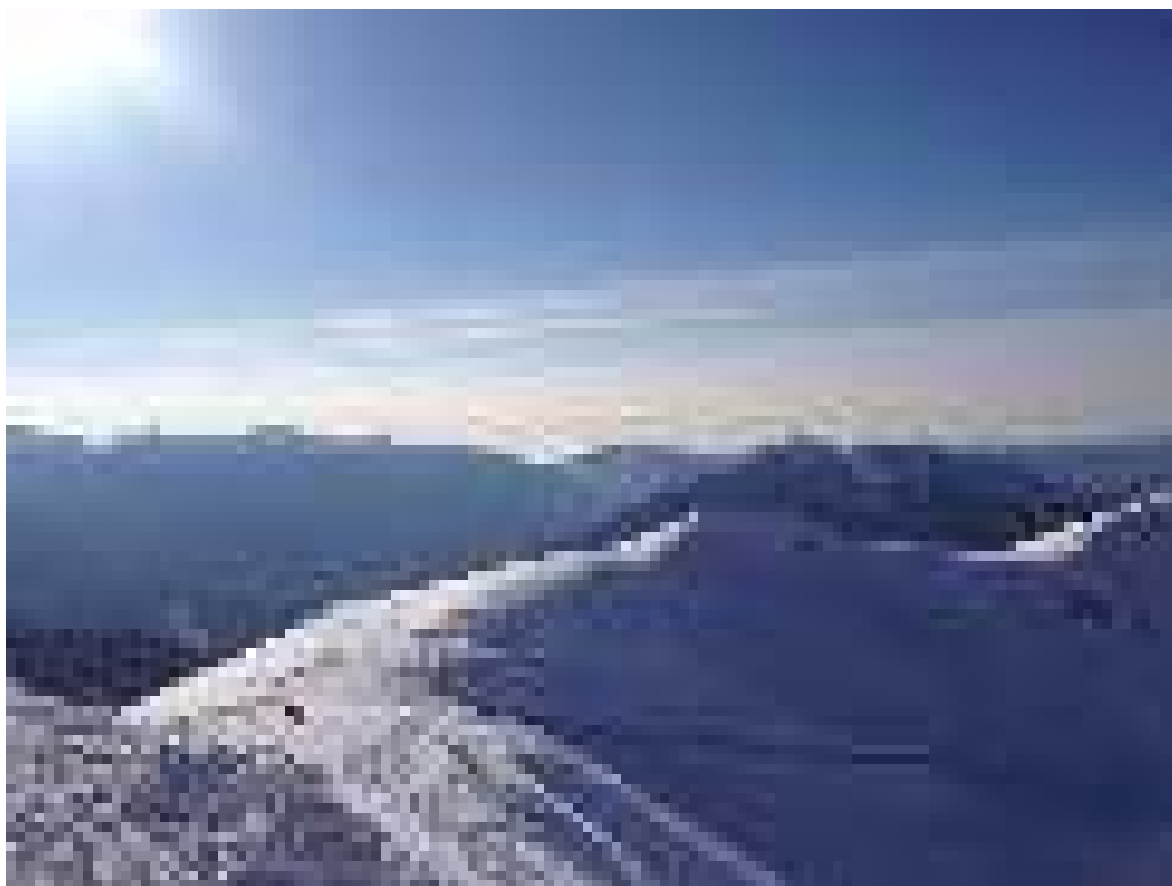
Acknowledgement.

This work was supported in part by grant of the Russian Foundation for Basic Research (Grant No. 15-02-09106) and Program "Nanostructures: Physics, chemistry, biology, technology basics" of Presidium of Russian Academy of Sciences. We are grateful to the Joint Supercomputer Center of RAS for the possibility of using their computational resources for our calculations.

References

- [1] S. L. Kovalenko, T. V. Pavlova, B. V. Andryushechkin, O. I. Kanishcheva, K. N. Eltsov (to be published).
- [2] G. Kresse and J. Hafner, *Phys. Rev. B* **47**, 558 (1993).
- [3] G. Kresse and D. Joubert, *Phys. Rev. B* **59**, 1758 (1999).
- [4] J. P. Perdew, K. Burke, and M. Ernzerhof, *Phys. Rev. Lett.* **77**, 3865 (1996).
- [5] S. Grimme, *J. Comput. Chem.* **27**, 1787 (2006).
- [6] H. Jonsson, G. Mills, K. W. Jacobsen, *Classical and Quantum Dynamics in Condensed Phase Simulations*; World Scientific: Singapore (1998).
- [7] Li Huang, Yi Pan, Lida Pan, Min Gao, Wenyan Xu, Yande Que, Haitao Zhou, Yeliang Wang, Shixuan Du, and H.-J. Gao, *Appl. Phys. Lett.* **99**, 163107 (2011).

Tuesday, March 21



©A.Golubina

Carbon Nanotubes as Nanoreactors: Synthesis & Analysis of Low-Dimensional Materials

Andrei N. Khlobystov

School of Chemistry, University of Nottingham, University Park, Nottingham, NG7 2RD, U.K.
Nanoscale & Microscale Research Centre (nmRC), University of Nottingham, NG7 2RD, U.K.
Andrei.Khlobystov@nottingham.ac.uk

Carbon nanotubes are the world's tiniest test tubes that can be filled with a wide range of different molecules. Due to extreme confinement within the nanoscale channel of a host-nanotube dynamic and structural behaviour of the guest-molecules can change drastically as compared to their free, unconfined state. For example, translational and rotation molecular motions both are substantially affected within the nanotube, while new packing arrangements of the guest-molecules arise as a result of severe space restrictions within the nanotube channel. The previous studies clearly demonstrate the nanotube as a powerful template for the formation of low-dimensional materials. The next challenge is to employ carbon nanotubes as reaction vessels for specific chemical transformations leading to unique functional materials.

Transmission electron microscopy (TEM) is invaluable for characterization of structures inside nanotubes, but also it can promote transformations within the sample due to electron beam (e-beam) interactions with atoms. Provided that the amount of energy transferred from collisions of the e-beam with molecules is known, transformations in molecules promoted during TEM analysis can be interpreted as chemical reactions. Such approach, which we term *ChemTEM*, utilizes the e-beam of TEM as an imaging tool and a source of energy simultaneously, thus allowing to discover previously unforeseen chemical reactions inside nanotubes and to assess the impact of nanoscale confinement on the pathways of these reactions. Two examples of reactions of polycondensation of perchlorocoronene (PCC) and octathiacirculene (OTC) leading to a zigzag Cl-terminated graphene nanoribbon and a ribbon-like S-containing polymer respectively have recently been discovered by *ChemTEM* [1]. Under similar conditions an inorganic complex $[\text{Mo}_6\text{I}_{14}]^{2-}$ demonstrated polycondensation of the octahedral complexes into extended polyiodide structure $[\text{Mo}_6\text{I}_{12}]_n$ inside single-walled carbon nanotubes, with the nanotube playing a role of a reservoir of electron density facilitating the initial steps of the reaction [2]. Similarly, catalytic activities of sub-nm metal clusters consisting of ~10-60 atoms have been studied and compared by *ChemTEM*, revealing interesting trends within periods [3] and groups [4] of transition metals and demonstrating unusual reactions between the metals and carbon nanotube.

ChemTEM allows to discover reactions inside carbon nano test tubes and to unravel their mechanisms. As the role of the host-nanotube and its impact on products of the reactions are being understood, the same principles can be harnessed to control preparative-scale synthesis in order to improve important chemical processes [5] or to deliver new materials inaccessible by other means.

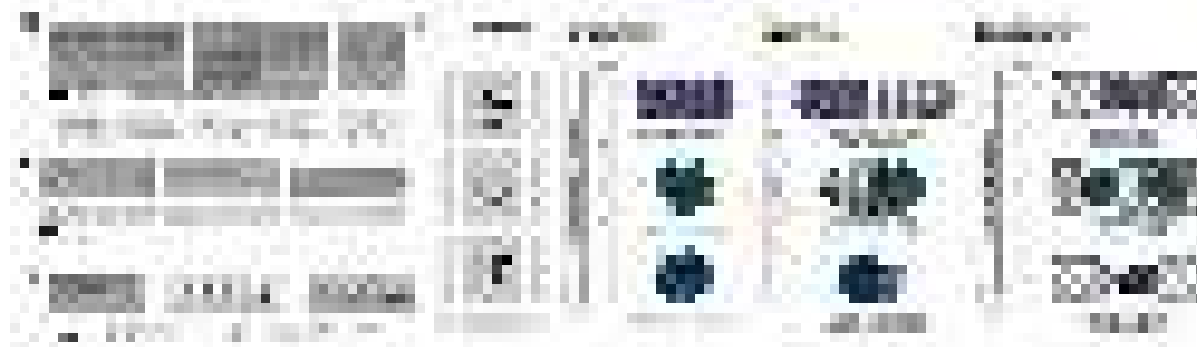


Fig. 1. Reactions of polycondensation of (a,b) PCC to graphene nanoribbon and (c) $[\text{Mo}_6\text{I}_{14}]^{2-}$ to $[\text{Mo}_6\text{I}_{12}]_n$. (d) Comparison of metal-carbon reactions and interactions with atomic resolution is enabled by *ChemTEM* method.

References

- [1] T. W. Chamberlain et al., ACS Nano, submitted (2017).
- [2] A. Botos et al., J. Am. Chem. Soc., **138**, 8175 (2016).
- [3] T. Zoberbier et al., J. Am. Chem. Soc., **134**, 3073 (2012).
- [4] T. Zoberbier et al., Small, **12**, 1649 (2016).
- [5] S. A. Miners et al., Chem. Soc. Rev., **45**, 4727 (2016).

Phonon contribution to electrical resistance of acceptor-doped single-wall carbon nanotubes assembled into transparent films

V. I. Tsebro,¹ A. A. Tonkikh,^{2,3} D. V. Rybkovskiy,^{2,3} E. A. Obratsova,⁴ E. I. Kauppinen,⁵ and E. D. Obratsova²

¹*P. N. Lebedev Physical Institute, Russian Academy of Sciences, 53 Leninsky Prospect, 119991 Moscow, Russia*

²*A. M. Prokhorov General Physics Institute, Russian Academy of Sciences, 38 Vavilov Street, 119991 Moscow, Russia*

³*Faculty of Physics, Southern Federal University, 5 Zorge Street, 344090 Rostov-on-Don, Russia*

⁴*Shemyakin and Ovchinnikov Institute of Bioorganic Chemistry, Russian Academy of Sciences,
16/10 Miklukho-Maklaya Street, 117871 Moscow, Russia*

⁵*Department of Applied Physics, Aalto University, School of Science, Post Office Box 15100, FI-00076 Espoo, Finland
RybkovskiyD@gmail.com*

Transparent conducting netlike single-wall carbon nanotube (SWCNT) films are promising candidates for the production of transparent electrodes for photovoltaic devices, displays, and other optoelectronic applications. The sheet resistance of such films can be significantly decreased by filling the nanotube inner channels with strong electron acceptors.

We present results of electrical resistance measurements of pristine and acceptor-doped SWCNTs assembled into transparent films in the temperature range of 5 to 300 K. The doping was accomplished by filling the nanotubes with iodine or CuCl from the gas phase. After doping the films resistance appeared to drop down by one order of magnitude, to change the nonmonotonic temperature behavior, and to reduce the crossover temperature. The experimental data have been perfectly fitted in frames of the known heterogeneous model with two contributions: from the nanotube bundles (with quasi-one-dimensional conductivity) and from the interbundle electron tunneling. The doping was observed to decrease the magnitudes of both contributions.

To interpret the changes in the nanotube part after doping we applied the model of phonon constraint of charge carrier backscattering and used the relationship between the electronic and phonon band structures of the SWCNTs. In the undoped SWCNT films the main contribution to conductivity comes from metallic nanotubes due to the intervalley scattering via phonons near the K point of the phonon bands. After doping the samples with iodine and CuCl the Fermi level becomes shifted into the valence band of the semiconducting tubes, which start to participate in the conductivity, and intravalley scattering processes with low energy phonons become possible. The values of the Fermi level shift into the valence band are estimated to be equal to -0.6 eV in the case of iodine doping and -0.9 eV in the case of CuCl doping. These values are in qualitative agreement with the optical absorption data.

[1] V. I. Tsebro, A. A. Tonkikh, D. V. Rybkovskiy, E. A. Obratsova, E. I. Kauppinen, and E. D. Obratsova, Phys. Rev. B **94**, 245438 (2016).

Modification of Single-Walled Carbon Nanotube Optical Properties by Graphene Nanoribbon Filling

Alexander Chernov^{1,2}, Pavel Fedotov¹, Elena Obraztsova^{1,3}

¹. Prokhorov General Physics Institute, RAS, Vavilov Str. 38, 119991, Moscow, Russia

². Institute of Physics II, University of Cologne, Zùlpicher Str. 77, 50937, Cologne, Germany

³. National Research Nuclear University MEPhI (Moscow Engineering Physics Institute), Kashirskoe hwy. 31, 115409, Moscow, Russia
al.chernov@nsc.gpi.ru

Single-walled carbon nanotubes (SWCNTs) can serve as a template for the growth of narrow nanoribbons inside. The hallmark of graphene nanoribbons (GNRs) formed inside SWCNTs is their long length and width dependence on the nanotube diameter. Several different molecules can be used for filling and further transformation into different types of GNRs [1-4]. Along with the additional spectral features corresponding to the response from the encapsulated GNRs, precise modification of nanotubes optical properties can be performed. The internal nanotube environment affects the optical transition energies of SWCNTs.

We perform SWCNT filling by coronene molecules with transformation of molecules into GNRs at different parameters and study optical response of composite materials. Depending on the GNR type we detect changes in optical absorption and nanotube photoluminescence (see Fig.1). GNRs absorption and emission are located in the visible spectral range [3]. GNR filling results in the energy shifts of the nanotubes optical transitions, which can be clearly seen by the changes in the photoluminescence peak positions. Certain nanotube geometries demonstrate increased photoluminescence intensity upon filling. The origin of the peak position shifts and intensity changes is explained by energy transfer, dielectric screening and mechanical strain induced after the GNR formation. Encapsulation of molecules and GNRs in SWCNTs can be used for modification of optical properties of nanotubes by changing their internal environment.

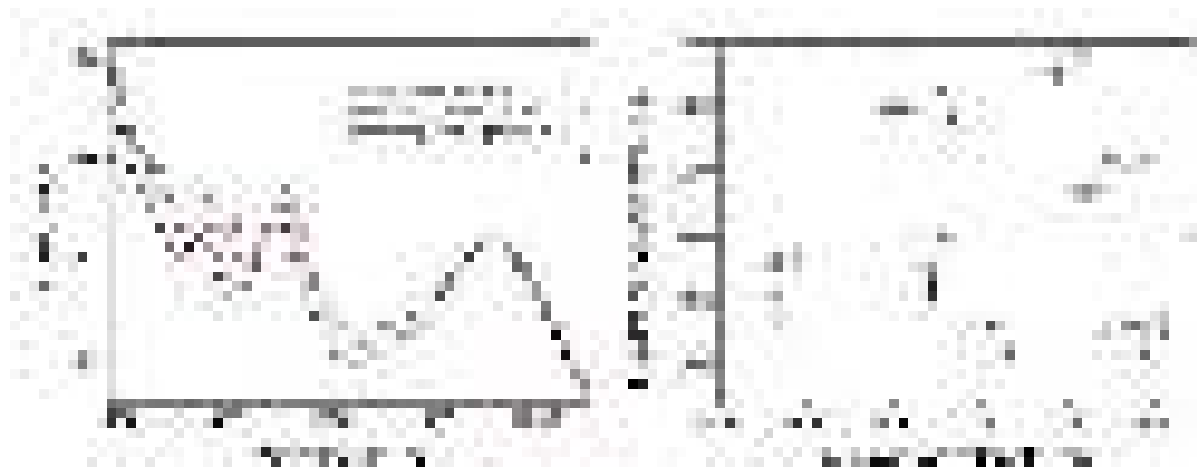


Fig. 1. Left – absorption spectra of pristine single-walled carbon nanotubes (black), nanotubes with formed inside short (red) and long (blue) graphene nanoribbons. Right image – photoluminescence excitation map with peaks corresponding to emission peak positions of different nanotube geometries before filling (black) and after formation of graphene nanoribbons inside (red and blue colors for tubes with encapsulated short and long ribbons respectively).

Acknowledgement

The work was supported by RFBR grants 15-32-70005 mol_a_mos and 16-02-00979.

References

- [1] A. Chuvilin, E. Bichoutskaia, M. C. Gimenez-Lopez, T. W. Chamberlain, G. A. Rance, N. Kuganathan, J. Biskupek, U. Kaiser and A. N. Khlobystov, *Nature Nanotechnology*, **10**, 687 (2011).
- [2] A. V. Talyzin, I. V. Anoshkin, A. V. Krasheninnikov, R. M. Nieminen, A. G. Nasibulin, H. Jiang and E. I. Kauppinen, *Nano Letters*, **11**, 4352 (2011).
- [3] A. I. Chernov, P. V. Fedotov, A. V. Talyzin, L. I. Suarez, I. V. Anoshkin, A. G. Nasibulin, E. I. Kauppinen, V. L. Kuznetsov and E. D. Obraztsova, *ACS Nano*, **7**, 6346 (2013).
- [4] A. I. Chernov, P. V. Fedotov, A. S. Krylov, A. N. Vtyurin and E. D. Obraztsova, *J. Nanoelectron. Optoelectron.*, **10**, 012504 (2016).

Carbon nanotube filling by inorganic compounds

L. G. Bulusheva^{1,2}, Yu. V. Fedoseeva^{1,2}, G. N. Chekhova¹, A. L. Chuvilin³, C.P. Ewels⁴, A.V. Okotrub^{1,2}

¹Nikolaev Institute of Inorganic Chemistry SB RAS, Novosibirsk 630090, Russia

²Novosibirsk State University, Novosibirsk 630090, Russia

³CIC nanoGUNE Consolider, Donostia-San Sebastian 20018, Spain

⁴Institut des Matériaux Jean Rouxel, CNRS-Université de Nantes, France

Corresponding author e-mail: bul@niic.nsc.ru

Carbon nanotubes (CNTs) having confined inner space protected by chemically resistant shells are promising for sorption, storage, and delivery of various compounds as well as carrying out specific reactions, which are difficult or impossible carried out in other conditions.

Here, we focus on processes of inclusion of mercury(II) chloride, cisplatin, and tetrachloroaurate hydrogen into CNTs. The first compound, HgCl_2 , is extremely toxic and bioaccumulating pollutant and search of the ways of its effective sorption is an important ecological task. The second compound, $\text{PtCl}_2(\text{NH}_3)_2$, is an anti-cancer drug, which should be deliver to certain place of a human body. The third compound, HAuCl_4 , is widely used for preparation of gold nanoparticles, which may find the use in catalysis and photonics. Before the filling, single-walled or multi-walled CNT (SWCNTs and MWCNTs) nanoreactors have been purified from catalytic particles and pre-opened via a heating in air. Melt-phase technique was used in the case of HgCl_2 , whereas $\text{PtCl}_2(\text{NH}_3)_2$ and HAuCl_4 were inserted from a solution. Efficiency of filling process and structure of inclusions in CNT cavities were analyzed by high-resolution transmission electron microscopy (HRTEM). Composition of the products of syntheses and changes in electronic structure of CNTs and inclusions as compared to that of initial components were determined using X-ray photoelectron spectroscopy (XPS) and near-edge X-ray absorption fine structure (NEXAFS) spectroscopy. The type of the doping of CNTs after the filling was evaluated from Raman scattering.

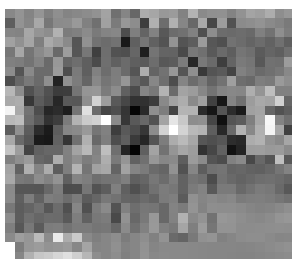


Fig. 1. HRTEM image of Hg_2Cl_2 @MWCNT

We show that CNTs easily absorb toxic mercury dichloride HgCl_2 , and guide its transformation into dimercury dichloride Hg_2Cl_2 in the cavity (Fig. 1). Simulations of high-resolution transmission electron microscopy images reveal alignment of the [001] direction of Hg_2Cl_2 nanocrystals with nanotube axis. The chemical state of host SWCNTs remains almost unchanged except for *p*-doping from the guest Hg_2Cl_2 nanocrystals. In the case of MWCNTs, the nanotube walls are chlorinated owing to interaction of realizing chlorine with the defects. The reduction of $\text{Hg}(\text{II})$ occurs owing to donation of electronic density from a CNT, which catalyses the interior redox reactions. Possible mechanisms of the reduction process are proposed from quantum-chemical calculations within density functional theory (DFT).

We found that a cage molecule curcubit[6]uril helps in inserting of $\text{PtCl}_2(\text{NH}_3)_2$ into SWCNT. DFT calculations reveal a confinement of the inner space of the curcubit[6]uril and size of cisplatin that provides an energy gain with hosting of $\text{PtCl}_2(\text{NH}_3)_2$ inside curcubit[6]uril molecule. That molecule has a suitable interaction with CNT wall thus carrying cisplatin into nanotube. An interaction of curcubit[6]uril with HAuCl_4 produces metallic nanoparticles, which size are controlled by the CNT interior. Comparison of XPS and Raman data for two filled samples detects that Au nanoparticles accept electron density from CNTs, while cisplatin@curcubit[6]uril system acts as an electron donor.

The work was partially supported by the Russian Foundation for Basic Research (grant 16-53-150003) and the FP7-PEOPLE-2013-IRSES #612577 (NanoCF) grant.

Enhancing the conductivity of single-walled carbon nanotubes films

Albert G. Nasibulin^{1,2}

¹ Skolkovo Institute of Science and Technology, Nobel str. 3, Moscow, Russia 143026

² Department of Applied Physics, Aalto University School of Science, Puumiehenkuja 2, 00076, Espoo, Finland

Corresponding author e-mail a.nasibulin@skoltech.ru

Single-walled carbon nanotube (SWCNT) films are a strong candidate for the replacement of commonly used transparent electrodes, such as indium-tin oxide (ITO), which have several drawbacks and depleted raw material supply. SWCNT networks have been demonstrated potential advantages in performance and fabrication cost reduction in comparison with ITO. Furthermore, high flexibility of the SWCNTs opens avenues beyond the ITO, i.e. creation of completely new components, urgently needed in the flexible, transparent and stretchable electronics.

We demonstrated an aerosol CVD process to dry-deposit large area SWCNT-networks with tuneable conductivity and optical transmittance on wide range of substrates including flexible polymers [1-2]. These SWCNT-networks can be chemically doped to approach the ITO performance [3-5]. Wide application potential of our SWCNT films is demonstrated by successful applications in the field effect transistors, photovoltaic devices, and supercapacitors. [6-8].

[1] Nasibulin, A. G., Moisala, A., Brown, D. P., Jiang, H. and Kauppinen, E.I., Chemical Physics Letters 402, 227 – 232 (2005).

[2] Kaskela, A., Nasibulin, A.G., Zavodchikova, M., Aitchison, B., Papadimitratos, A., Tian, Y., Zhu, Z., Jiang, H., Brown, D.P., Zakhidov, A., and Kauppinen, E.I., **10**, 4349 (2010).

[3] Nasibulin, A. G., Kaskela, A. O., Mustonen, K., Anisimov, A. S., Ruiz, V., Kivistö, S., Rackauskas, S., Timmermans, M. Y., Pudas, M., Aitchison, B., Kauppinen, M., Brown, D. P., Okhotnikov, O. G., Kauppinen, E. I., ACS Nano 5, 3214-3221 (2011).

[4] Mustonen, K., Laiho, P., Kaskela, A., Susi, T., Nasibulin A.G. and Kauppinen, E.I. (2015) Applied Physics Letters 107, 143113.

[5] Gorkina, A. L., Tsapenko, A. P., E. P. Gilshteyn, T. S. Koltsova, Tatiana V. Larionova, A. Talyzin, A. S. Anisimov, I. V. Anoshkin, E. I. Kauppinen, O. V. Tolochko, A. G. Nasibulin, Carbon 100, 501 (2016).

[6] Sun, D-M., Timmermans, M.Y., Kaskela, A., Nasibulin, A.G., Kishimoto, S., Mizutani, T., Kauppinen, E.I., and Ohno, Y., Mouldable all-carbon integrated circuits, Nature Communications 4, 2302 (2013).

[7] Cui, K., Anisimov, A.S., Chiba, T., Fujii, S., Kataura, H., Nasibulin, A., Chiashi, S., Kauppinen, E., and Maruyama, S., Air-Stable High-Efficiency Solar Cells with Dry-Transferred Single-Walled Carbon Nanotube Films, Journal of Materials Chemistry A 2, 11311 (2014).

[8] Gilshteyn, E. P., Kallio, T., Kanninen, P., Fedorovskaya, E. O. Anisimov, A. S., Nasibulin, A. G. RSC Adv., 6, 93915 (2016).

Nonlinear optics of excitons in transition metal dichalcogenides monolayers

M.M. Glazov¹, L.E. Golub¹, G. Wang², X. Marie², T. Amand², B. Urbaszek²

¹*Ioffe Institute, 194021, St.-Petersburg, Russia*

²*Universite de Toulouse, INSA-CNRS-UPS, LPCNO, 31077 Toulouse, France*
glazov@coherent.ioffe.ru

Monolayers of transition metal dichalcogenides (TMDs) with MoS₂ and WSe₂ being the most prominent examples are actively studied nowadays due to prospects for creation of van der Waals heterostructures, where layers of different materials can be isolated and then assembled in a tailored sequence [1]. TMD monolayers have, like graphene, a hexagonal lattice and a hexagonal Brillouin zone with two valleys at the K_+ and K_- zone edges. However, unlike graphene, TMD monolayers are semiconductors with the band gap the K_+ and K_- point of about 2 eV. These materials demonstrate remarkable optical properties controlled by the robust excitons, Coulomb-correlated electron-hole pairs, with the binding energies on the order of several hundreds millieV [2,3]. High binding energies are related with relatively large carrier effective masses and weak screening. For the same reasons, the exchange interaction between the electron and the hole is enhanced by orders of magnitude as compared with conventional III-V or II-VI quantum wells [4].

Typically, in semiconductors, Wannier-Mott excitons form a series of $1s, 2s, 2p, \dots$ hydrogen-like states. In TMD monolayers the binding energies of the excitonic states strongly differ from the two-dimensional hydrogen atom model. This difference is mainly caused by the unusual screening of the Coulomb interaction since the polarizability of the monolayer exceeds by far the polarizability of the surrounding media [3].

The excited excitonic states play an important role in the nonlinear optical properties such as two-photon absorption and second harmonic generation. Here we present the results of theoretical and experimental studies of the fine structure of the excited excitonic states, mainly focusing on s -shell and p -shell states. We also address the nonlinear optics of TMD monolayers, including second order nonlinearity responsible for the second harmonic generation and the third order nonlinearity responsible for the two-photon absorption [5,6].

We demonstrate that p - and s -shell excitons are mixed due to the specific D_{3h} point symmetry of the TMD monolayers. The microscopic model of the mixing is developed within the kp -perturbation theory. It is shown that both long- and short-range parts of the electron-hole exchange interaction provide the mixing. Hence, both s - and p -shell excitons are simultaneously active in single- and two-photon processes providing an efficient mechanism of the second harmonic generation. It is shown that the linear in the wavevector terms in the interband optical matrix elements are allowed in TMD monolayers. These terms are evaluated and shown to contribute to the nonlinear response of TMD monolayers as well. The nonlinear susceptibility responsible for the second harmonic generation is calculated. In agreement with experiment we observe giant enhancement of the second harmonic generation efficiency at the excitonic states. The theory is further compared with experiment in terms of relative strengths of the response at various excitonic states. The experimental observation that the dominant contribution to the nonlinear susceptibility is provided by the ground, $1s$, exciton state allows us to conclude that the main mechanism of the second order response is provided by the linear in the wavevector terms in the interband optical matrix element.

[1] A. K. Geim and I. V. Grigorieva, *Nature* **499**, 419 (2013).

[2] K. F. Mak, K. He, C. Lee, G. H. Lee, J. Hone, T. F. Heinz, and J. Shan, *Nature Mater.* **12**, 207 (2013).

[3] A. Chernikov, T. C. Berkelbach, H. M. Hill, A. Rigosi, Y. Li, O. B. Aslan, D. R. Reichman, M. S. Hybertsen, and T. F. Heinz, *Phys. Rev. Lett.* **113**, 076802 (2014).

[4] M. M. Glazov, T. Amand, X. Marie, D. Lagarde, L. Bouet, and B. Urbaszek, *Phys. Rev. B* **89**, 201302(R) (2014).

[5] G. Wang, X. Marie, I. Gerber, T. Amand, D. Lagarde, L. Bouet, M. Vidal, A. Balocchi, and B. Urbaszek, *Phys. Rev. Lett.* **114**, 097403 (2015).

[6] M. M. Glazov, L. E. Golub, G. Wang, X. Marie, T. Amand, B. Urbaszek, arXiv:1610.06780 (2016)

Electronic and optical properties of lithium doped graphene nanoribbons

Alexander Gruneis

*Physical Institute University of Cologne, Zùlpicher Str. 77, 50937 Cologne
Germany*

We perform a spectroscopic characterization of chemically functionalized graphene nanoribbons (GNRs) with a width of $N=7$ atoms using angle-resolved photoemission spectroscopy (ARPES) and ultra-high vacuum (UHV) Raman and photoluminescence. ARPES of Li doped GNRs shows a quasiparticle band gap renormalization from 2.4 eV to 2.1 eV and an increase in the effective mass of the conduction band carriers by a factor of four [1]. Using a UHV-Raman system, it is shown that Li doping also reduces the Raman intensity by one order of magnitude, and results in phonon energy shifts, suggesting the importance of lattice expansion and dynamic effects.

Incorporation into optoelectronic devices requires the alignment-preserving transfer of parallel GNRs onto insulating substrates. Here, the bubbling transfer is applied and the photophysics of such samples characterized by polarized Raman and photoluminescence spectroscopies. The Raman scattered light and the photoluminescence are polarized along the nanoribbon axis. The Raman cross section as a function of excitation energy has distinct excitonic peaks associated with transitions between the one-dimensional parabolic subbands. Photoluminescence of GNRs is intrinsically low but can be strongly enhanced by hydrogenation which causes the formation of sp^3 defects. In-situ measurements of the photoluminescence during the hydrogenation suggests a peculiar dependence of the photoluminescence intensity on the H/C stoichiometry.

[1] Senkovskiy et al. Adv. Electr. Materials (2017) at press.

Charge Transport in carbon Nanotube Films Studied by Terahertz Spectroscopy

B.P. Gorshunov^{1,2*}, E.S. Zhukova^{1,2}, J.S.Starovatykh¹, M.A. Belyanchikov¹, A. Grebenko¹, A. Bubis¹,
A.S.Prokhorov^{1,2}, V.I. Tsebro⁴, A.A. Tonkikh², D.V. Rybkovskiy², E.I. Kauppinen⁵, A.G.Nasibulin^{3,5,6},
and E.D. Obraztsova²

¹Moscow Institute of Physics and Technology, Dolgoprudny, Moscow Region, 141700 Russia

²A.M. Prokhorov General Physics Institute, RAS, Moscow, 119991 Russia

³Skolkovo Institute of Science and Technology, Nobel str. 3, 143026, Moscow, Russia

⁴P.N. Lebedev Physical Institute, RAS, 53 Leninsky Prospect, 119991 Moscow, Russia

⁵Department of Applied Physics, Aalto University, School of Science, P.O. Box 15100, FI-00076 Espoo, Finland

⁶National University of Science and Technology "MISIS", Leninsky Ave, 4, Moscow, 119049, Russia

*Corresponding author: bpgorshunov@gmail.com

Electrical transport mechanisms of 2D carbon nanotube networks are presently under intensive studies. However, related experimental data still remain ambiguous and controversial. We report on terahertz-infrared spectra of optical conductivity and dielectric permittivity of thin transparent macro-scale free-standing films

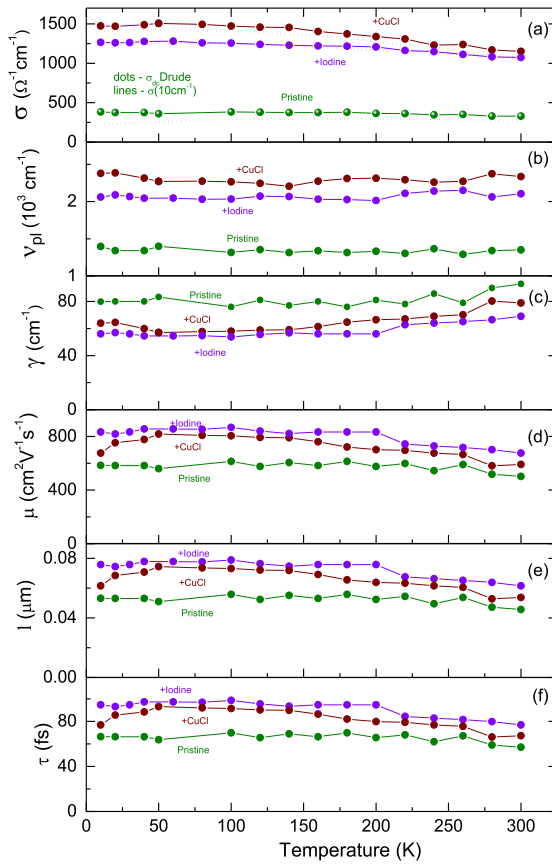


Fig.1. Temperature dependencies of effective parameters of charge carriers of pristine, CuCl- and iodine-doped SWCNT films determined by processing the spectra within the framework of the Drude conductivity model. (a). Dc conductivity (dots) and conductivity at a frequency of 10 cm⁻¹ (dashed lines). (b). Plasma frequency. (c). Scattering rate. (d). Mobility. (e). Mean-free path. (f). Collision time. For the calculations the Fermi velocity was taken as $v_F=8 \cdot 10^7$ cm s⁻¹) and the effective mass as $m^*=0.2 m_e$, where m_e is the free electron mass.

composed of pristine and CuCl- and iodine-doped single-walled carbon nanotubes (SWCNTs) measured in the frequency range from 7 to 25 000 cm⁻¹ and at temperatures from 5 to 300 K. Controversially to the existing results, we did not observe clearly the so-called terahertz conductivity peak. Instead, typical metallic frequency and temperature behavior of the conductivity and dielectric permittivity was discovered at terahertz frequencies and attributed to the high quality interconnected SWCNT network providing free pathways for charge carriers. Applying Drude conductivity model, we determined temperature and doping dependences of effective parameters of the carriers in the films: plasma frequency, scattering rate, scattering time, mobility, mean-free path (Fig.1). In pristine films, clear signatures of the tunnel gap are detected that governs the dc and the ac transport at low temperatures (below 100-150 K). The obtained results demonstrated a great potential of the material in the field of electromagnetic applications at frequencies up to few terahertz. We show that the terahertz-infrared spectroscopy is an effective contactless technique that allows to study microscopic transport mechanisms in carbon nanotube layers.

The work was supported by the Russian Ministry of Education and Science (Program ‘5stop100’) and RSF project 15-12-30041”Formation of films of filled single-wall carbon nanotubes”; part of the experiments we performed at the MIPT Center of Collective Usage. We acknowledge fruitful discussions with S.Tretiak, G.Fedorov, M.Shuba and the assistance of Z.V.Gagkaeva and L.S.Kadyrov in spectroscopic measurements.

High Quality Carbon Nanotube-Amorphous Silicon heterojunction solar cells

Pramod M Rajanna¹, Alena Alekseeva¹, Danila S Saranin², Sergei Bereznev³, Oleg Sergeev⁴, Albert G Nasibulin¹

1. Skolkovo Institute of Science and Technology, Skolkovo Innovation Center, Building 3, Moscow 143026, Russia

2. MISIS, Leninsky Ave 4, Moscow 119049, Russia

3. Tallinn University of Technology, Ehitajate tee 5, 19086 Tallinn, Estonia

4. NEXT ENERGY EWE-Forschungszentrum für Energietechnologie e. V., Carl-von-Ossietzky-Straße 15, 26129 Oldenburg, Germany

Corresponding Author: Pramod M Rajanna pramod.mulbagal@skolkovotech.ru

Solar photovoltaic (PV) devices, or solar cells are a promising way to convert sunlight to electricity, the photovoltaic effect, has always fascinated scientists. The objective of the people involved in this field are threefold: (1) to improve the power conversion efficiency of the devices (2) to develop processes for lower production costs (3) to ensure that module performance is maintained for several decades in outdoor conditions, thereby providing more energy than used in production.

Until now, in the solar PV market, many different technologies exist, each with a different price and performance trade off. Crystalline silicon (c-Si) technology, has been dominant with nearly 80% market share, yielding record efficiency of ~25% [1-3]. However, there are some drawbacks like limited availability of the Si feedstock, high production costs, and long energy payback time.

Several approaches have been proposed to reduce the cost like compromise on the efficiency and use of cheaper materials to achieve substantial reduction in costs like CdTe, CIGS and a-Si. Additionally, many types of organic-based solar cells have been proposed. However, efficiency of these devices is too low and their reliability is very limited [4].

However, in the last few decades, nanomaterials and nanotechnologies have made dramatic contributions to the development of solar cells due to their low material usage and tunable structure at the nanoscale. Moreover, recent advances and breakthroughs in carbon materials have enabled them to be frontrunners in several devices. Especially in the case of PV devices, the family of carbon nanomaterials has advantages in terms of flexibility, surface area, carrier mobility, chemical stability, and optoelectronic properties. This fulfills the requirement of heterojunction based solar cells. Several studies have been reported with C-Si and carbon nanomaterials as heterojunction solar cells with photo conversion efficiencies of about 15% [5]. But, owing to the complexity of problems for C-Si based devices as aforementioned, an attractive alternative is hydrogenated amorphous silicon (a-Si:H) which can be deposited as thin film at very low temperatures ~150 deg C with advanced deposition techniques & process technology [6].

In this work we demonstrate that a-Si:H and high quality pristine single walled carbon nanotubes (SWCNT) can form very good C/a-Si heterojunction solar cells. The novelty of the work involved is in the very low energy consuming process technology for fabrication of C/a-Si heterojunction with stable efficiency of >6% and high open-circuit voltage exceeding 750mV.

2. Acknowledgement.

This research was supported by the Ministry of Education and Science of the Russian Federation (project identifier RFMEFI58114X0006).

3. References

- [1] Masuko K, Shigematsu M, Hashiguchi T, Fujishima D, Kai M, Yoshimura N, Yamaguchi T, Ichihashi Y, Yamanishi T, Takahama T, Taguchi M, Maruyama E, Okamoto S. Achievement of more than 25% conversion efficiency with crystalline silicon heterojunction solar cell. *IEEE Journal of Photovoltaics* 2014; 4: 1433–1435.
- [2] Zhao J, Wang A, Green MA, Ferrazza F. Novel 19.8% efficient “honeycomb” textured multicrystalline and 24.4% monocrystalline silicon solar cells. *Applied Physics Letters* 1998; 73: 1991–1993.
- [3] Yamamoto K, 25.1% efficiency Cu metallized heterojunction crystalline Si solar cell. 25th International Photovoltaic Science and Engineering Conference, Busan, Korea, November 2015.
- [4] M. Jorgensen, K. Norrman, S. A. Gevorgyan, T. Tromholt, B. Andreasen and F. C. Krebs, *Adv. Mater.*, 2012, 24, 580–612.
- [5] N. S. Lewis, *Science* 2007, 315, 798.
- [6] Matsui T, Sai H, Suezaki T, Matsumoto M, Saito K, Yoshida I, Kondo M. Development of highly stable and efficient amorphous silicon based solar cells. *Proc. 28th European Photovoltaic Solar Energy Conference*, 2013; 2213–2217.

Circular polarization control with metallic artificial structures

Kuniaki Konishi

*Institute for Photon Science and Technology, The University of Tokyo, Hongo, Bunkyo-ku, Tokyo, 113-0033, Japan
kkonishi@ipst.s.u-tokyo.ac.jp*

Circularly polarized light (CPL) sources are important for a variety of applications, such as circular dichroism spectroscopy, spin state control in quantum information technology and ultrafast magnetization control. Metallic artificial structures, or Metamaterials, are promising candidates to develop novel devices with a lot of flexibility in their design for CPL control. The symmetry of a material plays a crucial role in polarization sensitive optical phenomena; therefore it is necessary to employ metamaterials with appropriate symmetries to achieve proper circular polarization control. We have studied the effect of circular polarization in planar chiral metamaterials for controlling linear circular polarization, and triangle-arrayed metamaterials for controlling nonlinear circular polarization. In this presentation, we show the recent progress of our research related to these topics.

We have found that planar chiral metamaterials exhibit strong optical activity [1], and clarified that the origin of the enhanced polarization effect is the plasmonic resonance [2,3]. We have also developed several new applications for this structure, including polarization control in the terahertz (THz) frequency region [4,5,6]. Recently, we have developed a new THz polarization control device employing enantiomeric handedness switching of chiral metamaterial realized by MEMS technology [7]. In the THz regime where polarization devices are still lacking, the presented device can for example be used to create a simple and practical polarization-modulated THz imaging system when combined with other new types of THz devices, such as the THz camera [8].

Nonlinear processes forbidden in homogeneous media can be allowed in metamaterials, thereby offering a unique opportunity to study the interplay between the shapes and mutual arrangements of individual nanoentities. This is especially important for second-order nonlinear optical phenomena and second-harmonic generation in arrays of metal nanoparticles, and has accordingly been investigated extensively [9]. We have demonstrated that triangle-arrayed metallic periodic structures, which are achiral nanostructures with threefold rotational symmetry, exhibit a unique polarization effect in a second-order nonlinear process: a circularly polarized fundamental beam produces a counter-circularly polarized second-harmonic beam [10]. The presented relationships between polarization selection rules and rotational symmetries of nanostructures are of importance for developing wavelength-conversion devices that function in wavelength regions where other methods of polarization control are unavailable.

References

- [1] M. Kuwata-Gonokami Makoto Kuwata-Gonokami, N. Saito, Y. Ino, M. Kauranen, K. Jefimovs, T. Vallius, J. Turunen and Y. Svirko, *Phys. Rev. Lett.*, **95**, 227401 (2005).
- [2] K. Konishi, T. Sugimoto, B. Bai, Y. Svirko and M. Kuwata-Gonokami, *Opt. Express*, **15**, 9575 (2007).
- [3] K. Konishi, B. Bai, Y. Toya, Jari Turunen, Y. Svirko and M. Kuwata-Gonokami, *Opt. Lett.*, **37**, 4446 (2012).
- [4] N. Kanda, K. Konishi and M. Kuwata-Gonokami, *Opt. Express*, **15**, 11117 (2007).
- [5] N. Kanda, K. Konishi and M. Kuwata-Gonokami, *Opt. Lett.*, **34**, 3000 (2009).
- [6] N. Kanda, K. Konishi and M. Kuwata-Gonokami, *Opt. Lett.*, **39**, 3274 (2014).
- [7] T. Kan A. Isozaki, N. Kanda, N. Nemoto, K. Konishi, M. Kuwata-Gonokami, K. Matsumoto and I. Shimoyama, *Appl. Phys. Lett.*, **102**, 221906 (2013).
- [8] T. Kan, A. Isozaki, N. Kanda, N. Nemoto, K. Konishi, H. Takahashi, M. Kuwata-Gonokami, K. Matsumoto and I. Shimoyama, *Nature Commun.*, **6**, 8422 (2015).
- [9] N. Nemoto, N. Kanda, R. Imai, K. Konishi, M. Miyoshi, S. Kurashina, T. Sasaki, N. Oda and M. Kuwata-Gonokami, *IEEE Trans. THz Sci. Technol.*, **6**, 175 (2016).
- [10] M. Kauranen and A. V. Zayats, *Nature photon.*, **6**, 737 (2012).
- [11] K. Konishi, T. Higuchi, J. Li, J. Larsson, S. Ishii, and M. Kuwata-Gonokami, *Phys. Rev. Lett.*, **112**, 135502 (2014).

Carbon nanotube based composites in periodic structures: electromagnetic properties and band structure in microwaves

D. Bychanok^{1,2,a}, K. Piasotski¹, D. Meisak¹, G. Gorokhov¹, P. Kuzhir^{1,2}

¹*Institute for Nuclear Problem of Belarus State University, Belarus*

²*Ryazan State Radio Engineering University, Russia*

^a*dzmitrybychanok@ya.ru*

In the recent decade, advances in the area of electromagnetic materials have demonstrated great potential for technological use of electromagnetic metamaterials. The ability to shape precisely their individual elements, meta-atoms, offers a great advantage for not only controlling their individual response but also allowing the design of collective (or effective) response of the whole material, which may not be achieved by individual elements. Furthermore, it was shown that by designing the overall structure of the metamaterial it is possible to create materials with entirely new properties, e.g. with graded refractive index.

The periodic structures with space-dependent refractive index are well known and widely used in optics [1,2]. The idea of present communication is to fabricate and investigate the electromagnetic properties of periodic, lossy, multi-walled carbon nanotubes (MWCNT) – based structures in Ka-band (26-37 GHz).

MWCNTs [3] produced by CVD technique [4] were used as conductive fillers (1 wt.%) in epoxy composites. The fabrication details can be found elsewhere [5,6]. The samples were prepared in form of plane-parallel plates. The MWCNT-content in investigated materials was above percolation threshold and the samples were macroscopically conductive. To form periodic structure the MWCNT-based composites were stacked layer by layer and separated with non-conductive polymer.

The electromagnetic properties of obtained periodic structures based on nanocarbon composite materials were investigated both experimentally and theoretically. Experimentally observed electromagnetic response of investigated samples in Ka-band was similar to the typical stepwise behavior of “artificial plasma” materials [7], or photonic crystals.

To model the electromagnetic properties, the long-wave approximation and matrix-method described in detail in our recent papers [8,9] were used. Additionally the plane wave expansion method [10] for theoretical calculations of band diagrams inherent to obtained periodic structures was utilized.

The work is supported by Federal Focus programme of Ministry of Education and Science of Russian Federation, project ID RFMEFI57715X0186.

[1] A. Paddubskaya et al., J. Appl. Phys. **119**, 135102 (2016).

[2] K. Batrakov et al., Sci Rep.; **4**: 7191 (2014).

[3] <http://nano.bsu.by/products/mwcnt>

[4] A. Okotrub et al, Nanotechnologies in Russia **3**, 191200 (2008).

[5] S. Bellucci et al, Journal of Nanoscience and Nanotechnology, **11**, 9110-9117, (2011).

[6] D. Bychanok et al., Journal of Applied Physics, **113**, 124103-6 (2013).

[7] A. Sánchez ; S. Orozco, Proceedings of International Conference on Electromagnetics in Advanced Applications (ICEAA), Turin, 1325-1328 (2015).

[8] D. Bychanok et al., Applied Physics Letters, **108**, 013701, (2016).

[9] D.S. Bychanok et al. Technical Physics, **61**, No. 12, 1890–1894 (2016).

[10] A. J. Danner An introduction to the plane wave expansion method for calculating photonic crystal band diagrams, University of Illinois (2002).

Wednesday, March 22



©M.Rybin

High Electron Mobility, Quantum Hall Effect and Anomalous Optical Response in Atomically Thin InSe

D. A. Bandurin¹, A. V. Tyurnina^{2, 3}, Y. Cao^{1, 2}, A. Mishchenko¹, V. Zólyomi², I. V. Grigorieva¹,
V. I. Fal'ko^{1,2}, A. K. Geim¹

¹*School of Physics & Astronomy, University of Manchester, Oxford Road, Manchester M13 9PL, United Kingdom*

²*National Graphene Institute, University of Manchester, Manchester M13 9PL, United Kingdom*

³*Skolkovo Institute of Science and Technology, Nobel St 3, 143026 Moscow, Russia*

denis.bandurin@manchester.ac.uk

Since the first isolation of graphene there have been intensive search for new 2D materials but so far only two decent competitors to graphene have emerged. These are few-layer dichalcogenides such as MoS₂ and WSe₂ and multilayer black phosphorous. 2D dichalcogenides have proven to be highly stable and, after long efforts, low-temperature mobilities of about 10,000 cm²/Vs were achieved for 6-10 layer devices [1], [2]. Unfortunately, it is notoriously difficult to make good electric contacts to 2D dichalcogenides. For example, no quantum Hall effect was so far observed in any of them. In addition, their intrinsic (phonon-limited) mobility at room temperature is only about 100 cm²/Vs, which limits potential applications. On the other hand, 2D black phosphorous [3] promises much higher mobility of 1,000 cm²/Vs at room temperature but is so poorly stable under ambient conditions that most research has been done so far on a near-surface gas in essentially bulk crystals rather than on true 2D crystals. Even for such thick samples, a mobility of 6,000 cm²/Vs was achieved only recently allowing the observation of the quantum Hall effect in the near-surface hole gas.

In this talk we will report the electronic and optical properties in few-layer InSe, Fig. 1a. This 2D material is already known to be relatively stable under ambient conditions so that previously it was possible to do optical studies of few-layer flakes despite their degradation. To avoid working with partially decomposed samples and make working electronic rather than only optical devices, we encapsulated few-layer InSe in an inert atmosphere, Fig. 1b. This allowed room-temperature mobilities of about 1,000 cm²/Vs and low-temperature ones >12,000 cm²/Vs. The quantum Hall effect was clearly observed in such devices, Fig. 1c. [4]. Their optical properties turned out to be nontrivial, too. For example, main-gap luminescence in monolayer InSe is totally absent for fundamental reasons, contrary to a previous report on decomposed InSe. Our work will lead to high follow-up interest, and we would not be surprised if researchers currently dealing with 2D dichalcogenides and black phosphorous will soon switch their attention to the new kid on the block.



Fig. 1. a, Schematic representation of the monolayer and bilayer InSe crystal structures. Purple and red spheres correspond to indium and selenium atoms, respectively. **b**, Optical micrograph of an InSe device. **c**, Quantum Hall effect in the InSe device as a function of back-gate voltage.

References

- [1] X. Cui et. al Nat. Nanotechnol. **10**, 534 (2015).
- [2] B. Fallahazad et. al. Phys. Rev. Lett. **116**, 086601 (2016).
- [3] L. Li et al. Nat. Nanotechnol. (2016).
- [4] D. A. Bandurin et. al., Nat. Nanotech. (2016).

Terahertz Radiation Induced Photocurrents in Topological Insulators

Vasily Bel'kov

Ioffe Institute, Polytechnicheskaya str. 26, St. Petersburg, 194021 Russia

E-mail: bel@epi.ioffe.ru

We report on the observation of photogalvanic effects in epitaxially grown Sb_2Te_3 and Bi_2Te_3 as well as HgTe-based three-dimensional topological insulators. It was shown that asymmetric scattering of Dirac fermions driven back and forth by the terahertz electric field results in a *dc* electric current caused by the linear photogalvanic effect. The effect is forbidden in the bulk of centrosymmetric Sb_2Te_3 and Bi_2Te_3 . Because of the "symmetry filtration" in these materials the *dc* current is generated in the surface states only. Polarization, frequency and temperature dependences of the photocurrent were studied and analyzed.

The effect provides an optoelectronic access to characterize three-dimensional topological insulators. Indeed being sensitive to the surface symmetry and scattering details the photogalvanic effect allows one to study the high frequency conductivity of the surface states and homogeneity of sample surfaces. In particular, measuring the polarization dependence of the photogalvanic current and scanning a terahertz laser beam spot across the sample is capable of mapping of the electronic properties of the surface states and the local domain orientation. An important advantage of the proposed method is that it can be applied to study topological insulators at room temperature

Under certain experimental conditions *dc* photocurrent generation is driven by the trigonal photon drag effect. It arises due to the dynamical momentum alignment by time- and space-dependent radiation electric field and implies the radiation-induced asymmetric scattering in the electron momentum space. The effect was investigated in both *n* and *p*-type $(\text{Bi}_{1-x}\text{Sb}_x)_2\text{Te}_3$ three-dimensional topological insulators with different antimony concentrations *x*.

In three-dimensional topological insulators based on 80-nm strained HgTe films cyclotron-resonance-induced photocurrents excited by terahertz radiation have been detected and investigated. The data enable us to extract the electron mobility and the cyclotron mass as a function of the Fermi energy. Analysis of the photocurrent in gated topological insulator samples provides a sensitive method to probe the cyclotron masses and the mobility of two-dimensional Dirac surface states, when the Fermi level lies in the bulk energy gap or even in the conduction band.

The origin of the observed photogalvanic effects is discussed in terms of asymmetric scattering of topological insulator surface carriers in the momentum space.

Optically Induced Terahertz Emission from 3D Topological Insulators

**Petr. A. Obraztsov¹; Pavel A. Chizhov¹, Oleg E. Tereshenko²,
Konstantin A. Kokh³, Natsuki Nemoto⁴, Kuniaki Konishi⁴**

¹*A.M. Prokhorov General Physics Institute, RAS, Moscow, Russia*

²*Rzhanov Institute of Semiconductor Physics, SB RAS, Novosibirsk, Russia*

³*V.S. Sobolev Institute of Geology and Mineralogy, SB RAS, Novosibirsk, Russia*

⁴*Institute for Photon Science and Technology, University of Tokyo, Tokyo Japan*

We report experimental observation of terahertz emission from bulk crystals and epitaxial films of three-dimensional topological insulators Bi₂Se₃ and Bi₂Te₃ under excitation with femtosecond laser pulses in visible and near-IR spectral range. The excitation of any surface of the 3D topological insulator with obliquely incident arbitrary polarized femtosecond laser pulses induces THz response, which depends on the polarization state and incidence angle of the excitation light. The performed polarization sensitive measurements suggest separate contributions from bulk and surface of TI crystal to the THz generation process. The bulk contribution does not feel the polarization state of the incidence light and decreases with reducing the topological insulator crystal thickness. The surface contribution, on the contrary, is extremely sensitive to the excitation light helicity and linear polarization rotation due to unusual band structure of topological insulator surface. The topologically protected surface states cause very pronounced polarization dependence in agreement with the recent theoretical and experimental studies on light induced spin and electron currents in materials having Dirac-cone band structure. Moreover we demonstrate that 3D TI provide a possibility to control the transient behavior of induced surface photocurrents on ultrafast time scale purely with light polarization and therefore control the polarization of emitted THz radiation.

Local Electronic Confinement in Covalent Graphene Derivatives and its Impact on the Corresponding Raman Response

Vojislav Krstić*, Maria Kolečnik-Gray

Department of Physics, Friedrich-Alexander-Universität Erlangen-Nürnberg (FAU), Staudtstraße 7, 91058 Erlangen, Germany

*corresponding author: vojislav.krstic@fau.de

Covalent functionalization of graphene is a continuously progressing field of research. The optical properties of such derivatives attract particular attention. In virtually all optical responses, however, an enhancement in peak intensity with increase of sp^3 carbon content is observed.

To elucidate this general phenomenon we present a phenomenological model [1] which takes into account the circumstance that upon covalent functionalization confined π -conjugated domains surrounded by sp^3 carbon regions in graphene monolayers are formed. [2,3] In particular, such confined regions are known to lead to an additional quantization of the local electronic spectrum giving rise to photoluminescent activity.

Our model incorporates the modulation of the Raman intensities through the photoluminescence active regions and correlates the individual D- and G-mode intensities to the degree of functionalization.

Through this, evaluations of Raman spectra of covalently functionalized graphene using our model also circumvent the ambiguities and information loss encountered in evaluations in the degree of functionalization using the ratio of D- and G-mode intensities. To underpin our model, we carried out experiments [1] employing Raman spectroscopy and an *in situ* electrostatic doping technique (Fig. 1).



Fig.1. Schematic set-up for *in situ* electrostatic doping of a graphene(oxide) monolayer during Raman measurements using light of energy $h\nu$ for excitation of the Raman modes.

Acknowledgement

Financial support is acknowledged from the Deutsche Forschungsgemeinschaft (DFG-SFB 953 “Synthetic Carbon Allotropes”, A1, B12), the European Research Council (ERC grant no. 259286), the grant no. EI 938/3-1, and the Graduate School Molecular Science (GSMS). The research leading to these results has received partial funding from the European Union Seventh Framework Programme under grant agreement no. 604391 Graphene Flagship.

References

- [1] P. Vecera, S. Eigler*, M. Kolečnik-Gray, V. Krstić*, A. Vierck, J. Maultzsch, R. A. Schäfer, F. Hauke, A. Hirsch*;
*corresponding authors, *submitted*
- [2] J. Robertson, E.P. O'Reilly, *Phys. Rev. B* **35**, 2946-2957 (1987).
- [3] F. Demicheli, S. Schreiter, A. Tagliaferro, *Phys. Rev. B* **51**, 2143-2147 (1995).

Optical Characterization and Kinetics of Photoinduced Carriers of 2D Transition Metal Dichalcogenides

ED. Mishina, S.D. Lavrov, A.P. Shestakova, V.G. Morozov

*Moscow Technological University (MIREA), Vernadsky ave. 78, 119454 Moscow, Russia
mishina_elena57@mail.ru*

1. Introduction

Monolayers of transition metal dichalcogenides (TMD), such as MoS₂, WS₂, MoSe₂, WSe₂ are direct bandgap semiconductors. This fact provides their unique properties and makes them very well fitting complements to graphene. Several optoelectronic devices were suggested and assembled using TMD/graphene heterostructures such as phototransistors [1] and field-effect transistors [2]. Carrier dynamics is one of the most important properties in semiconductor devices, such as high electron mobility transistor and field-effect transistor, both of which are capable for realizing terahertz ultrahigh-speed operation.

In this paper we report the methodology of optical characterization of TMD monolayers and results of such characterization. For WSe₂ monolayers transient reflectivity is measured in an optical pump-probe experiment providing information about carrier dynamics. The model is suggested to describe the obtained results based on the method of nonequilibrium statistical operator for the case of strong photoexcitation (degenerated plasma).

2. Results

The monolayers (MLs) of WSe₂ were obtained by the mechanical exfoliation from the bulk layered crystals onto on pre-cleaned annealed SiO₂(285nm)/Si substrate. Optical characterization implies the following steps: visualization by reflection microscopy; crystallographic structure, symmetry and edge defects determination by second harmonic generation (SHG) microscopy; monolayer identification by photoluminescence (additionally the thickness can be checked by atomic force microscopy (AFM)). Visualization of the thin layers is based on the optical properties of high refractive index layer (TMD) on top of Fabry-Perot cavity, the thickness of SiO₂ layer is chosen in order to provide minimal reflectivity accompanied by maximal contrast. However, it is not possible by this method to distinguish between 1-3 MLs. The latter can be achieved by photoluminescence (PL) microscopy on wavelength of excitonic resonance. Due to exponential dependence of PL intensity on the thickness, only ML flakes will be seen as bright spots, the method is proved to be even more precise than conventional AFM. SHG microscopy controls the quality of the flakes (it is also quite useful for large area CVD layers due to their polycrystallinity), in particular edge effects, consisting in increasing or decreasing SHG intensity at the edges due to higher concentration of defects, including absorption of extrinsic molecules [3].

To measure the relaxation time for hot photocarriers in monolayer, the two-color pump-probe experiment was performed at room temperature using the amplified Ti-sapphire laser and frequency doubler with the wavelengths of 800 and 400 nm and pulse widths of 50 and 150 fs for the probe and pump beams, respectively. The pump fluence equals to 2 mJ/cm², which provides the two-dimensional carrier density equals to 10¹⁴ cm⁻². The differential reflectivity of a WSe₂ monolayer was obtained and fitted within the two-time relaxation model which is commonly used for direct band semiconductors [9]. The resulting values of the relaxation times are $\tau_1 \approx (0.67 \pm 0.02)$ ps and $\tau_2 \approx (57 \pm 2)$ ps. τ_1 can be identified with the carrier-phonon relaxation time, τ_2 with carrier recombination.

We formulate a microscopic model describing interaction between photo-injected carriers and optical phonons in mono layer TMDs. The model takes account of the spin-valley structure of the conduction and valence bands. The evolution equations for the carrier and phonon quasi-temperatures are derived and the carrier-phonon relaxation time is estimated. For carrier density taken from the experiment we obtained the value of relaxation time 1 ps. It is of the same order of magnitude as carrier-phonon relaxation times for many other highly photoexcited polar semiconductors [4] and quite close to the value of τ_1 obtained in our experiments.

3. Acknowledgement.

The work is supported by Russian Science Foundation, (Grant 14-12-01080) and Ministry of Education and Science (State task for the Universities).

4. References

- [1] W. Zhang, Chih-Piao Chuu, Jing-Kai Huang, et al, Scientific Reports **4**, 3826 (2014)
- [2] H. Du, T. Kim, S. Shin, et al, Appl. Phys. Lett. **107**, 233106 (2015)
- [3] E. Mishina, N. Sherstyuk, A. Shestakova, et al, Semiconductors **49**, 791 (2015)
- [4] V.G. Morozov, C. Dekeyser, N. Ilyin, E. Mishina, Solid St. Commun **251**, 32 (2017)

Molybdenum disulphide composite materials for energy applications

Victor O. Koroteev^{*1,2}, A.A. Kotsun^{1,2}, D.A. Bulushev^{2,3}, A.L. Chuvilin^{4,5}, L.G. Bulusheva^{1,2},
A.V. Okotrub^{1,2}

¹Nikolaev Institute of Inorganic Chemistry, SB RAS, 3 Acad. Lavrentiev ave., 630090 Novosibirsk, Russia

²Novosibirsk State University, 2 Pirogov str., 630090 Novosibirsk, Russia

³Borisev Institute of Catalysis, SB RAS, 5 Acad. Lavrentiev ave., 630090 Novosibirsk, Russia

⁴CIC nanoGUNE Consolider, E-20018 San Sebastian, Spain

⁵IKERBASQUE, Basque Foundation for Science, Bilbao, Spain

koroteev@niic.nsc.ru

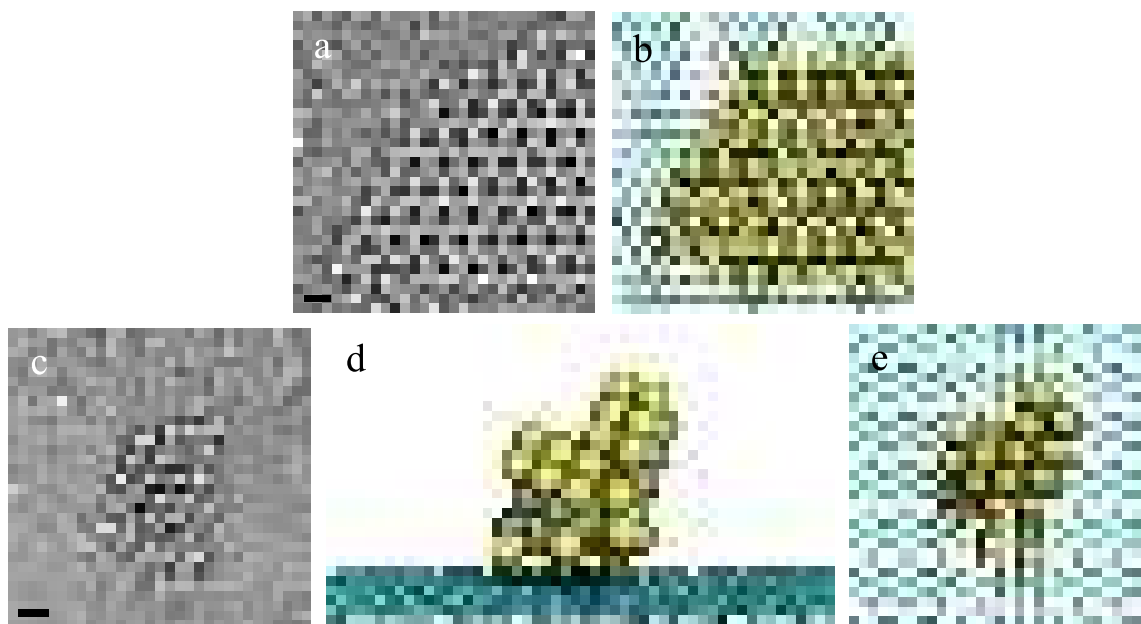
Combination of low dimensional carbon nanostructures, possessing high electrical conductivity and specific surface, with semiconducting nanoparticles containing transitional metals allows creation of new class of hybrid materials with outstanding properties for different applications. Molybdenum disulfide in combinations with carbon-based nanostructures could serve as perfect anode material for lithium storage [1,2] or catalyst [3,4]. Theoretical electrochemical capacity of carbon based materials is limited to 372 mAh/g, while the capacity of hybrids could reach 1150 mAh/g [5].

In this work, we are different techniques, which allows the production of MoS₂ particles on carbon nanotube or few layer graphene support.

For the applications, where electric conductivity and high availability of sulphide nanoparticles is significant, such as Li-ion battery materials and supercapacitors we propose to use aligned carbon nanotubes arrays, because of its porous structure and electric connectivity. The arrays, covered with MoS₂ were tested as a Li-ion battery anode material and supercapacitor electrode, achieving high specific capacity in both cases.

Catalytic properties of MoS₂ layers and nanoparticles on few layer graphene (Fig. 1) were tested on formic acid decomposition reaction. The reaction resulted production of hydrogen with selectivity up to 50% and organic products, such as methyl formate starting from 125°C.

Fig. 1. represents TEM images of MoS₂ monolayer (a) and nanoparticle (c) and corresponding atomic structures (b, d, e).



This work was financially supported by the Russian Science Foundation grant No. 16-13-00016.

References

- [1] K. Chang, W. Chen, L. Ma, H. Li, H. Li, F. Huang, Z. Xu, Q. Zhang, and J.-Y. Lee, *J.Mater.Chem.* **21**, 6251 (2011).
- [2] G. Huang, T. Chen, W. Chen, Z. Wang, K. Chang, L. Ma, F. Huang, D. Chen, and J. Y. Lee, *Small* **9**, 3693 (2013).
- [3] Y. Li, H. Wang, L. Xie, Y. Liang, G. Hong, and H. Dai, *Journal American Chemical Society* **133**, 7296 (2011).
- [4] P. Ge, M. D. Scanlon, P. Peljo, X. Bian, H. Vubrel, A. O'Neill, J. N. Coleman, M. Cantoni, X. Hu, K. Kontturi, B. Liu, and H. H. Girault, *Chem.Commun.* **48**, 6484 (2012).
- [5] K. Chang and W. Chen, *ACS Nano* **5**, 4720 (2011).

Electronic and spin structure of Bi-graphene-like system

Oleg E. Tereshchenko

*A.V. Rzhano Institute of Semiconductor Physics SB RAS, Lavrentiev av. 13, 630090 Novosibirsk, Russian Federation
Novosibirsk State University, 630090 Novosibirsk, Russian Federation
teresh@isp.nsc.ru*

In recent years a new field has emerged in condensed-matter physics based on the realization that the spin-orbit interaction can lead to topological insulating electronic phases and on the prediction and observation of these phases in real materials and heterostructures. Generally, Rashba spin-orbit coupling becomes larger in materials with heavier atoms due to the larger atomic spin-orbit coupling. The group-V semimetal bismuth (Bi) is a promising candidate to investigate the graphene-like properties and surface Rashba effect, since the energy splitting of the bands is fairly large owing to the heavy atomic mass of the Bi atom.

The aim of this work is to develop the methods of preparation (substrate surface preparation, evaporation rate, ...) and to study the electronic structure of Bi/InAs(111) interfaces using state-of-the-art spin- and angular resolved photoemission spectroscopy (SR ARPES).

The Bi deposition on InAs(111)A-(2x2) surface at room temperature (RT) leads to the epitaxial growth with forming well-ordered (1x1) hexagonal Bi phase above one monolayer. The dispersion measured by ARPES shows no gap at the surface, indicating surface metallization. The dispersion near the Fermi level (0-0.5 eV) is a typical for bismuth states characterized by Rashba-type. Spin-resolved ARPES demonstrates the presence of spin-polarized states directly at the Fermi level. Below the Fermi level these states cross the gap of InAs forming linear dispersion with crossing point at 0.25 eV below the Fermi level. The presence of Bi-induced states in the gap of InAs with linear dispersion is similar to graphene with two important differences: states are spin-polarized and located at Γ point. It is found that the surface Fermi level position at InAs(111)A is unpinned and can be changed in controllable way by Bi adsorption-desorption process.

Another behavior is observed when deposition takes place at elevated temperature. At 1 ML of Bi coverage the InAs(111)A-($\sqrt{3}\times\sqrt{3}$)Bi structure is formed which consists of three 60° oriented domains. The electronic structure of InAs(111)A-($\sqrt{3}\times\sqrt{3}$)Bi surface is significantly different from those observed on InAs(111)A-(1x1)Bi. First of all, the dispersion contains a small gap, which can be considered in the first approximation as a gap in the primarily Rashba states. The appearance of a gap is probably induced by the strong spin-orbit interaction in bismuth layer and reduced structural surface symmetry. In this case, the polarized states remain, and the presence of the gap may allow considering this system as a promising candidate for the spin-transistor system. The observed dispersion can also be interpreted as the graphene-like Dirac state with a gap. Moreover, 2D electron states in the quantized states at the InAs surface are hybridized with Bi states that should lead to increase of Rashba splitting in 2D states of InAs.

Structure and Spin Dynamics of Si-Vacancies in SiC

S.A. Tarasenko

*Ioffe Institute, 194021 St. Petersburg, Russia
tarasenko@coherent.ioffe.ru*

1. Introduction

Silicon carbide (SiC) has been attracting growing attention due to diversity of its polytypes with remarkable and tunable electric and optical properties as well as radiation stability. Of particular interest for fundamental research in optics and applications in sensorics and spintronics are color centers associated with silicon vacancies or divacancies [1-6]. The silicon-vacancy center (V_{Si}) possesses the half-integer spin $3/2$. It can be selectively initialized and read-out by optical means and efficiently manipulated by a radiofrequency (rf) field. Because of a narrow broadening together with a high sensitive of spin sublevels to an external magnetic field, temperature, mechanical pressure, etc., V_{Si} can be utilized as efficient room-temperature sensors, particularly through the optically detected magnetic resonance (ODMR).

In this talk, we discuss the structure and spin dynamics of V_{Si} in 4H SiC, the spin fluctuations caused by interaction with environment in an ensemble of V_{Si} , as well as applications of V_{Si} for magnetic field and temperature measurements. We show that the high spin $3/2$ provides additional functionality.

2. Fine structure

The fine structure of a V_{Si} center is determined by the real atomic arrangement of the vacancy which is described by the C_{3v} point group. At zero magnetic field, the ground state is split in two Kramers doublets with the spin projections $m = \pm 1/2$ and $\pm 3/2$ along the crystal c -axis, the zero-field splitting is about 70 MHz for the $V_{Si}(V_2)$ center. An external magnetic field \mathbf{B} splits the levels $m = \pm 1/2$ and $\pm 3/2$ further and, at certain fields, one observes the level anticrossings: LAC-1 between the states with $\Delta m = 1$ and LAC-2 between the states with $\Delta m = 2$. Application of a resonant rf field allows one to manipulate the V_{Si} spin states. In addition to the commonly studied "allowed" rf-driven spin transitions between the states with $\Delta m = 1$, the trigonal pyramidal symmetry of V_{Si} enables the "forbidden" spin transitions with $\Delta m = 2$ [5]. In the vicinity of the LACs, the intensity of photoluminescence demonstrates resonance-like behavior. The sharpest resonance is detected for "forbidden" LAC-2 with $\Delta m = 2$. This phenomenon can be used for a purely optical sensing of dc magnetic fields with nanotesla resolution [5]. Experiment shows that the effect is robust up to at least 500 K, suggesting a simple, contactless method to monitor weak magnetic fields in a broad temperature range.

The excited state of the V_{Si} center has a similar structure. Here, however, the value of the zero-field splitting has a giant thermal shift of about 2.1 MHz/K [6]. The thermal shift has been observed by ODMR in the excited state using the ground state as an ancilla or, alternatively, by monitoring the photoluminescence intensity in the vicinity of the excited-state level anticrossing. The findings suggest that a pure optical integrated magnetic field and temperature sensor can be implemented on the same V_{Si} centers.

3. Spin fluctuations

The spin and optical properties of V_{Si} centers can be also efficiently studied by probing the fluctuations stemming from the interaction of the centers with environment. Owing to the fundamental connection between fluctuations and dissipation processes, such a noise spectroscopy is a powerful tool for studying the spin dynamics in conditions close to thermal equilibrium and beyond [7]. We develop a microscopic theory of spin fluctuations for V_{Si} centers and discuss the control of the noise power spectrum by a rf field. It is shown that spin fluctuations in an ensemble of V_{Si} centers can be probed by measuring the correlation function of the luminescence intensity $g^{(2)}$.

- [1] H. Kraus, V.A. Soltamov, D. Riedel, S. V  th, F. Fuchs, A. Sperlich, P.G. Baranov, V. Dyakonov, and G.V. Astakhov, Room-temperature quantum microwave emitters based on spin defects in silicon carbide, *Nat. Physics* **10**, 157 (2014).
- [2] D.J. Christle, A.L. Falk, P. Andrich, P.V. Klimov, J. Hassan, N.T. Son, E. Janz  n, T. Ohshima, and D.D. Awschalom, Isolated electron spins in silicon carbide with millisecond coherence times, *Nat. Materials* **14**, 160 (2015).
- [3] M. Widmann, S.-Y. Lee, T. Rendler, N.T. Son, H. Fedder, S. Paik, L.-P. Yang, N. Zhao, S. Yang, I. Booker, A. Denisenko, M. Jamali, S.A. Momenzadeh, I. Gerhardt, T. Ohshima, A. Gali, E. Janz  n, and J. Wrachtrup, Coherent control of single spins in silicon carbide at room temperature, *Nat. Materials* **14**, 164 (2015).
- [5] D. Simin, V.A. Soltamov, A.V. Poshakinskiy, A.N. Anisimov, R.A. Babunts, D.O. Tolmachev, E.N. Mokhov, M. Trupke, S.A.T., A. Sperlich, P.G. Baranov, V. Dyakonov, and G.V. Astakhov, All-Optical dc Nanotesla Magnetometry Using silicon vacancy fine structure in isotopically purified silicon carbide, *Phys. Rev. X* **6**, 031014 (2016).
- [6] A. N. Anisimov, D. Simin, V. A. Soltamov, S. P. Lebedev, P. G. Baranov, G. V. Astakhov, and V. Dyakonov, Optical thermometry based on level anticrossing in silicon carbide, *Sci. Reports* **6**, 33301 (2016).
- [7] N.A. Sinitsyn and Y.V. Pershin, The theory of spin noise spectroscopy: a review, *Rep. Progr. Phys.* **79**, 106501 (2016).

Surface modification, stability and spin polarization of excited electrons in tetradymite topological insulators

Lada V. Yashina (1), Jaime Sánchez-Barriga (2), Oliver Rader (2)

(1)Department of Chemistry, Moscow State University, Leninskie Gory 1/3, 119991, Moscow, Russia

(2)Helmholtz-Zentrum Berlin fuer Materialien und Energie, Albert-Einstein-Str. 15, 12489 Berlin, Germany

Yashina@inorg.chem.msu.ru

Three-dimensional topological insulators (TIs) are characterized by spin-polarized Dirac-cone surface states that are protected from backscattering by time-reversal symmetry. Within the past few years, TIs have attracted a lot of interest due to their unique electronic structure with spin-polarized topological surface states (TSSs), which may pave the way for these materials to have a great potential in multiple applications. However, to enable consideration of TIs as building blocks for novel devices, stability of TSSs toward oxidation should be tested. We investigate the behavior of the topological surface states on Bi_2X_3 ($\text{X} = \text{Se}, \text{Te}$) by valence-band and core level photoemission in a wide range of water and oxygen pressures both in situ (from 10⁻⁸ to 0.1 mbar) and ex situ (at 1 bar). We find that no chemical reactions occur in pure oxygen and in pure water. Water itself does not chemically react with both Bi_2Se_3 and Bi_2Te_3 surfaces and only leads to slight *p*-doping. In dry air, the oxidation of the Bi_2Te_3 surface occurs on the time scale of months, in the case of Bi_2Se_3 surface of cleaved crystal, not even on the time scale of years. The presence of water, however, promotes the oxidation in air, and we suggest the underlying reactions supported by density functional calculations. All in all, the surface reactivity is found to be negligible, which allows expanding the acceptable ranges of conditions for preparation, handling and operation of future Bi_2X_3 -based devices. Among the family of TIs with a tetradymite structure, Sb_2Te_3 is of *p*-type and appears to be the least explored material since its TSS is unoccupied in the ground state, a property that allows the use of optical excitations to generate spin currents relevant for spintronics. Here, we report relatively fast surface oxidation of Sb_2Te_3 under ambient conditions. We show that the clean surface reacts rapidly with molecular oxygen and slowly with water, and that humidity plays an important role during oxide layer growth. In humid air, we show that Sb_2Te_3 oxidizes on a time scale of minutes to hours, and much faster than other tetradymite TIs. The high surface reactivity revealed by our experiments is of critical importance and must be taken into account for the production and exploitation of novel TI-based devices using Sb_2Te_3 as a working material.

Control of the spin polarization of topological surface states (TSSs) using femtosecond light pulses opens novel perspectives for the generation and manipulation of dissipationless surface spin currents on ultrafast time scales. Using time-, spin-, and angle-resolved spectroscopy, we directly monitor the ultrafast response of the spin polarization of photoexcited TSSs to circularly polarized femtosecond pulses of infrared light. We achieve all-optical switching of the transient out-of-plane spin polarization, which relaxes in about 1.2 ps. Our observations establish the feasibility of ultrafast optical control of spin-polarized Dirac fermions in TIs and pave the way for optospintronic applications at ultimate speeds.

[1] Volykhov A., Sánchez-Barriga J., Sirotina, A., Neudachina V., Frolov, A., Gerber E., Kataev E., Senkovskiy B., Khmelevsky N., Aksenenko A., Korobova N., Knop-Gericke A. Rader O., Yashina L. Rapid surface oxidation of Sb_2Te_3 as indication for a universal trend in the chemical reactivity of tetradymite topological insulators *Chemistry of Materials* 28 (2016) 8916–8923

[2] Yashina, L.; Sánchez-Barriga, J.; Scholz, M.; Volykhov, A.; Sirotina, A.; Neudachina, V.; Tamm, M.; Varykhalov, A.; Marchenko, D.; Springholz, G.; Bauer, G.; Knop-Gericke, A.; Rader, O. Negligible Surface Reactivity of Topological Insulators Bi_2Se_3 and Bi_2Te_3 Towards Oxygen and Water *ACS nano* 7 (2013) 5181-5191

[3] Sánchez-Barriga J., Golias E., Varykhalov A., Kornilov O., Braun J., Yashina L.V., Schumann R., Minár J., Ebert H., Rader O. Ultrafast spin-polarization control of Dirac fermions in topological insulators *Physical Review B* 93 (2016) 155426

[4] Sánchez-Barriga J., Varykhalov A., Braun J., Xu S.-Y., Alidoust N., Kornilov O., Minár J., Hummer K., Springholz G., Bauer G., Schumann R., Yashina L. V., Ebert H., Hasan M. Z., Rader O. Photoemission of Bi_2Se_3 with Circularly Polarized Light: Probe of Spin Polarization or Means for Spin Manipulation? *Physical Review X* 4, 011046 (2014)

Poster session



©A.Golubina

Thermal conductivity of carbon nanotubes and their nanocomposites

M. V. Avramenko, D. V. Chalin, S. B. Rochal

*Department of Nanotechnology, Faculty of Physics, Southern Federal University, Rostov-on-Don, 5 Zorge Str., 344090, Russia
avramenko.marina@gmail.com*

Current progress in electronics and optoelectronics stimulates an interest in investigation of thermal conductivity of different materials, because performance and stability of nanoelectronic devices are specified by the cooling effectiveness. Due to a combination of unique electrical and thermal properties, carbon nanotubes (CNTs) and their polymer nanocomposites are considered to be the promising materials for development of the new-generation nanoelectronic devices [1, 2]. Unfortunately, despite the great number of both theoretical and experimental papers, thermal conductivity of CNTs and their polymer nanocomposites is still a matter of intense debate.

In our work we present a simple model of a polymer/CNT nanocomposite consisting of arbitrarily oriented CNTs of equal mean length embedded in a polymer matrix. Considering thermal conductivity of such a system at $T < 100$ K, we suppose that phonon mean free path is comparable to the CNTs mean length and phonons are scattered only at the ends of nanotubes, so heat transport is described in the frame of the Landauer's approach [3] as ballistic one. Low-frequency dynamics of CNTs and van der Waals interaction between a CNT and its environment is studied by means of the continuous theory [4] and its generalized version [5]. We demonstrate that our model is a convenient tool for estimation of the upper limit of a polymer/CNT nanocomposite thermal conductivity and analysis of other thermodynamic properties of single- and multi-walled nanotubes and their nanocomposites, which are also determined by the phonon spectrum and peculiarities of its reconstruction when the complex system is formed and influenced by the environment.

This work was supported by the RSF grant No. 15-12-10004.

[1] A. Jorio, M.S. Dresselhaus and G. Dresselhaus, *Carbon Nanotubes: Advanced Topics in the Synthesis, Structure, Properties and Applications*, Vol. **111** (Springer, Berlin, 2008).

[2] *Carbon Nanotubes Applications on Electron Devices*, edited by J. M. Marulanda (InTech, 2011).

[3] R. Landauer, IBM Journal of Research and Development, **1**, 223 (1957).

[4] S. B. Rochal, V. L. Lorman and Yu. I. Yuzyuk, Physical Review B, **88**, 235435 (2013).

[5] M. V. Avramenko, I. Yu. Golushko, S. B. Rochal, A. E. Myasnikova, Physica E, **68**, 133 (2015).

Polyaniline coated carbon buckypapers for the supercapacitor applications

Ekaterina O. Fedorovskaya^{1,2}, Konstantin M. Popov², Lyubov G. Bulusheva^{1,2}, Alexander V. Okotrub^{1,2}.

¹ Novosibirsk State University, 630090, 2, Pirogova str., Novosibirsk, Russia

² Nikolaev Institute of Inorganic Chemistry, SB RAS, 630090, 3, Acad. Lavrentiev Ave., Novosibirsk, Russia
fedorovskaya-eo@yandex.ru

Electrochemical capacitors, known as supercapacitors, have attracted great interest as promising energy storage devices due to their higher power energy density and longer cycle performance than the conventional dielectric capacitors. Recently, buckypapers based on carbon materials such as graphene or nanotubes have attracted attention as a promising material for capacitor electrodes. Carbon buckypapers commonly possess large specific surface area, remarkable chemical inertness and physical stability. 3D network of the carbon material in the buckypapers provides fast charge/discharge processes and high stability of a capacitor. Formation of three-dimensional conducting network from buckypaper coated with a layer of polyaniline, involved in the Faraday processes, seems to be promising for obtaining of high-capacitance supercapacitors. Extensive 3D carbon network in this system provides a good quality coating of polyaniline.

The binder-free buckypaper films were prepared by a filtration of aqueous dispersion of carbon nanotubes (CNTs) or graphene and treated by a HNO₃/H₂SO₄ mixture through a polyester filter. CNTs synthesized by a catalytic chemical vapor deposition (CCVD) method at two different temperatures 720 and 800°C. Graphene was prepared by reduction of graphite oxide synthesized by Hammers. Polyaniline was deposited by the electrochemical oxidation of aniline in acid solution in a three-electrode cell comprising of an Ag/AgCl electrode using potentiostatic and galvanostatic mode. Buckypaper films were used as working electrodes.

A study of the electronic structure of the carbon nanotubes and composites was carried out by. The morphology, functional structure and defectness of samples were determined by Raman and IR spectroscopy and scanning electron microscopy. The electrochemical measurements were carried out on a potentiostat Elins PI-30-Pro working in potentiodynamic mode. Electrochemical measurements showed that the capacity of carbon buckypaper electrode increases with the polyaniline coating formation. Furthermore, specific capacity and the morphology of the composites based on the carbon buckypaper depend on polyaniline synthesis conditions.

The work was financially supported by the Russian Foundation for Basis Research (grant No. 16-33-00441).

Optimization of polymer fibers properties by introducing of carbon nanotubes

S.N. Bokova-Sirosh^{1,*}, E.A. Obratsova^{1,2}, E.D. Obratsova¹

¹ A.M. Prokhorov General Physics Institute RAS, 38 Vavilov str., 119991, Moscow, Russia

² M.M. Shemyakin & Yu. A. Ovchinnikov Institute of Bioorganic Chemistry, RAS, 10/16 Miklukho-Maklaya, 117997 Moscow, Russia

*Corresponding author bokova.sirosh@gmail.com

Polymer fibers - very perspective and marketable material. Application of polymer fibers is very wide: from military applications, sporting goods and equipment. In turn, the carbon nanomaterials have unique physical and chemical properties, including: a high degree of mechanical strength and an ability of material to absorb mechanical energy. The combination of this properties result in a significant improvement in the properties of the modified material. There are a number of works devoted to introduction of single-wall carbon nanotubes (SWNTS) into polymeric materials [1], but SWNTS are quite expensive. During the research it was noted that the multi-walled carbon nanotubes (MWNT) could also be used to achieve the result delivered, which also have potential for use in this area.

In this work the raw carbon material and modified fibers have been investigations by Raman scattering and scanning electron microscopy (SEM). The Raman spectra of initial fibers have shown typical signals corresponding to C-C ring stretching, and the vibrations of amide group. The Raman spectra have shown a presence of carbon nanostructures in the raw soot. The introduction of carbon nanostructures into the polymer fibers was made from a suspension. The SEM and Raman studies of fibers enriched with carbon nanostructures have not revealed their presence in the fiber. A small amount of filler could be a reason of such result.

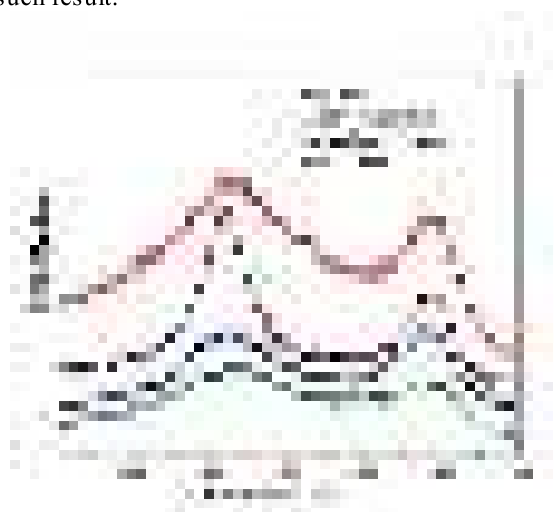


Fig. 1 Raman spectra of the thermal carbon soot and blast soot.

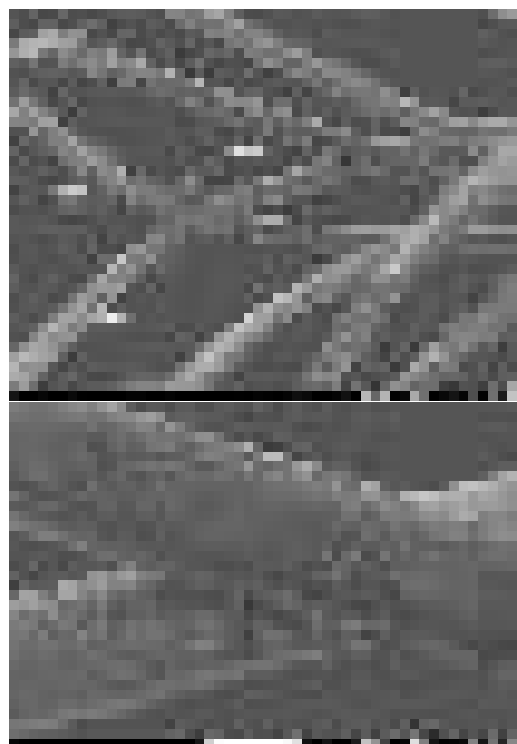


Fig. 2 SEM imaging of modified fibers.

Acknowledgements: This research was supported by the RAS research programs and RFBR15-32-70013 mol_a_mos.

[1] S.N. Bokova et al. "Optical Diagnostics of Polymeric Fibers Containing Single-Wall Carbon Nanotubes", *Journ. of Nanoelectronics and Optoelectronics* 4 (2009) 232-235.

Observation of Trions in Single-Walled Carbon Nanotubes Doped In Acid Medium

T.V. Eremin^{1,2}, E.D. Obraztsova^{1,2}

¹Physics Department of M.V. Lomonosov Moscow State University, Moscow, Russia

²A.M.Prokhorov General Physics Institute, RAS, Moscow, Russia

timaeeremin@yandex.ru

Doping of single-walled carbon nanotubes leads to spectacular changes of their optical and electronic properties. Commonly used doping technique via filling the nanotubes with dopants molecules deals with films or powders of nanotubes making photoluminescence studying complicated due to the fast irradiative relaxation of electronic excitations in bundles. However, doping can also be performed via adding of dopants to the solution of individual nanotubes.

We report a comprehensive study of changes of optical properties of single-walled carbon nanotubes caused by doping in acid medium. In this work, hydrochloric acid was added to an aqueous solution of nanotubes wrapped with sodium cholate. Besides the suppression of RBM modes in the Raman spectrum and the suppression of the first optical transition in the optical absorption spectrum, we have observed an appearance of a new band in the photoluminescence spectrum with the energy about 200 meV less than the main photoluminescence band (Fig.1a). This new band was assigned to trions, quasiparticles consisting of two holes and one electron [1] (Fig.1b).

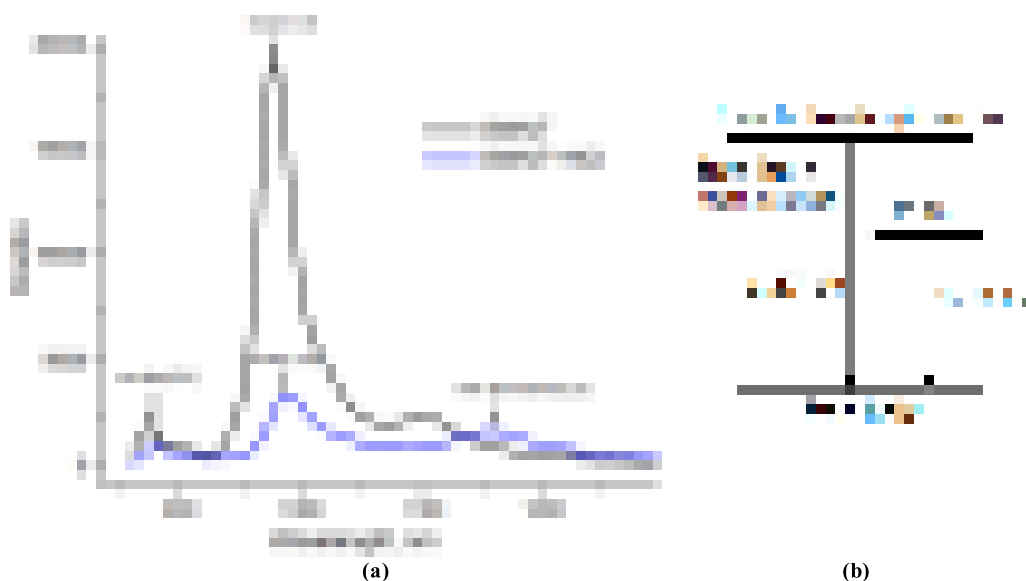


Fig.1 (a) Photoluminescence spectrum of initial SWNT suspension (black line) and SWNT suspension with added HCl (blue line).

Excitation wavelength is 570 nm; (b) the energy level diagram.

Acknowledgements. The work was supported by RSF project 15-12-30041 and RFBR project 16-02-00979.

[1] Matsunaga, Ryusuke, Kazunari Matsuda, and Yoshihiko Kanemitsu. "Observation of charged excitons in hole-doped carbon nanotubes using photoluminescence and absorption spectroscopy." *Physical Review Letters* 106.3 (2011): 037404.

Electronic structure of fluorinated double-walled carbon nanotubes

Yu.V. Fedoseeva^{1,2}, L.G. Bulusheva^{1,2}, A.V. Okotrub^{1,2}, E.V. Lobiak¹, P.N. Gevko¹, E. Flahaut^{3,4}

¹Nikolaev Institute of Inorganic Chemistry SB RAS, 630090 Novosibirsk, Russia

²Novosibirsk State University, 630090 Novosibirsk, Russia

³Centre Interuniversitaire de Recherche et d'Ingenierie des Materiaux, Universite Paul-Sabatier, France

⁴CNRS, Institut Carnot Cirimat, F-31062 Toulouse, France

⁵Institut Langevin, CNRS, ESPCI Paris, PSL Research University, CNRS, F-75005 Paris, France

Corresponding author e-mail: fedoseeva@niic.nsc.ru

Fluorination of carbon nanotubes is gateway to modify chemical and physical properties of nanotube surface and wide field of their applications. Functionalization of double-walled carbon nanotubes (DWCNTs) are especially interesting, since chemically modified outer shells possess new physicochemical characteristics, while unmodified inner shells preserve electronic properties characteristic for single-wall CNTs. In this work fluorinated double-walled carbon nanotubes (F-DWCNTs) received using different fluorination techniques were comparatively studied. Fluorination of DWCNTs were carry out by treatment with help of gaseous F_2 and XeF_2 at 200 °C, by mixture BrF_3 and Br_2 at room temperature and CF_4 radio-frequency plasma. Additionally, we study the influence of admixture of HF catalysis in the F_2 gas on the composition and electronic state of fluorinated DWCNTs. The DWCNTs fluorinated at various concentration of BrF_3 in the mixture of BrF_2 and Br_2 were also compared. Purified and oxygenated by acid treatment DWCNTs were used for fluorination. Transmission electron microscopy reveals preserving double-walled structure of DWCNTs and decrease diameter of nanotube ropes after fluorination. The most significant changes are observed in the DWCNTs fluorinated by fluorine gas. X-ray photoelectron spectroscopy reveals that fluorine concentration on surface of the fluorine DWCNTs depends on fluorination techniques. DWCNTs fluorinated by F_2 have the most fluorine content, the stoichiometry of outer fluorinated shell was estimated to be $CF_{0.5}$. While DWCNTs fluorinated by BrF_3 , XeF_2 and CF_4 -plasma have surface stoichiometry $CF_{0.3}$, $CF_{0.15}$ and $CF_{0.22}$. Raman spectroscopy demonstrates that fluorination induces changes in the vibration structure of DWCNTs. The intensities of “radial breathing” modes decrease and D-modes increase with increasing fluorination degree. The structural modifications of the fluorinated DWCNT samples were studied by optical absorption spectroscopy. Inner shells of DWCNTs remain intact after fluorination procedures. Differences in the electronic structure of fluorinated DWCNTs are observed by near-edge x-ray absorption fine structure spectroscopy (NEXAFS). Comparison of the NEXAFS F K-spectra of fluorinated DWCNTs allows suggesting that local surroundings of CF-groups located on the DWCNT surface are various and depend on the applied fluorination procedure. In order to

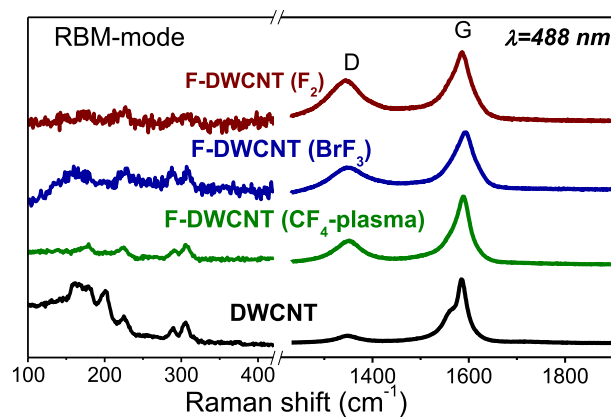


Fig. 1. Raman spectra of F-DWCNT fluorinated by different techniques using F_2 , BrF_3 and CF_4 -plasma together with reference spectrum of DWCNTs.

analyze NEXAFS FK-edge spectra, quantum-chemical modeling were performed in the framework of density functional theory using Z+1 approximation. According to modeling, the distribution of fluorine atoms on the surface of DWCNTs were proposed for fluorinated DWCNT produced by different fluorination techniques. Fully fluorinated areas were found to be in the F-DWCNT fluorinated by F_2 , while fluorination by BrF_3 , XeF_2 , and CF_4 lead to formation of fluorinated carbon chains, surrounded by non-fluorinated carbon areas. It was discovered that presence of oxygen-containing groups on the surface of DWCNT leads to the increase fluorine concentration and changing the electronic structure of fluorinated DWCNTs.

Authors would like to acknowledge the support of the Russian Foundation for Basic Research (Grant № 16-53-150003).

Purification of metallic and semiconducting single-walled carbon nanotubes

^{*1}Bagdasarova K.A., ^{1,2}Eremina V.A., ³Obraztsova E.A., ⁴Bondarenko G.N., ¹Obraztsova E.D.

¹A.M. Prokhorov General Physics Institute RAS, 119991, RF, Moscow, Vavilov str., 38

²Faculty of Physics, M.V. Lomonosov Moscow State University, 119991, RF, Moscow, Leninskie gory, 1

³Shemyakin-Ovchinnikov Institute of Bioorganic Chemistry RAS, 117997, Moscow, RF, Miklukho-Maklaya str., 16/10 .

⁴A.V. Topchiev Institute of Petrochemical Synthesis RAS, 119991, RF, Moscow, Leninsky pr., 29

^{*}bkarin@mail.ru

The sorting of single-walled carbon nanotubes (SWCNT) by aqueous two phase extraction (ATPE) method [1, 2] was used to separate nanotubes over electrical conductivity type. However, as a result of the method, separated fractions contain not only metallic or semiconducting SWCNT, but also the polymers and the surfactants (PEG, Dx, SC and SDS) which were used for separation.

The presence of above mentioned polymers and surfactants in separated fractions doesn't effect on their optical properties, but doesn't allow clearly estimate their electrophysical characteristics.

The structures of separated fractions were studied by IR-spectroscopy analysis, absorbance spectroscopy and SEM. The purification of separated fractions from carbohydrate phases was carried out by a few different methods, based on SWCNT sedimentation in different settler solutions. As last ones, the sulfuric acid, ethanol - sodium chloride and sodium thiocyanate water solutions were used.

The sedimentation methods lead to SWCNTs bundles formation (see Fig. 1). Then, the subsequent ultracentrifugation was used to finally remove the supernatant solution. This isab efficient way to purify the initial fraction.



Fig. 1. Bundles of carbon nanotubes after acid treatment.

The work was supported by RFBR- 16-52-540003 and RFBR- 15-32-70014.

[1] C. Y. Khripin, J. A. Fagan, and M. Zheng, J. Am. Chem. Soc., 135 (18), 6822-6825, (2013).

[2] V.A. Eremina, P.A. Obraztsov, P.V. Fedotov, A.I. Chernov, and E.D. Obraztsova, Phys. Status Solidi B, 1-6, (2016).

Sorted semiconducting single-walled carbon nanotubes for transistor sensor applications

V.A. Eremina^{1,2}, A.I. Chernov², J. Shook³, A. Zakhidov⁴, E.D. Obraztsova^{1,2}

¹Physics Department of M.V. Lomonosov Moscow State University, 1 Leninskie gori, Moscow, Russia

²A.M. Prokhorov General Physics Institute, RAS, 38 Vavilov street, 119991 Moscow, Russia

³Physics Department, Texas State University, San Marcos, TX 78666, USA

⁴Materials Science, Engineering, and Commercialization, Texas State University, San Marcos, TX 78666, USA
erjomina@physics.msu.ru

Single-walled carbon nanotubes (SWCNTs) is a promising material for transistor applications [1]. According to their geometrical structure, SWNTs may have different types of conductivity - metallic or semiconducting [2]. For using them as transistors, one needs pure semiconducting nanotubes. However, in the result of synthesis, there are nanotubes with both types of conductivity in a mixture.

Using aqueous two phase extraction technique [3,4,5] we have obtained the exceptional results of sorting: up to 99% purity of semiconducting nanotubes (Fig 1a).

We used the sorted fraction to fabricate back gated, interdigitated electrode field effect transistor (Fig. 1b).



Fig.1. a) UV-vis-NIR absorbance spectrum of pure semiconducting fraction of arc-SWCNTs with an average diameter of 1.4 nm and the photo of 30 ml of this suspension. b) SEM image of semiconducting SWCNTs integrated on interdigitated electrode.

Acknowledgements

The work was supported by RSF-15-12-30041 and RFBR-16-52-540003 projects.

References

- [1] Baughman, Ray H., Anvar A. Zakhidov, and Walt A. de Heer. "Carbon nanotubes-the route toward applications." *Science* 297.5582 (2002): 787-792.
- [2] Dresselhaus, Mildred S., et al. "Carbon nanotubes" (2000) *Springer Netherlands*.
- [3] Khripin, Constantine Y., Jeffrey A. Fagan, and Ming Zheng. "Spontaneous partition of carbon nanotubes in polymer-modified aqueous phases." *Journal of the American Chemical Society* 135.18 (2013): 6822-6825.
- [4] Eremina, Valentina A., Pavel V. Fedotov, and Elena D. Obraztsova. "Copper chloride functionalization of semiconducting and metallic fractions of single-walled carbon nanotubes." *Journal of Nanophotonics* 10.1 (2016): 012515-012515.
- [5] Eremina, Valentina A., Obraztsov, Petr A., Fedotov, Pavel V., Chernov, Alexandr I., and Obraztsova, Elena D. "Separation and optical identification of semiconducting and metallic single-walled carbon nanotubes" (2016) *Physica Status Solidi (b)*, DOI 10.1002/pssb.201600659.

Sorting of large diameter carbon nanotubes using gel chromatography

Pavel V. Fedotov¹, Alexander I. Chernov^{1,2}, Elena D. Obraztsova^{1,2}

¹A.M. Prokhorov General Physics Institute, RAS, 38 Vavilov Street, 119991, Moscow, Russia

²National Research Nuclear University MEPhI (Moscow Engineering Physics Institute), 31 Kashirskoe hwy., 115409, Moscow, Russia

fedotov@physics.msu.ru

Single-walled carbon nanotubes (SWCNTs) are one of the most interesting materials today. They are appeared to be useful in various fields of applications. For instance nanotubes can be used as a nanoscale reactor to synthesize novel 1D materials [1, 2]. The ultimate mechanical, chemical and physical properties of SWCNTs, basically, their stability upon various stresses and a tunability of their properties, make nanotubes perfect candidate for such advanced application areas. High homogeneity of crystalline structure as well as electronic and optical properties appears to be one of the main requirements for SWCNTs. If one would like to apply nanotubes as a nanoreactor, an efficient method of producing high purity monodispersed nanotubes with different diameters and geometries should be developed.

One way to produce monodispersed SWCNTs is based on utilizing specific sorting technique. The SWCNT gel chromatography is an efficient sorting method that allows extracting single-chirality nanotubes [3]. It was demonstrated that one can obtain highly monodispersed SWCNTs with small diameter via temperature-controlled gel chromatography. However, in order to apply nanotubes as nanoreactor large diameter monodispersed nanotubes are also in high demand. The applicability of a gel chromatography method to sort large diameter SWCNTs has not been well-studied yet.

In this work we tried to sort large diameter SWCNTs (av. diameter is 2 nm) by temperature-controlled gel chromatography. We show the evidence of selectivity to both a conductivity type and a diameter of nanotubes.

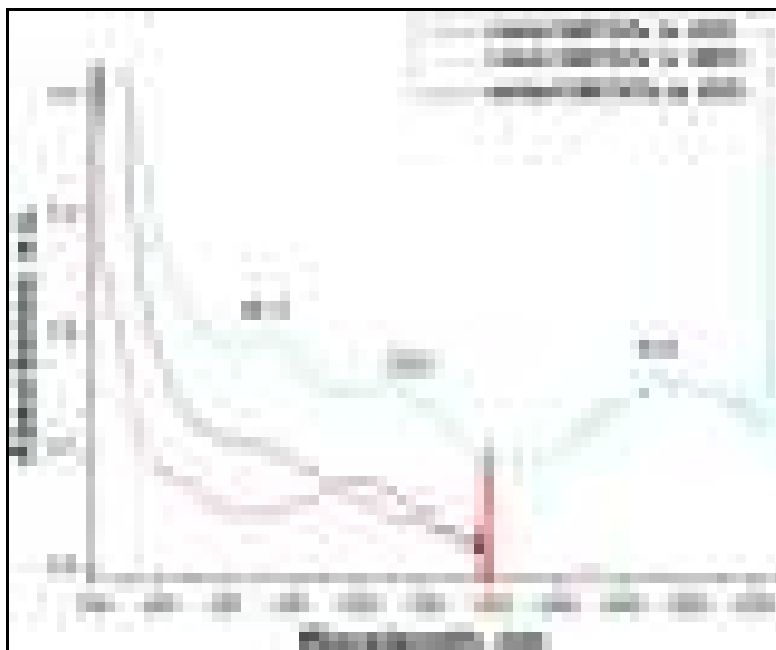


Fig.1. The optical absorption spectra of initial SWCNTs in H₂O and MEK (methyl ethyl ketone) and extracted fraction of nanotubes.

The work was supported in frames of project 15-12-30041 of Russian Science Foundation. P.V. Fedotov thanks grant SP-170.2015.3 of Ministry of Education and Science of Russian Federation. A.I. Chernov thanks RFBR grant 15-32-70005.

[1] Alexander I. Chernov, Pavel V. Fedotov, Alexander V. Talyzin *et al* "Optical Properties of Graphene Nanoribbons Encapsulated in Single-Walled Carbon Nanotubes", ACS nano (2013), 7 (7), pp 6346–6353

[2] Pavel V. Fedotov, Valentina A. Eremina, Alexander A. Tonkikh, *et al* "Enhanced optical transparency of films formed from sorted metallic or semiconducting single-walled carbon nanotubes filled with CuCl", Phys. Status Solidi B 253 (2016), No. 12, 2400–2405

[3] Huaping Liu, Takeshi Tanaka, Yasuko Urabe, and Hiromichi Kataura "High-Efficiency Single-Chirality Separation of Carbon Nanotubes Using Temperature-Controlled Gel Chromatography", ACS nano (2013), 13 (5), pp 1996–2003

Investigation of optical properties of nanohorn aqueous suspensions for biological applications

O. A. Gurova^{1, 2}, L.V. Omel'yanchuk^{2, 3}, A. V. Okotrub^{1, 2}

¹Nikolaev Institute of Inorganic Chemistry SB RAS, Lavrenteva Str. 3, Novosibirsk 630090,

²Novosibirsk State University, Pirogova Str. 2, Novosibirsk, 630090,

³Institute of Molecular and Cellular Biology SB RAS, Lavrenteva Str. 8/2, Novosibirsk 630090

e-mail: olga.gurov@gmail.com

In last time, inorganic nanomaterials have growing application in industry, and need to study their biological activities due to security issues. On the other hand, it is expected that controlled interaction between nanoparticles and cells or organisms can be used to create new methods of medical treatment of disease [1]. Carbon nanohorns (CNH) penetrating in biological tissue can effectively absorb and convert infrared (IR) radiation in heat which necessary for the local heating of tissue and organs. Thus, CNH can be used to prevent the growth of tumors using a method of hyperthermia.

The aims of this work are investigation of the properties of aqueous suspensions of carbon nanohorns and testing of penetration nanohorns in *Drosophila melanogaster* tissues.

In this study, we used carbon nanohorns powders synthesized by evaporation of a graphite target by arc discharge [2] and electron of beam emitted from an electron accelerator (fig.1(a)) [3]. CNH were oxidized for giving hydrophilic properties [4]. Nanohorns structure was characterized by scanning electron microscopy, infrared, optical and Raman spectroscopy. Thermal properties of structural and morphological features of the aqueous suspensions of the original and modified CNH were investigated.

Implementation of CNH in tissue of *Drosophila melanogaster* larva carried out through the culture medium. In experiment larvae have genotype *hs-Gal4 UAS-GFP.nls*. Then larvae irradiated IR - laser. The heated nanohorns caused "heat shock" reaction (response of cells to stress). After 4 hour, GFP-reporter luminescence was observed. The GFP synthesized in response to "heat shock" reaction.

According to the results, it showed that, after oxidation, aqueous suspensions nanohorns absorb in the IR region stronger than the initial sample (fig.1(b)). Oxidation of samples also leads to an improvement of the thermal properties nanohorns. It is showed that the nanomaterials are capable of penetrating into the tissues of *Drosophila* larvae, it is seen by the fluorescent GFP signal in the imaginal discs.

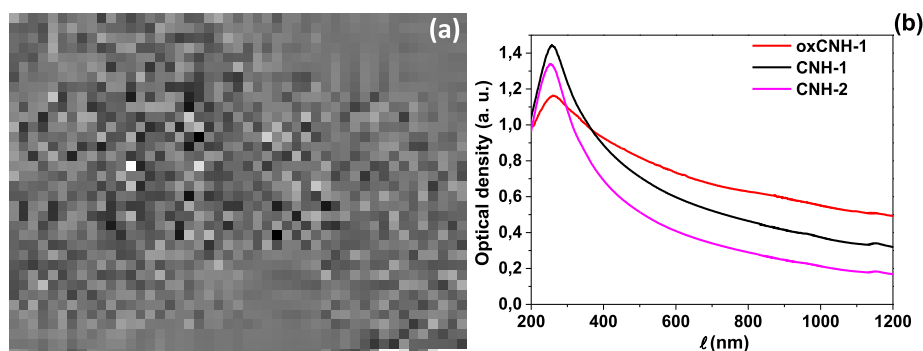


Fig.1 (a) TEM images of CNH synthesized evaporation of a graphite target by electron of beam emitted from an electron accelerator
(b) optical absorption spectra of carbon nanohorn suspension in distilled water.

Authors would like to acknowledge the support of the Russian Foundation for Basic Research (RFBR), grant № 16-32-00311.

[1] Heister E. et. al. Are Carbon Nanotubes a Natural Solution? Applications in Biology and Medicine. *ACS Appl. Mater. Interfaces* **5**, 1870-1891 (2013).

[2] Okotrub A.V. et. al. Synthesis of closed multilayer carbon particles in the electric discharge. *Inorganic materials* **32**, 974-978 (1996).

[3] Shimizu H et al. Method and device for producing carbon nanohorn. Patent WO 2012073700 A1. – 07.06.2012.

[4] Datsyuk V. et. al. Chemical oxidation of multiwalled carbon nanotubes. *Carbon N. Y.* **46**, 833-840 (2008).

The Mechanism of Resistance Switching in Films Based on Partially Fluorinated Graphene.

A.I. Ivanov¹, N.A. Nebogatikova^{1,2}, I.V. Antonova^{1,2*}

¹Rzhanov Institute of Semiconductor Physics SB RAS, Novosibirsk, Russia

²Novosibirsk State University, Novosibirsk, Russia

*antonova@isp.nsc.ru

Recently a wide range of materials are used for the fabricating of memristors. Structures based on graphene oxide (GO) showing resistive switching represent the great interest, but these memristor devices were found to exhibit unstable resistive effect. Fluorographene (FG) is more stable derivative of graphene, and partially fluorinated graphene with variable properties is considered as a promising material for fabricating of memristors [1]. It is known that resistive switching is observed in two-phase systems. Hence, it is necessary, that fluorinated graphene to contain a second phase providing resistive switching.

Original procedure for preparing fluorinated graphene in aqueous hydrofluoric acid solution has been developed in our laboratory [2]. In this report we have investigated the resistive switching effect in the composite films of fluorinated graphene with dimethylformamide (DMF) – FG-1, N-methylpyrrolidone (NMP) – FG-2 and without organic additives – FG-3 used at the stage of graphene suspension creation. DMF is an active compound forming a functional groups. DMF and water chemically react to form formate, that is functional group with a low activation energy. NMP is stable compound, which does not form functional groups in an aqueous medium. It was found, that if suspension of fluorographene not contained any organic additives, (Fig.1a), the resistive switching is not observed in fabricated films. Structures based on suspension with NMP exhibit resistive relatively weak switching effect (less than 0,4 a.u.), while adding DMF in suspension leads to change in resistance of films in 10 – 20 times.

Thus, the strongest resistive effect is observed for fluorographene films with functional groups of dimethylformamide (Fig.1a). The current-voltage characteristics of these samples have been studied on the mechanism responsible for the current in the structure. As it turned out, the current-voltage dependence is described the mechanism of Frenkel-Poole, linear regions are observed in the coordinate of $\ln(I/U)$ depending on the $U^{1/2}$ (Fig.1b) with trap activation energy of 80 meV. A schematic representation of the Frenkel-Poole conduction mechanism shown in Fig.1c.

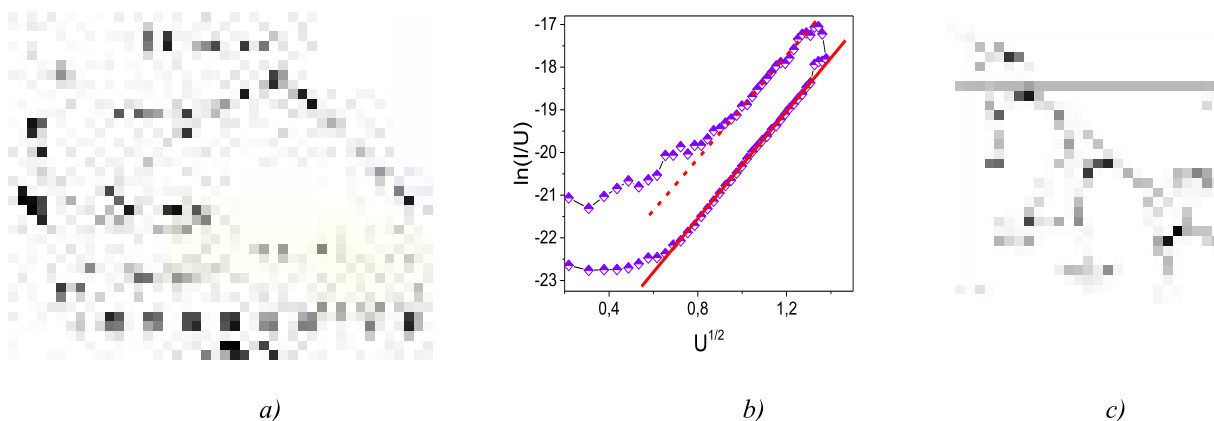


Fig.1: a) Dependences of the relative change in current as a function of fluorination time for suspension with different organic additives (NMP and DMF) and without one, the contact material to the film are indicated in brackets, b) Current - voltage characteristics for FG-1 structure in the coordinate axes $\ln(I/U)$ depending on the $U^{1/2}$, c) a schematic representation of the Frenkel-Poole conduction mechanism.

The influence of different organic additives on the resistive switching effect in films of fluorinated graphene, origin of this effect and current flow mechanism are discussed in this report. The presence of substance traces affects on the formation of conductive paths in partially fluorinated graphene films, chemical functional groups to form a conductive phase in two-phase systems. Stability of resistive switching is provided by capsulation of organic functional groups by fluorinated graphene flakes.

This study was partially financed by the Russian Science Foundation (grant No. 15-12-00008).

[1] Kurkina I. I. et al. Resistive switching effect and traps in partially fluorinated graphene films //Journal of Physics D: Applied Physics 49.9 (2016): 095303.

[2] Nebogatikova N. A. et al. Functionalization of graphene and few-layer graphene films in an hydrofluoric acid aqueous solution //Nanotechnologies in Russia 9. 1-2(2014): 51-59.

Electromagnetic properties of reduced graphene oxide films

M. Kanygin^{1,2,*}, O. Sedelnikova^{1,2}, E. Korovin², K. Dorozhkin²,
V. Suslyayev², L. Bulusheva^{1,3}, A. Okotrub^{1,3}

¹Nikolaev Institute of Inorganic Chemistry SB RAS, 3 Acad. Lavrentiev ave., Novosibirsk, Russia

²Tomsk State University, 36 Lenina st., Tomsk, Russia

³Novosibirsk State University, 2 Pirogova st, Novosibirsk, Russia

Corresponding author e-mail: mkanygin@gmail.com

Due to the quite effective interaction of carbon materials with electromagnetic radiation, these materials are widely used for many practical applications. Nowadays many researches are focused on the graphene materials and their interaction with electromagnetic radiation due to the unique properties of this kind of material [1-3]. One of the simplest way of graphene synthesis is a process of graphene oxide reduction. It should be note that efficiency of graphene interaction with radiation as well as other graphene properties are strongly depend on the method and conditions of graphene synthesis. In this work we present results of investigation influence of graphene synthesis conditions during graphene oxide chemical or thermal reduction on obtained graphene electromagnetic properties.

Graphene material was synthesized by liquid exfoliation of graphite oxide during the sonication process. Graphite oxidation was done by Hummers' method. Electronic structure initial material and materials after reduction was investigated by XPS and NEXAFS methods, which were performed at the Berlin Synchrotron Center BESSY-II using radiation from the Russian–German beamline. Graphene oxide reduction was performed chemically by staying at hydrazine hydrate vapors and thermally at 200°C. According to the UV-spectroscopy conductive layers were formed as a results of both reduction methods. XPS spectroscopy analysis of initial and reduced material demonstrate changes in the material electron structure and remove part of oxygen from the samples. Electromagnetic properties of initial and reduced graphene oxide films were investigated in the low-frequency the range from 1 kHz to 2 MHz on laboratory impedancemeter and in the THz range from 220 GHz to 720 GHz on terahertz spectrometer STD-21. Influence of reduction process conditions on the transmission and absorption of electromagnetic radiation by graphene material was found.

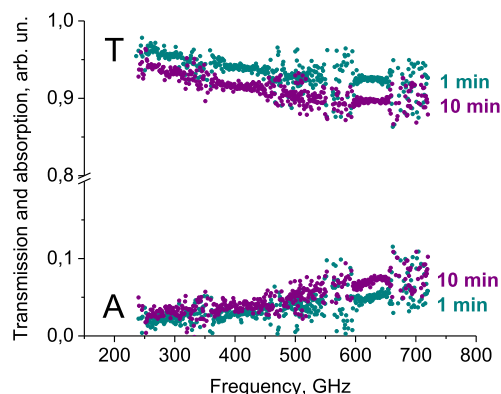


Fig.1. Transmission and absorption of THz radiation by chemically reduced graphene oxide with different reduction time.

Authors would like to acknowledge the support of the Russian Foundation for Basic Research (RFBR), grant № 16-32-00311.

[1] P. Kumar, F. Shahzada, S. Yu, S. Man Hong, Y.-H. Kim, Ch. Min Koo, Carbon, **94**, 494 (2015).

[2] Zhengang Lu, Limin Ma, Jiubin Tan, Heyan Wang, Xuemei Ding, Nanoscale, **8**, 16684 (2016).

[3] K. Batrakov, P. Kuzhir, S. Maksimenko, A. Paddubskaya, S. Voronovich, Ph. Lambin, T. Kaplas, Yu Svirko, Scientific Reports, **4**, 7191 (2014).

A novel strategy to fabricate Co-MWCNTs hybrids: Influence of MWCNT nature on the hybrid formation

M. Kazakova^{*1,2}, A. Andreev¹, A. Ischenko^{1,2}, V. Kuznetsov^{1,2}.

¹ Borekov Institute of Catalysis SB RAN, Russia

² Novosibirsk State University, Russia

Corresponding author e-mail: mas@catalysis.ru

MWCNTs, filled with metals, can be used for various applications in nanotechnology, biomedical sciences, memory device technology, and in catalysis. In the present work, the influence of the MWCNT nature was investigated on the features of Co-MWCNT hybrids formation. MWCNTs were synthesized by CVD method of ethylene decomposition over the bimetallic Fe-Co catalysts with different metal loadings and various supports at 680°C (the surface area of MWCNT was 115-380 m²/g, the average particle diameter of 7.2-18.6 nm). The obtained MWCNTs were designated as MWCNT-1, MWCNT-2 and MWCNT-3, correspondingly. An important step of the hybrid preparation is the creation of the anchoring sites for Co on the MWCNTs surface. To achieve that, functionalized MWCNTs containing surface carboxylic groups (ca. 0.8 groups per 1 nm²) were produced by the treatment with boiling concentrated nitric acid. Co-containing samples were prepared by the impregnation of as synthesized and functionalized MWCNTs with the aqueous solutions of Co (II) salts followed by calcination under an Ar atmosphere and reduction in H₂ flow at 350°C. The samples with Co content of 5-20 wt.% on the different types of MWCNTs were obtained. For the investigation of the structure and morphology of Co-containing MWCNTs, TEM, XRD, IF ⁵⁹Co NMR methods were used. The all samples with Co content up to 10 wt.% mainly contain Co particles within the channels of MWCNTs. Co particles inside the channels of MWCNTs with average diameter of 7.2 and 9.4 nm have rounded shape and the average diameter of 3-5 nm, which is determined by the internal diameter of the channels. The samples produced using MWCNTs with an average diameter of 18.6 nm contain elongated Co particles of more than 100 nm inside the MWCNTs.



Fig. 1. TEM images of the different type of initial MWCNTs and TEM images of 10 wt.% Co/MWCNT with different type of MWCNT, correspondingly.

MWCNTs modification by Co metal nanoparticles can potentially alter the dielectric and magnetic permeability of the MWCNTs thus making Co/MWCNT hybrids a new material for electro-magnetic applications such as radiofrequency shielding.

The reported study was funded by RFBR, according to the research project No. 16-32-60046 mol_a_dk.

Electrical Resistivity and Raman Signal of Graphene Films with Varying Fluorine Content

MariarKoleśnik-Gray^{1*}, Vitalii A. Sysoev², Lyubov G. Bulusheva², Alexander V. Okotrub² and Vojislav Krstić^{1*}

¹Department of Physics, Friedrich-Alexander-Universität Erlangen-Nürnberg (FAU), Staudtstr. 7, 91058 Erlangen, Germany

²Nikolaev Institute of Inorganic Chemistry, Siberian Branch of Russian Academy of Sciences (NIIC SB RAS), 3, Acad. Lavrentiev Ave., Novosibirsk, 630090, Russia.

*corresponding authors: vojislav.krstic@fau.de, maria.kolesnik-gray@fau.de

Covalent functionalization as a means for the modification of optoelectronic properties of graphene is a rapidly expanding field of fundamental and applied research. The reason for this is the disruption of the sp^2 -carbon lattice by the formation of sp^3 -bonds.

Here, we investigate the electrical resistivity at room temperature of few 10s of nm thin fluorographene [1-3] films of varying fluorine content and correlate the results with the generally observed Raman lines' intensity increase for higher degree of functionalisation in experiments.

In our measurements we find an unusual dependence of the thin film resistivity on the degree of fluorination. Also we observed that the dependence of the ratio of the D- and G-mode on the laser wavelength is comparable for low and high fluorinated graphene. Specifically, the ratio increases with wavelength (405 to 532 nm).

These observations are attributed to the aforementioned introduction of sp^3 -bonds of the graphene. While the resistivity reflects the propagation of the charge-carriers in the fluorinated graphene film, where both covalently bound fluorine and interflake-junctions represent scattering centres, the Raman activity is associated with allowed phonon modes in the system only.



Fig. 1. High-angle SEM image of a 200 nm thin fluorographene film on top of a SiO₂/Si substrate.

Acknowledgement

Financial support is acknowledged from the Deutsche Forschungsgemeinschaft (DFG-SFB 953 “Synthetic Carbon Allotropes”, A1, B12) and European Framework 7 IRSES Project No. 612577 (“NanoCF”).

References

- [1] V. I. Sysoev, A. V. Gusel'nikov, M. V. Katkov, I. P. Asanov, L. G. Bulusheva and A. V. Okotrub, *J. Nanophoton.* **10**, 012512 (2015).
- [2] A. Vyalikh, L. G. Bulusheva, G. N. Chekhova, D. V. Pinakov, A. V. Okotrub and U. Scheler, *J. Phys. Chem. C* **117**, 7940 (2013).
- [3] A. V. Okotrub, K. S. Babin, A. V. Gusel'nikov, I. P. Asanov and L. G. Bulusheva, *phys. stat. sol. (b)* **247**, 3039 (2010).

Conductive graphene-based layers for printing photonic and optoelectronic devices

I.A. Kotin¹, R.A. Soots¹, I.V. Antonova^{1,2}

¹Rzhanov Institute of Semiconductor Physics SB RAS, Novosibirsk, Russia

²Novosibirsk State Technical University, Novosibirsk, Russia

kotin@isp.nsc.ru

Today additive manufacturing such as 3D and 2D printing takes very large niche in fabrication of various devices. Especially, inkjet printing is one of the ways to create devices for photonics and optoelectronics. Since inkjet printing is very cheap and simple technique, it can replace common techniques in some areas, such as flexible, elastic and wearable electronics, photonics and optoelectronics. Fabrication of different photonic and optoelectronic devices by inkjet printing is required production of high conductive layers. There are different types of conductive inks [1,2]. First, it is conductive inks contained metal nanoparticles (NPs) typically made from silver, gold, copper and aluminum. Patterns printed by such inks have very high conductivity. However, silver and gold NPs inks are very expensive and copper and aluminum NPs are subjected to degradation because they can be oxidized. Second type is conductive polymer inks. The most promising polymer material for printed electronics is poly(3,4-ethylenedioxythiophene) (PEDOT) due to their high conductivity, solubility in water and so on. Disadvantages of conductive polymers are lower conductivity than metallic NPs inks and layer degradation at ambient condition. Recently graphene-based conductive layers have attracted much attention due to remarkable properties of graphene such as high conductivity, large carrier mobility. Moreover, it is flexible and very strong which make it promising for photonics and optoelectronics. There are simple and cheap techniques of large yield graphene production today, for example, by liquid phase exfoliation, electrochemical exfoliation.

In this report we demonstrate inkjet printing of conductive patterns using graphene-based inks with and without conductive polymer poly(3,4-ethylenedioxythiophene)-poly(styrenesulfonate) (PEDOT:PSS). We make a comparison of parameters these two conductive inks such as resistivity, time and thermal stability etc. (Fig.1). In addition, we make comparison graphene-based inks with silver inks. By inkjet printing of graphene-based inks one can make different photonic and optoelectronic devices such transparent conductors, light emission devices, solar cells and other terahertz devices.

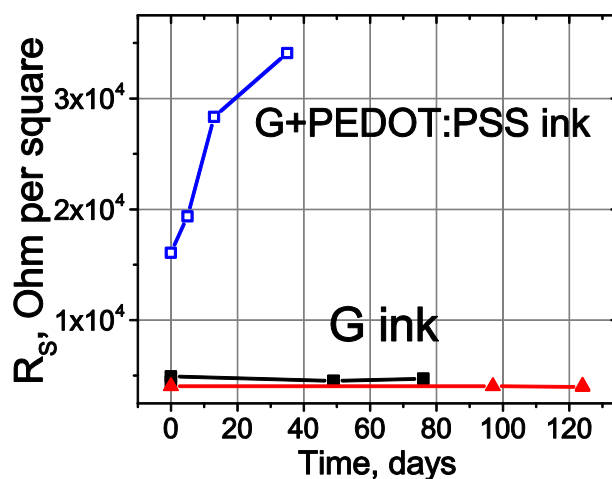


Figure 1. Time stability conductive layers printed by graphene and graphene-PEDOT:PSS inks.

Acknowledgement

This study was financially supported by the Russian Science Foundation (grant No. 15-12-00008).

References

- [1] Cummins G. and Desmulliez M.P.Y., *Inkjet printing of conductive materials: a review*, Circuit World, 38, 193 (2012)
- [2] Kamyshny A. and Magdassi S., *Conductive nanomaterials for printed electronics*, Small, 10, 3515 (2014)

The nature of atomic defects in epitaxial monocrystalline graphene on Ni(111) surface

S.L. Kovalenko¹, O.I. Kanishcheva^{1,2}, T.V. Pavlova¹, B.V. Andrushechkin¹, K.N. Eltsov¹

¹ A.M. Prokhorov General Physical Institute RAS, 119991 Moscow, Ulitsa Vavilova 38, Russia

² Moscow Institute of Physics and Technology, 1417019 Dolgoprudny, Moscow Region, 9 Institutskiy per., Russia

(corresponding author: S.L. Kovalenko, e-mail: stanislav.l.kovalenko@gmail.com)

We present results of a study of atomic defects in graphene formed on Ni(111) surface by thermal programmed growth from propene molecules (C_3H_6): at the beginning, propene is adsorbed on the nickel surface at room temperature and then the sample is annealed at 500 °C under UHV conditions. This method allows us to form monocrystalline graphene with size of Ni(111) target. The formed carbon layer does not have any discontinuities and in STM-images it is always observed as a hexagonal lattice with period $\approx 2.5\text{\AA}$ corresponding to the atomic lattice of graphene. Low electron energy diffraction on C/Ni(111) surface demonstrate sharp hexagonal pattern without any extra features. The graphene layer is a strict monolayer, because there is no any standing electron waves of $(\sqrt{3}\times\sqrt{3})R30^\circ$ structure around atomic defects which are typical for free-standing graphene and/or multilayer graphene and graphite. In STM images, single atomic defects have size of a single atomic cell. Associations of such defects are organized into so called «garlands» which are not located in boundaries between graphene domains because there is no phase shift of the atomic lattice of graphene. It means that epitaxial graphene layer actually is monocrystalline. The defects differ from well-known vacancy defects, Stone-Wales defects and extended defects formed at the boundaries between graphene domains with different location of carbon rings over the nickel lattice [1].

For analysis of the structure of the atomic defects in the monocrystalline graphene we have applied calculations based on density functional theory (DFT). In STM observation, we have found that graphene layer grows by forming islands separated by uncovered nickel islands. At the end of filling of surface with graphene layer, we have observed transformation of nickel islands into one-dimensional structures ending with «garland» of atomic defects. This observation graphene growth allows us to suggest that the single defect contains nickel atoms. DFT calculations have been made for several models with nickel atoms arranged in graphene single or double vacancies at different positions over the nickel lattice. Experimental STM images of the defects fit better with images calculated for models with one nickel atom in a single graphene vacancy over nickel atom in the substrate (on top) or with one nickel atom in a double graphene vacancy.

This work was supported by RFBR grant №15-02-09106 and Program "Nanostructures: Physics, chemistry, biology, technology basics" of Presidium of Russian Academy of Sciences.

[1] H. Tetlow, J. Posthuma de Boer, I.J. Ford, D.D. Vvedenskyb, J. Coraux, L. Kantorovich, Physics Reports 542 (2014) 195–295.

Optical limiting in heated aqueous suspension of detonation nanodiamonds and carbon nanotubes

R.Yu. Krivenkov, K.G. Mikheev, T.N. Mogileva, G.M. Mikheev

Institute of Mechanics UB RAS, 34, str. T. Baramzinoy, Izhevsk, 426067, Russia
roman@udman.ru

Optical limiting (OL) investigations in suspensions of carbon nanoparticles attracts attention in terms of development of optical limiters performing in a wide spectral range. A significant amount of studies of the OL in the suspensions of carbon nanotubes (CNTs) has been carried out to date. Light scattering on gas bubbles in host liquid, which arise due to local heating of suspended carbon nanoparticles is believed to be the main mechanism of the OL in the CNTs suspensions [1–3]. The OL in the detonation nanodiamonds (DNDs) suspensions is also concerned with nonlinear light scattering [4, 5], the mechanism of which has not been defined exactly yet.

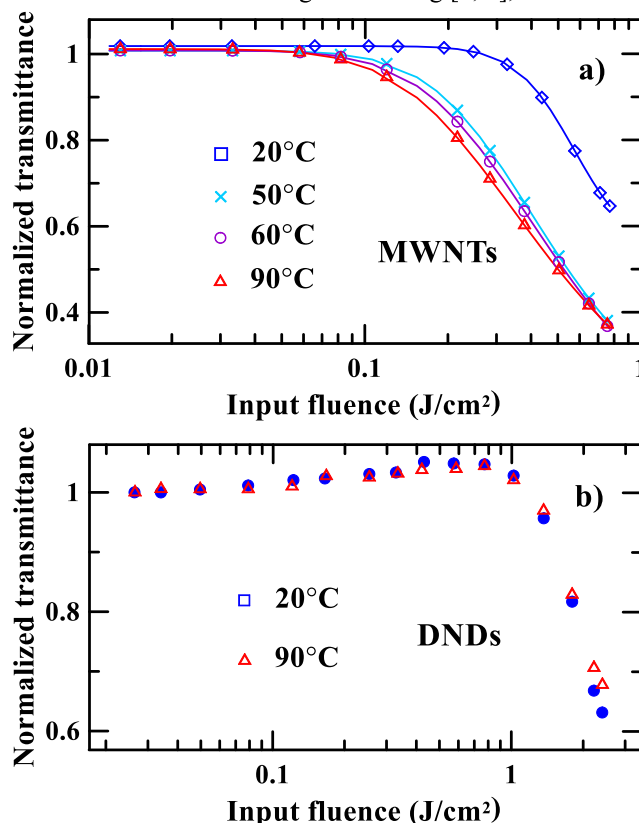


(Fig., a). This indicates that influence of gas bubbles on the OL is in accordance with [1, 3]. Heating of aqueous

DNDs suspensions at the same conditions does not affect the OL performance (Fig., b). However, the formation of microplasmas and strong nonlinear light scattering is observed in the beam waist during the OL process. This all indicate that the OL in aqueous DNDs suspensions is not concerned with the formation of gas bubbles. The

OL in aqueous DNDs suspensions is due to the microplasmas formation that leads to strong nonlinear light scattering.

Acknowledgement

This work was financially supported by RFBR (project No 16-42-180147_r_ural_a).

References

- [1] L. Vivien, P. Lancon, D. Riehl, F. Hache and E. Anglaret, *Carbon*, **40**(10), 1789 (2002).
- [2] J. Wang and W. J. Blau, *Journal of Physical Chemistry C*, **112**(7), 2298 (2008).
- [3] J. Wang, D. Früchtl, Z. Sun, J. N. Coleman and W. J. Blau, *Journal of Physical Chemistry C*, **114**(13), 6148 (2010).
- [4] G. M. Mikheev, A. P. Puzyr', V. V. Vanyukov, K. V. Purtov, T. N. Mogileva and V. S. Bondar', *Technical Physics Letters*, **36**(4), 358 (2010).
- [5] V. V. Vanyukov, T. N. Mogileva, G. M. Mikheev, A. P. Puzir, V. S. Bondar and Y. P. Svirko, *Applied Optics*, **52**(18), 4123 (2013).
- [6] V. V. Vanyukov, T. N. Mogileva, G. M. Mikheev, A. V. Okotrub and D. L. Bulatov, *Journal of Nanoelectronics and Optoelectronics*, **7**(1), 102 (2012).
- [7] G. M. Mikheev, R. Y. Krivenkov, K. G. Mikheev, A. V. Okotrub and T. N. Mogileva, *Quantum Electronics*, **46**(8), 719 (2016).

In this paper we performed comparative study of temperature influence on the OL in aqueous suspensions of CNTs and DNDs using z-scan technique. The results of this study indicate that the OL in aqueous DNDs suspension is concerned with nonlinear light scattering on microplasmas.

The production technology of multiwalled CNTs (MWNTs) used in the experiments is presented in [6]. MWNTs have a diameter of 15 – 20 nm and a length less than 1 mm. The production technology of aqueous DNDs suspension is described in [5]. The average nanoparticles clusters size of DNDs in the suspension was 50 nm. In the experiments suspensions of MWNTs and DNDs were filled into 1 mm-thickness optical cells, with the linear transmittance of MWNTs and DNDs suspensions being of 8% and 30%, respectively. The experiments were carried out using z-scan technique on 532 nm laser setup, with the laser pulses duration being of 14 ns [7]. The laser radiation was focused by lens with focal length of 150 mm. The beam waist diameter was 90 μm and the Rayleigh length $z_0 = 7$ mm.

We found out that heating of aqueous MWNTs suspension from room temperature of 20°C to 90°C significantly improves the OL efficiency

Influence of temperature on optical limiting of detonation nanodiamonds suspension in engine oil

K.G. Mikheev¹, R.Yu. Krivenkov¹, T.N. Mogileva¹, A.P. Puzyr², V.S. Bondar², D.L. Bulatov¹, G.M. Mikheev¹

¹*Institute of Mechanics UB RAS, 34, str. T. Baramzinoy, Izhevsk, 426067, Russia*

²*Institute of Biophysics Siberian Branch of RAS, Federal Research Center "Krasnoyarsk Science Center SB RAS", Akademgorodok, Krasnoyarsk, Russia, 660036
k.mikheev@udman.ru*

Optical limiting (OL) is a nonlinear optical phenomenon at which the transmittance of the medium under study nonlinearly decreases, with increasing the incident radiation power density [1]. The OL in various carbon nanomaterials suspensions has been investigated intensively [2,3], since these materials are widely recognized as very promising for the OL applications [4]. It was shown that the aqueous detonation nanodiamonds (DNDs) suspensions are well suited for developing and creating an optical limiter capable to work in a wide spectral range [5]. However such an optical limiter could not perform both at temperatures close to 100 °C and below 0 °C, since the state of aggregate of host liquid changes. One of the ways to improve it is to use a non-freezing host liquid, e.g. engine oil. Our preliminary experiments have shown the DNDs suspensions in engine oil to be super stable and they have not developed sediment after seven years. Moreover, DNDs suspensions with nanoparticles clusters average size (D_{aver}) 110 and 320 nm in engine oil are more stable than that in water, while the OL efficiency in these suspensions increases with increasing the D_{aver} [3]. It makes study of the OL of DNDs suspensions in engine oil relevant in terms of creation of optical limiters capable to work in a wide temperature range. In this paper we study the influence of temperature on the OL properties of the DNDs suspension in engine oil and, since the mechanisms of the OL in aqueous and oil DNDs suspensions could be different, we also discover the mechanism of the OL in oil suspensions of DNDs.



Fig. The normalized transmittances of the (a) 50 and (b) 110 nm DNDs suspensions in engine oil as functions of z/z_0 measured at different temperatures. The input pulse energy was 88 μJ , the diffraction length of the beam (z_0) was 6.9 mm.

In our experiments we used DNDs which were obtained by a known technology [6]. The 1 wt.% suspensions of DNDs were obtained in engine oil for the experiments. For preparation of engine oil suspensions of DNDs, the particles with an average size of clusters $D_{\text{aver}}=50$ nm and $D_{\text{aver}}=110$ nm in hydrosols were used. OL study was carried out by z-scan technique; 532 nm radiation of YAG:Nd³⁺-laser with passive Q-switching was used as an excitation source [7]. Laser pulse duration was 13.6 ns. In order to heat the suspension, the cell was placed into the specially designed thermostat with two windows for laser beam, able to heat the whole sample up to 100°C and keep preset temperature constant.

In Fig. the results of z-scan study of 50 and 110 nm DNDs suspensions obtained at 532 nm at oil temperatures of 20°C and 100°C are presented. The z-scan data measured at temperatures of 20°C and 100°C are shown to be almost identical. The same results were obtained at middle temperature points for both suspensions. This indicates that increasing the engine oil temperature up to 100°C is not accompanied with the OL threshold changing. Therefore, independence of the OL

performance on the temperature makes it possible to use the DNDs suspension in engine oil as optical limiter at the temperature range of 20-100°C. In addition, this fact could be used to discover the nature of nonlinear scattering in the oil DNDs suspension.

Acknowledgement

This work was financially supported by RFBR (project No 16-38-00553).

References

- [1] K. Mansour, M.J. Soileau, E.V. Van Stryland, J. Opt. Soc. Am. B., **9**, 7, 1992.
- [2] I.M. Belousova, D. A. Videnichev, I. M. Kislyakov, T. K. Krisko, N. N. Rozhkova, S. S. Rozhkov, Opt. Mater. Express, **5**, 1, 2015.
- [3] V. V. Vanyukov, T. N. Mogileva, G. M. Mikheev, A. P. Puzyr, V. S. Bondar, Y. P. Svirko, Appl. Opt., **52**, 18, 2013.
- [4] J. Wang, Y. Chen, R. Li, H. Dong, L. Zhang, M. Lotya, J. N. Coleman and W. J. Blau. *Nonlinear Optical Properties of Graphene and Carbon Nanotube Composites* (Carbon Nanotubes - Synthesis, Characterization, Applications, InTech, 2011).
- [5] V. V. Vanyukov, G. M. Mikheev, T. N. Mogileva, A. P. Puzyr, V. S. Bondar, Y. P. Svirko, Appl. Opt., **54**, 11, 2015.
- [6] V.S. Bondar, A.P. Puzyr, Phys. Solid State, **46**, 4, 2004.
- [7] G. M. Mikheev, R. Yu. Krivenkov, K. G. Mikheev, A. V. Okotrub, T. N. Mogileva, Quantum Electron., **46**, 8, 2016.

Influence the aggregate's size of multiwalled carbon nanotube on dielectric properties of nanotube/polymer composites

Moseenkov S.I.¹, Kuznetsov V.L.^{1,2}, Suslyayev V.I.², Dorozhkin K. V.²

¹ Boreskov Institute of catalysis SB RAS, Novosibirsk, Russia

² National Research Tomsk State University, Tomsk, Russia

moseenkov@catalysis.ru

Due to their unique mechanical and electrical properties multiwalled carbon nanotubes MWCNT are widely used for different practical applications. The most often MWCNTs are used as a component of composite materials. Homogeneity of MWCNT distribution in composite matrixes is a key characteristic influencing on properties of resulting composite. Traditionally investigators are concentrated on the production of materials with uniform distribution of MWCNT composite matrices.

Generally, an increase in the content MWCNT composite nanotubes with uniform distribution in the matrix leads to an increase of its electrical conductivity and permittivity. This limits the possibility of EMI composites with controlled properties. Changing the type of MWCNT distribution in the composite can significantly extend the range of concentrations at which percolation threshold is achieved [1], and the flexibility to manage its physical properties.

Earlier we have shown that dielectric properties of MWCNT/polymer composite depends on the procedure for sample preparation [2]. The uniform distribution of MWCNTs in polymer matrixes results in the low percolation threshold, while the samples of composite with high content of MWCNTs had a high real and imaginary parts of dielectric permittivity.

In this paper, we have performed a comparative study of EMI response of two types of composites on the base of epoxy resins and MWCNTs with different type distribution of nanotubes in epoxy resin matrixes. Namely, (A) with uniform distribution of MWCNTs, and (B) with uniform distribution of MWCNT agglomerates of controlled size, preliminary isolated within polymethylmethacrylate shells (see Fig.1) We have changed the thickness of dielectric layer, diameter of aggregates and concentration of MWCNT's aggregates into epoxy matrices.

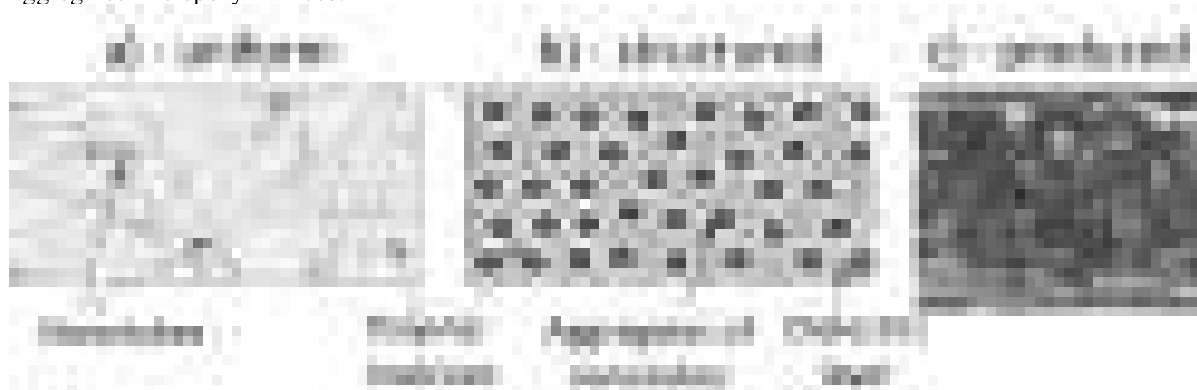


Fig. 1. Difference in structure for MWCNT composites with uniform (a) and structured (b) distribution of nanotubes. c) – SEM image of obtained MWCNT/epoxy composite.

The structure of MWCNT/epoxy composites was investigated using optical and scanning electron microscopy. Dielectric spectra of permittivity was obtained in range 430-720 GHz. It has shown that frequency dependence of dielectric permittivity of structured composites differs significantly from composites with uniform distribution of MWCNT. Thus the composites with the isolated MWCNT agglomerates demonstrate diminished reflectivity and increased absorbance of EMI.

This work was partially supported by project MK-7588.2016.3

[1] Pang, H., Xu, L., Yan, D.-X., Li, Z.-M., 2014. Conductive polymer composites with segregated structures. Progress in Polymer Science, Topical Issue on Nanocomposites 39, 1908–1933.

[2] Kazakova, M.A., Kuznetsov, V.L., Semikolenova, N.V., Moseenkov, S.I., Krasnikov, D.V., Matsko, M.A., Ishchenko, A.V., Zakharov, V.A., Romanenko, A.I., Anikeeva, O.B., Tkachev, E.N., Suslyayev, V.I., Zhuravlev, V.A., Dorozhkin, K.V., 2014. Comparative study of multiwalled carbon nanotube/polyethylene composites produced via different techniques: MWCNT/polyethylene composites produced via different techniques. physica status solidi (b) 251, 2437–2443.

Single walled carbon nanotube quantification method employing the Raman signal intensity

Irina I. Nefedova, Dmitri V. Lioubtchenko, Ilya V. Anoshkin, Igor S. Nefedov, Antti V. Räsänen

*Aalto University School of Electrical Engineering, Department of Radio Science and Engineering, Finland
irina.nefedova@aalto.fi*

CNT layers can be employed for transparent electrode fabrication [1, 2] fuel and solar cells, supercapacitors, etc. [3, 4]. A measurement technique for the number of carbon nanotubes in the CNT layer is needed. Non-destructive characterization techniques for carbon nanotube content measurements like scanning electron microscopy (SEM), atomic force microscopy (AFM) etc. do not allow to estimate the number of carbon atoms in the layer.

The quantification of the carbon nanotube contents in any layers and in polymer/dispersion systems transparent for the wavelength in the range of 633-740 nm has been developed. It is based on determination of the G peak intensity of the Raman spectrum, together with precise mass measurement and optical absorbance measurements. This method opens an opportunity for the quantitative mapping of sp^2 carbon atoms distribution in the SWCNT layers with a resolution limited by the focused laser spot size.

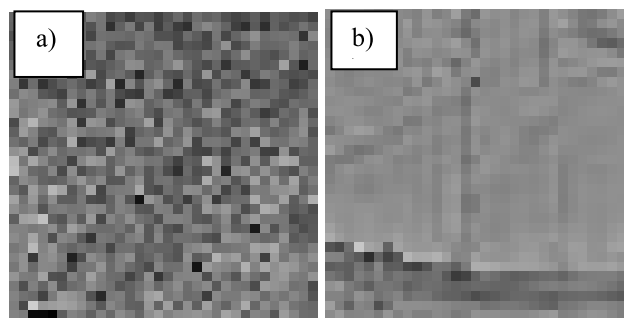


Figure 1. SEM (a) and TEM (b) images of the SWCNTs. In capture (b) both single walled CNTs and bundles of them are visible.

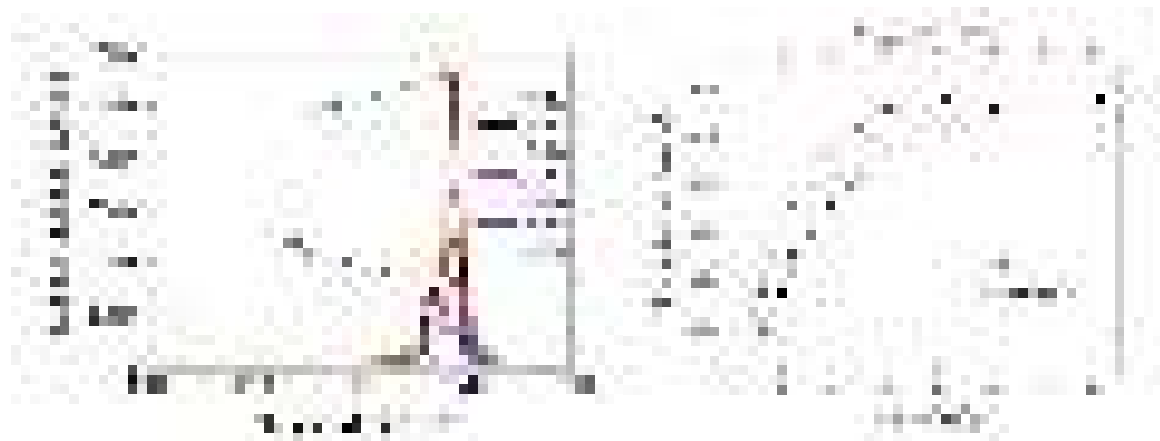


Figure 2. Raman spectra for SWCNT samples with different optical transparencies (%) and dependencies of the number of carbon atoms in the SWCNT layer, normalized to the surface area N_C/S and the number of SWCNTs in the layer, normalized to the surface area N_{SWCNT}/S on the Raman intensity I .

This work was financially supported in part by the Academy of Finland through the DYNAMITE project, by Nokia and Teknologiateollisuuden 100-vuotissäätiö Foundations and by Aalto ELEC Doctoral School. The authors are grateful prof. A.G Nasibulin for the fruitful discussion. This work was carried out using the Aalto University Nanomicroscopy Center (Aalto-NMC) facilities.

[1] L.B. Hu, D.S Hecht, G. Gruner, Chem Rev, 110, 5790, (2010).

[2] A.G Nasibulin, A. Kaskela, K. Mustonen, A.S Anisimov, V. Ruiz, S. Kivistö, et al., ACS Nano, 5, 3214, (2011)..

[3] M. Borghei, G. Scotti, P. Kanninen, T. Weckman, I.V. Anoshkin, A. Nasibulin, et al., Energy, 65, 612, (2014).

[4] A. Santasalo-Aarnio, M. Borghei, I.V. Anoshkin, A.G. Nasibulin, E.I Kauppinen, V. Ruiz, et al., Int. J. Hydrogen Energ., 37, 3415, (2012).

Branched Carbon nanostructures: Synthesis, Characterization and Application

E.A. Obratzova,^{1,2} D.V. Basmanov,² N.A. Barinov,² and D.V. Klinov^{1,2}

1 M.M.Shemyakin & Yu.A. Ovchinnikov Institute of Bioorganic Chemistry, Russian Academy of Sciences, Miklukho-Maklaya 10/16, 117997, Moscow, Russia

2 Scientific Research Institute of Physico-Chemical Medicine, Moscow, Malaya Pirogovskaya 1a, 119435, Russia

Carbon nanomaterials with various crystalline structures are among the most attractive objects in current material science. By simply changing the synthesis conditions one can obtain a wide range of materials beginning from graphene and nanotubes to diamond. Undeservedly little attention is received, to our opinion, by amorphous materials from nanocarbon family. In this work we describe the synthesis procedure and present the main characteristics of a branched carbon structures proved to be an outstanding material for efficient and easy high-resolution atomic force microscopy.



Figure 1. Schematic of the branched carbon nanostructures growth procedure.

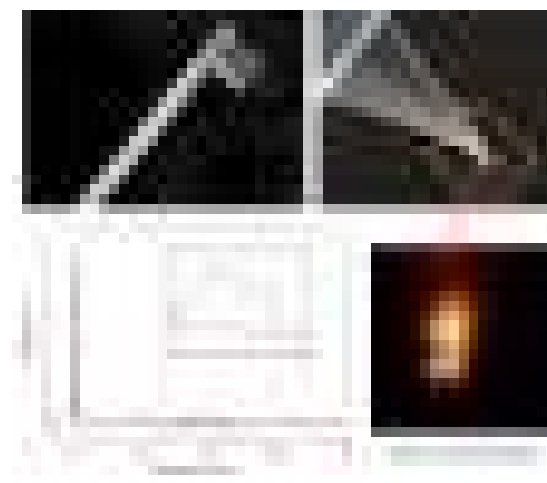


Figure 2. SEM images and Raman spectra of the nanostructures grown at the apex of an AFM probe.

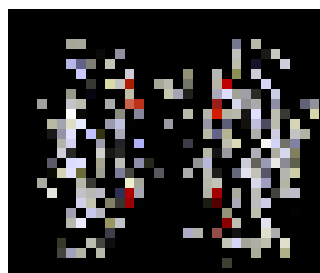


Figure 3. AFM images of the biotin-streptavidin complex showing the two units of the complex obtained for the first time using the AFM probes with branched carbon structures at the apex.

Acknowledgements: The work was supported by RFBR grant 15-32-70014.

1-Bromoadamantane Molecules Arrangement Inside Single-Walled Carbon Nanotube

Andrey Orekhov^{1, 2}, Andrey Chuvilin^{3, 4}, Alexander Tonkikh^{5, 6}, Dmitriy Rybkovskiy^{5, 6}, Elena Obraztsova⁶

¹ Shubnikov Institute of Crystallography of FSRC «Crystallography and Photonics» of RAS, Moscow, RUSSIA

² National Research Center «Kurchatov Institute», Moscow, RUSSIA

³ CIC nanoGUNE Consolider, Donostia - San Sebastian, SPAIN

⁴ IKERBASQUE Basque Foundation for Science, Bilbao, SPAIN

⁵ Faculty of Physics, Southern Federal University, 344090, Rostov-on-Don, Russia

⁶ Prokhorov General Physics Institute of Russian Academy of Sciences, Moscow, RUSSIA

Andrey.orekhov@gmail.com

Inner channel of single walled carbon nanotubes (SWCNT) could be used as a nanoreactor to create novel one-dimensional structures which are unstable in freestanding systems. Filling the SWCNT leads to changing of optical and electronic properties of nanocomposite making them suitable for application in photonic and optoelectronic devices. The formation of narrow 1D sp³ bonded structures is a very promising task on which a number of research groups are working to date. Diamondoid molecules are promising building blocks for this kind of system, but there are relatively few studies of such structures. Analysis of guest molecules arrangement could be performed by High-Resolution Transmission Electron Microscopy (HRTEM) technique. Application of the low voltage transmission electron microscopy allows to reduce the irradiation damage of the sample and to increase the TEM image contrast, which is important for materials with light elements.

The TEM measurements of 1-bromoadamantane@SWCNT were performed with a Titan 60-300 TEM/STEM microscope (FEL, The Netherlands) at acceleration voltage of 80 kV equipped with monochromator and CEOS image spherical aberration corrector. The chemical composition was estimated by X-ray Energy Dispersion Spectroscopy (EDS) technique. TEM image interpretation was carried out by comparison with simulated HRTEM images.

The presence of bromine atom in the molecule composition allows to use EDS technique for analysis of the filling result. In accordance to the presence of Br signal at EDS spectra obtained from filled SWCNT lead to the conclusion that the 1-bromoadamantane molecules successfully loaded into the nanotube. Analysis of HRTEM images revealed the carbon structures formation inside the nanotubes which are apparently formed as a result of the 1-bromoadamantane guest molecules arrangement. Besides, in the nanotube channel the free atoms migrating along the guest structures were observed. HRTEM images simulation was applied to confirm that migrating atoms correspond to bromine. The experimental and simulated data were in good agreements.

To summarize, the filling of SWCNT with 1-bromoadamantane molecules leads to formation of carbon structures with freestanding Br atoms inside the inner nanotube channel.

Acknowledgements.

The work was supported by RSF-15-12-10004.

Computer modeling of H-terminated linear carbon chains

A. V. Osadchy^{1,2}, E. D. Obraztsova^{1,2}, L.A. Savina³, V. V. Savin³

¹ A.M. Prokhorov General Physics Institute RAS, Vavilova 38, Moscow 119991, Russia

² National Research Nuclear University MEPhI (Moscow Engineering Physics Institute), Kashirskoye shosse 31, Moscow, 115409, Russia

³ Immanuel Kant Baltic Federal University, Nevskogo str., 14, Kaliningrad, Russia, 236041

Corresponding author e-mail: aosadchy@kapella.gpi.ru

The work is devoted to the theoretical study of hydrogen terminated linear carbon chains (LCC). LCC are the one-dimensional structures, consisting of chains of carbon atoms with alternating single and triple bonds of varying length. Free bonds at the ends of the chains are terminated by hydrogen atoms. The calculations have been performed using the density functional theory (DFT) with decomposition of electronic wave functions into plane waves as implemented in Quantum Espresso software package [1,2]. The stable configurations of carbon chains encapsulated in the single-wall carbon nanotubes of various diameters and isolated different lengths carbon chains have been calculated. A computer simulation of the band structure, infrared absorption spectra and Raman spectroscopy of carbon chains, encapsulated in single-wall carbon nanotubes and various lengths isolated chains have been performed. The weak influence of the single-walled carbon nanotube to the carbon chain band structure have been demonstrated. The resulting dynamics of the band gap width and the results of the simulation of the Raman spectra of chains are in good agreement with the published experimental and theoretical data [3,4].

Acknowledgements This work was supported by RFBR 15-02-09073 and RAS research programs.

[1] P. Giannozzi et al., *J. Phys. Condens Matter* 21, 395502 (2009).

[2] Arno Schindlmayr, P. Garcia-Gonzalez, et al., *Phys. Rev. B* 64, 235106 (2001)

[3] N.R. Arutyunyan, P.V. Fedotov, V.V. Kononenko, *Journal of Nanophotonics* 10, 012519 (2016).

[4] A. Milani, M. Tommasini, et. al., *Beilstein J. Nanotechnology*, 6, 480–491 (2015)

Electromagnetic properties of carbon nanotube based composites in Ka-band (26-37 GHz)

D. Meisak^{1,a}, K. Piasotski¹, G. Gorokhov¹, D. Bychanok^{1,2}

¹*Institute for Nuclear Problem of Belarus State University, Belarus*

²*Ryazan State Radio Engineering University, Russia*

^a*dariameysak@gmail.com*

Dispersive composite materials based on multiwall carbon nanotubes [1] in epoxy resin matrix are produced and their electromagnetic responses are investigated in Ka-band (26-37 GHz). Both theoretical and experimental results demonstrate high potential of fabricated composites to be used as compact effective absorbers in 26-37 GHz range.

Microwave measurements were carried out using a scalar network analyzer ELMIKA R2-408R [2]. All measurements were performed in a 7.2×3.4mm waveguide system. To analyze the electromagnetic properties of the investigated samples the standard procedure was used to convert S-parameters to dielectric permittivity spectrum [3] (see Fig.1).



Fig. 1. Dielectric permittivity spectra of epoxy resin based composites with various MWCNTs content.

Theoretical analysis shows that composites with MWCNTs [3] content 1.5%wt. are most promising for absorption applications in Ka-band.

To summarize, effective absorbing properties of composites may be achieved by addition of small amounts of multi-walled carbon nanotubes in commercially available epoxy resin matrix. Using dispersive materials may significantly improve absorption properties of composites. In fact, for composites with 1.5% MWCNTs the absorption coefficient within whole Ka-band is in the range from 84 up 100% inside the waveguide was experimentally observed. The predicted absorbing properties of the investigated composites in free space are close to theoretical maximum of 97-100% for whole Ka-band.

The work is supported by Federal Focus programme of Ministry of Education and Science of Russian Federation, project ID RFMEFI57715X0186.

[1] <http://nano.bsu.by/products/mwcnt>

[2] D. Bychanok et al. Progress In Electromagnetics Research C, **66**, 77-85 (2016).

[3] Standard test method for measuring relative complex permittivity and relative magnetic permeability of solid materials at microwave frequencies, ASTM D5568-08, 2009.

Photoluminescence and photoresponse from graphene oxide quantum dots/PANI/PVA-based composite

Tomskaya A.E., Kapitonov A.N., Popov V.I., Smagulova S.A.

North-Eastern Federal University, Yakutsk

ae.tomskaya@s-vfu.ru

Graphene pure, doped, or hetero-combination provides the basis for photodetectors. Changing the structure of graphene is used to configure the properties or for using of synergies. In addition to the above modifications, graphene can form intercalation compounds.

In this paper graphene intercalation compound with using graphene oxide quantum dots (GO-QDs), HCl doped polyaniline (PANI) and polyvinyl alcohol (PVA) was synthesized. GO-QDs were chosen due to the fact that they have the kinetic energy of formation of bonds more efficiently than that of graphite. We report a simple method for obtaining the GO-QDs with glucose as precursor for GO-QDs and with using the microwave radiation during production. [1] Produced by that method GO-QDs show a broadband radiation in the range from 300 nm to 1000 nm. The width of the emission band of GO-QDs is one of the widest among all semiconductor materials and their counterparts among the quantum dots. Broadband emission is due to the layered structure of the GO-QDs, which consists of a large conjugated system of delocalized π -electrons. Further, when excited at different wavelengths ranging from 300 nm to 800 nm broadband NGQDs photoresponse has an unusual negative photocurrent. In addition, GO-QDs demonstrate photoresponse from 300 nm to 800 nm with a sensitivity of up to 109 V/W at 409 nm.

For effective using of the GO-QDs in optoelectronic applications required to use an additional matrix to improve the electrical properties. As is well known, the PANI is a conductive polymer, consisting of emeraldine base (EB) and salt phases (ES). During intercalation PANI and GO-QDs EB region of PANI output protons from the groups OH/COOH(GO-QDs), which is essentially a manipulation of the carrier density separately from the interplanar interface of the GO-QDs.[2] Analysis of photoresponse upon UV-VIS irradiation of GO-QDs, PANI and their composite revealed that the polarity is controlled.

Addition of PVA promotes the creation of additional hydrogen bonds between oxygen functional groups in the GO-QDs/PANI/PVA composite and increases emission efficiency at high contents of PVA.[3] Strong illumination over a wide range of visible radiation was found in 10% of the weight of GO-QDs in the PVA matrix and at 15% of the weight of GO-QDs quenching of the photoluminescence as observed.

[1] Libin Tang, Rongbin Ji, Xueming Li, et al. *ACS Nano*, DOI: 10.1021/nn501796r, 2014.

[2] Sesha Vempati, Sefika Ozcan, and Tamer Uyar, *Applied Physics Letters*, 106, 051106, 2015.

[3] Meryem Goumri, Jany We'ry Venturini, Anass Bakour, Mohammed Khenfouch, Mimouna Baitoul, *Appl. Phys. A*, 122:212,

The surface electrochemical strong doping of single walled carbon nanotubes and graphene films

Alexander A. Tonkikh¹, Ivan I. Kondrashov¹, Valentina A. Eremina^{1,2}, Elena D. Obratsova¹

¹*A.M. Prokhorov General Physics Institute of Russian Academy of Sciences, Vavilov Strasse 38,*

Moscow 119991, Russia

²*M.V. Lomonosov Moscow State University, Faculty of Physics, Leninskie Gory Strasse 1,*

Moscow 119991, Russia

In the present investigation the surface electrochemical doping has been applied to study excitonic states and Raman mode features observed under the strong doping in single walled carbon nanotubes (SWCNTs) and graphene films. The doping procedure was carried out in double layer supercapacitor configuration with utilizing gel electrolytic system based on poly(vinyl alcohol) and H_2SO_4 . The samples of strongly doped SWCNTs and graphene were studied by in-situ Raman and UV-vis-NIR measurements. The Raman spectroscopy showed the upshift of the G-band when the applied a negative gate voltage. The in-situ UV-vis-NIR measurements under the negative gate voltage bias showed strong Burstein–Moss effect and density of states renormalization for SWCNTs.

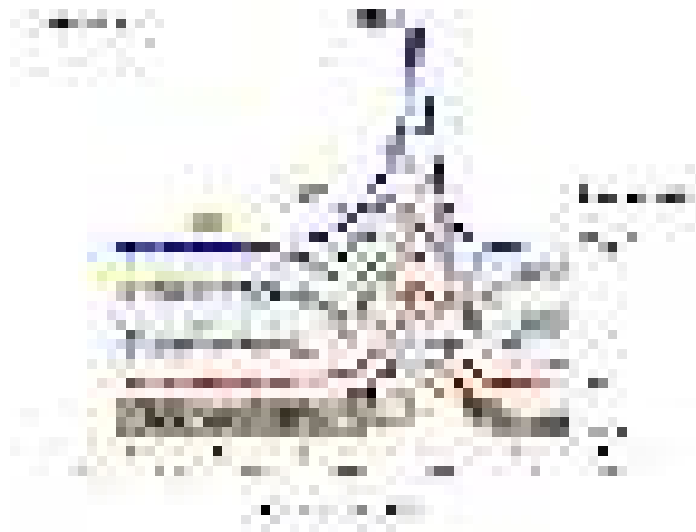


Fig.1. Raman spectra of electrochemically doped SWCNTs by gate voltage bias from +1,5V to -1,5V.

Graphene oxide suspensions for 2D Printing

Vasileva F.D.¹, Kapitonov A.N.²

Federal State Autonomous Educational Institution of Higher Education

"M. K. Ammosov North-Eastern Federal University"

Dorush21@mail.ru¹, kapitonov1944@mail.ru²

In response to its unique properties, graphene is attractive 2D material for the use in inkjet technology. Graphene-based 2D printing- one of the most prospective direction of modern electronics and photonics development. As opposed to the similar methods, 2D printing differs in low cost of technological process, ability to print on different substrates, including on flexible.

Due to some difficulties in obtaining graphene, graphene oxide is exceptionally prospective material for the use in 2D printing. In contrast to graphene, graphene oxide forms a stable aqueous suspensions, which does not require replacement of the solvent prior printing. Organic solvents in which graphene is stable, strongly impair the conductivity of the material and require high temperature for their removal, which is not desirable in flexible electronics.

In recent times, the most promising method for graphene oxide producing -electrochemical exfoliation of graphite in an aqueous of inorganic salt solutions [1]. This method, unlike the Hammer method, allows obtaining in a short time (10 - 20 min) sufficient amount of material and does not require the use of strong acids. And most importantly, it leads to the formation of weakly oxidized graphene, due to only marginal oxidation during the reaction. The mechanism of this reaction is described in detail in articles [2,3].

The scientific novelty of the work lies in the fact that it is possible to change the oxidation state of graphene depends on the electrolyte concentration. In its turn leads to the recovery possibility of oxidized graphene at a relatively low temperature and 2D printing technology use, where the flexible substrates which aren't maintaining high temperatures are applied.

Electrochemical exfoliation of graphite was carried out in an electrolyte based on an aqueous solution of ammonium sulfate $(\text{NH}_4)_2\text{SO}_4$. To determine the optimal concentration of the electrolyte, aqueous solutions were prepared $(\text{NH}_4)_2\text{SO}_4$ at the following concentrations: 0.05; 0.1; 0.15; 0.3 M. The reaction of electrolysis was conducted at a positive voltage (15V) on a graphite electrode. The reaction time was 15 minutes.

It has been shown that it is possible to change the oxidation state of graphene oxide, depending on the electrolyte concentration in the range 0,2-0,28 with standard deviation $\sigma = 0,02$.

The optimum concentration of electrolyte is 0.15 M for the graphene oxide with a low degree of oxidation 0.2.

The lateral size of graphene oxide flakes are not more than 400 nm, and the thickness right of 1-2 nm.

For the electrolyte concentration of 0.15M resistance at an annealing temperature of 300 ° C was 1.3 k Ω /□. Hall mobility - 7,1 cm²/V*s.

Thus, the received graphene oxide suspension at concentration of electrolyte 0.15 M is suitable for use in the inkjet 2D printing on flexible substrates.

[1] C.T.J. Low., et al. Carbon, **54** 1 (2013).

[2] K. Parvez., et al, J. Am. Chem. Soc, **136** 6083 (2014).

[3] K.W. Hathcock, J.C. Brumfield, C.A.Goss, E.A. Irene, R.W. Murray. Anal Chem, 67:2201-6.(1995);

Transfer of CVD grown graphene by lamination method for transparent conducting films

Popov V.I., Timofeev V.B., Nikolaev D.V., Timofeeva T.E., Smagulova S.A., Vinokurov P.V.

North-Eastern Federal University, 677000, Belinskogo str., Yakutsk, Republic of Sakha (Yakutia), Russia

pv.vinokurov@s-yfu.ru

Transparent conducting films are widely used in a variety of photovoltaic devices: LCDs, OLEDs, touch panels and solar cells. Currently, the Indium Tin Oxide is most common material for transparent conducting films due to its high conductivity and transparency, but high cost and fragility make it not suitable for flexible electronics. Therefore, new flexible material like carbon nanotubes and graphene are intensively investigated. Chemical vapor deposition (CVD) method is commonly used for growth of large area graphene. The main disadvantage is multiple step transfer process onto different substrates. Electrical properties of the transferred films strongly depend on substrate materials, used chemical reagents and transfer methods [1]. The promising method of graphene transfer onto polymer flexible substrate can be a laminating method [2, 3].

In this work we apply the direct transfer method of CVD grown graphene onto a transparent polymer substrate to obtain transparent conducting films. Standard laminator and laminating films were used for realizing of this transfer process. Copper foil with CVD grown graphene on it is attached to the polymer film by laminator. After the copper substrate etching, the transparent conducting films with improved electrical and optical characteristics were obtained.

References

- [1] И.В. Антонова, С.В. Голод, Р.А. Соотс, А.И. Комонов, В.А. Селезнев, М.А. Сергеев, В.А. Володин, В.Я. Принц ФТП, **45**, 6 (2014)
- [2] L.G.P. Martins, Yi Song, T. Zeng, M.S. Dresselhaus, et al., PNAS, **110**, 44 (2013)
- [3] Xu Ping, Kang Junmo, et al., ACS Nano, **8**, 9 (2014)

Stable Graphene Conformations from Pull and Release Experiments: A Different Application of Molecular Dynamics

Ruslan D. Yamaletdinov^{1,*}, Yuriy V. Pershin^{1,2}

¹*Nikolaev Institute of Inorganic Chemistry SB RAS, Novosibirsk 630090, Russia*

²*Department of Physics and Astronomy, University of South Carolina, Columbia, South Carolina 29208, USA*

*yamaletdinov@niic.nsc.ru

In this work, we explore various stable conformations of a graphene nanoribbon and, at the same time, demonstrate that the graphene folding can be realized in pull and release experiments. The main idea of such experiments, which are implemented here by numerical modelling, can be explained by three major steps of the proposed process: (i) graphene stretching by an external force, (ii) non-equilibrium dynamics after the force removal, and (iii) spontaneous emergence of a folded structure.

Unfortunately, the dynamics of such a process is not accessible analytically. Therefore, we have performed extensive numerical simulations with a goal of finding distinctive folded states, and determining the probabilities of their formation at various values of the pulling force and types of boundary conditions. Our molecular dynamics simulations demonstrate that, indeed, the above process folds flat graphene nanoribbons into various stable conformations. We have classified these conformations and analyzed the probabilities of their appearance as a function of the pulling force. Frequently observed conformations are exhibited in Fig. 1.

Importantly, we have found that the ground state of nanoribbons depends on their length. As it is shown in Fig. 2, the lowest energy state of very short nanoribbons is the flat one (state D in Fig. 1). As the nanoribbon length increases, the energy of a bilayer (wrinkle-like, state A) conformation becomes the lowest, and, at longer lengths, a spiral (rolled, state H) conformation turns into the ground state. Moreover, we emphasize that a significant role in the folding process is played by thermal fluctuations. It has been found that distinct folded states are generated in separate numerical experiments employing identical modelling parameters.

Physically, the folding occurs when the elastic potential energy of the stretched graphene is sufficient to overcome energy barriers separating the flat graphene from its folded conformations. In this way (as a part of its dynamics), the graphene may reach certain crumpled states that further develop into stable folded conformations. It should be emphasized that the process of folding by itself is not a simple process. According to our observations, very often the folded structure emerges through a continuous evolution of a locally nucleated bilayer graphene.

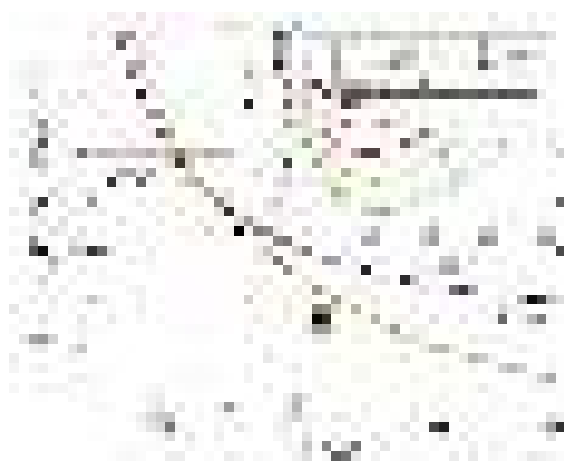


Fig. 2: Energies of A and H as functions of the nanoribbon length L . Dots and triangles represent MD simulations results, theoretical curves are represented by lines. Inset: the spiral conformation energy as a function of the inner radius of the spiral.



FIG. 1: A-G: Frequently observed conformations of a graphene nanoribbon. The conformation energy increases with the letter's position in the alphabet. H: Nanoribbon's ground state.

This work has been supported by the Russian Scientific Foundation grant No. 15-13-20021.

Diamond Refractive X-ray Lenses

M. Polikarpov^a, N.Klimova^a, I. Snigireva^b, V.Savin^a and A.A. Snigirev^a
^aImmanuel Kant Baltic Federal University (Kaliningrad, Russia), ^bESRF (Grenoble, France)

The intensive development of X-ray refractive optics' instrumentation and tools has given birth to X-ray refractive lenses which are now the standard elements at third-generation synchrotron radiation sources. In view of the global switch to the fourth generation of synchrotron sources and X-ray Free Electron Lasers, there is a growing need for x-ray optical elements fabricated from materials that can withstand extreme heat and radiation loads while still providing effective focusing and imaging. Diamond can satisfy all the requirements provided that a suitable lens manufacturing technology is available.

In our research, for the first time diamond planar refractive lenses were fabricated by laser micromachining in up to 1.2 mm thick diamond plates (both mono- and polycrystalline) which were grown by CVD and HPHT. Various linear lenses with apertures up to 1mm and radii of the parabola apex up to 500 μm were manufactured and analyzed with SEM, AFM, Raman spectroscopy and, of course, X-ray tests at the European Synchrotron Radiation Facility (ID06 beamline). A uniform intensity of the image of the focused X-ray beam showed the high quality of the lens's side walls and profile allowing to focus the X-radiation in accordance with the lens' demagnification factor. Planar lenses were followed by 2D parabolic X-ray refractive half lenses, which were also manufactured by laser micro-machining of single-crystal diamond. A single 2D lens had an aperture of 1 mm and parabola apex radii of 200 μm . Forming a compound refractive lens with 24 single lenses within, it has been successfully tested in the focusing and imaging modes both at the synchrotron sources and at the laboratory setups. Unique optical properties of diamond coupled with its excellent thermal qualities allows such lenses to be applied as focusing, imaging and beam-conditioning elements at high-heat flux beams of today and future X-ray sources.

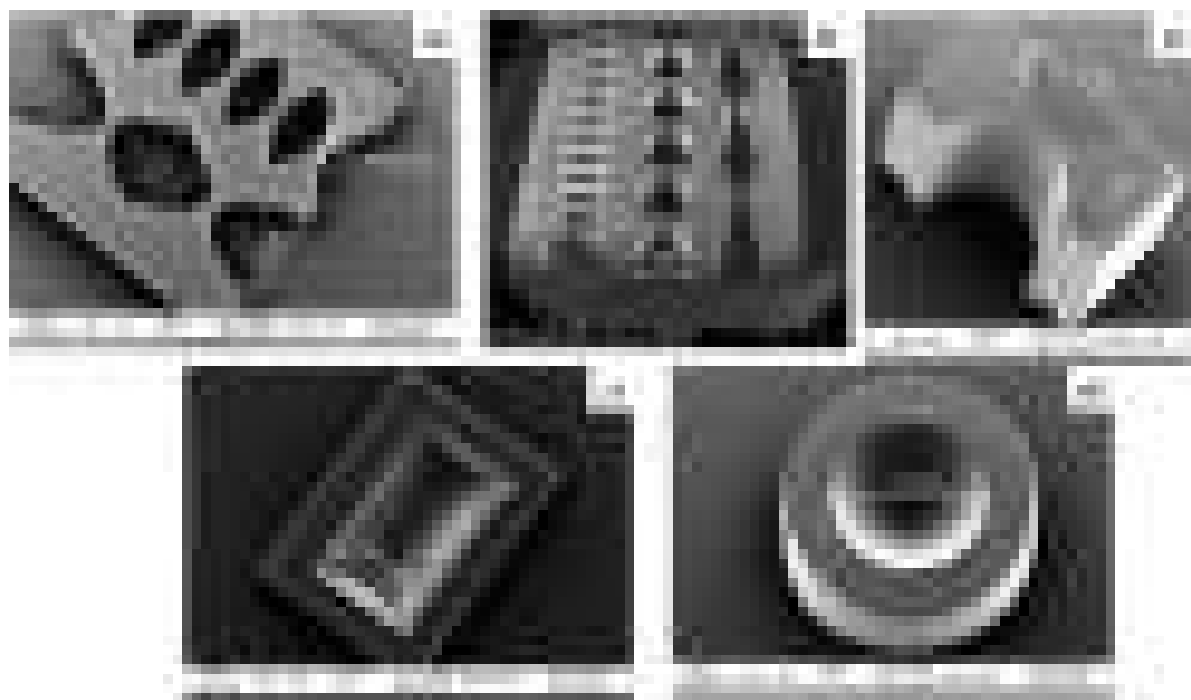


Fig.1. Diamond refractive x-ray lenses [1].

In addition, as lenses are made from single crystal, the Bragg law can be satisfied, depending on crystallographic orientation of the lens substrate or on the photon energy of incident-to-lens X-rays. Due to the Bragg diffraction, transmitted intensity might be dramatically reduced. This problem is well known in X-ray spectroscopy and is called "glitch". So we demonstrate the existence of the diffraction in the focusing mode of the refractive lens and measure the magnitude of the effect.

References

- [1] T. V. Kononenko, V. G. Ralchenko, E. E. Ashkinazi, M. Polikarpov, P. Ershov, S. Kuznetsov, V. Yunkin, I. Snigireva, & V. I. Konov, *Applied Physics A*, **122**, 152 (2016).

The work was supported by the Ministry of education and science of the Russian Federation (grants № 14. Y26.31.0002, № 02.G25.31.0086, state task №16.4119.2017/ПЧ).

Teasing of the Chiral Quantum State and Valley Tuning in van der Waals Heterostructures

Davit Ghazaryan¹, John R. Wallbank^{1,2}, Abhishek Misra¹, Yang Cao³, Tom L. Lane^{1,2}, Mark T. Greenaway⁴, Lawrence Eaves^{2,4}, Andre K. Geim³, Vladimir I. Fal'ko^{1,2}, Artem Mishchenko^{1,2}, Konstantin S. Novoselov^{1,2}

¹*School of physics and Astronomy, University of Manchester, Manchester M13 9PL, UK*

²*National Graphene Institute, University of Manchester, Manchester M13 9PL, UK*

³*Centre for Mesoscience and Nanotechnology, University of Manchester, Manchester M13 9PL, UK*

⁴*School of Physics and Astronomy, University of Nottingham, Nottingham NG7 2RD, UK.*

davit.ghazaryan@postgrad.manchester.ac.uk

Chirality is a fundamental property in the relativistic physics that has been also found in Dirac quasiparticles of cleaved graphene layers. Chiral nature of Dirac electrons is pivotal for such a phenomena's like half-integer quantum hall effect[1], absence of back scattering in p-n junctions [2], Klein tunneling[3], specific features in weak localization[4] etc. However, it has proved extremely difficult to directly visualize the chirality in electronic transport measurements. We will report the direct observation and manipulation of chirality and pseudospin degrees of freedom in the tunneling of electrons between two almost perfectly aligned graphene crystals. To this end, a strong in-plane magnetic field was used to resolve the contributions of the chiral states – a new technique for preparing graphene Dirac electrons in a particular quantum chiral state in a selected valley, which enables tunneling of valley-polarized electrons in monolayer and bilayer graphene, also allows one to selectively inject carriers propagating in the same direction and to probe pseudospin-polarized quasi-particles. In principle, the technique can be extended to tunneling devices in which surface states of topological insulators are used as electrodes; then, all-electrical injection of spin-polarized current with noninvasive tunneling contacts could reveal a number of exciting phenomena.

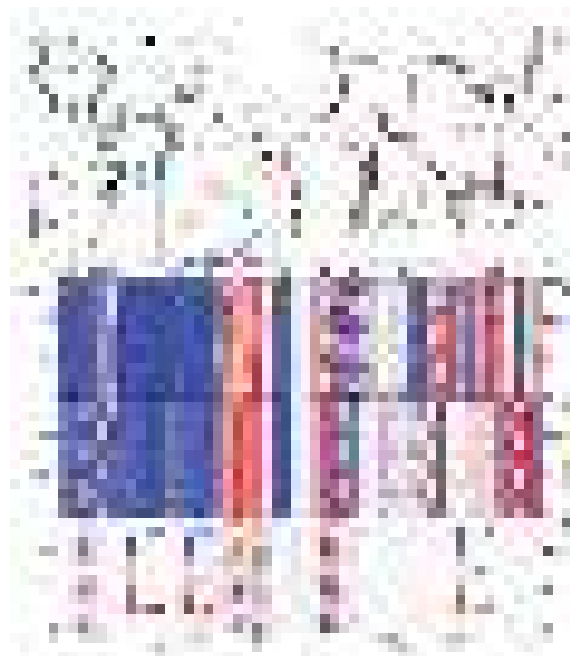


Fig. 1. a) Schematic representation of the BZ for the emitter (blue) and collector (red) graphene electrodes rotated by a small angle with respect to each other. Circles represent the Fermi surfaces in the two graphene layers. C) Resonance in dI/dV_b corresponding to (B). (D) As in (A) but with B field applied parallel to graphene layers. The Lorentz force leads to an additional momentum acquired by electrons when tunnelling from the emitter to the collector, which can be represented by a relative shift of the two BZs. (F) The resonant peak in dI/dV_b splits into six peaks in finite magnetic field (red curve), each corresponding to a resonance that occurs in each corner of the BZ (green and blue curves for K and K' valleys, respectively). Examples for particular resonant conditions for two corners of the BZ are shown in (D) and (E).

References

- [1] K. S. Novoselov et al., Nature 438, 197–200 (2005).
- [2] A. F. Young, P. Kim, Nat. Phys. 5, 222–226 (2009).
- [3] M. I. Katsnelson, K. S. Novoselov, A. K. Geim, Nat. Phys. 2, 620–625 (2006).
- [4] E. McCann et al., Phys. Rev. Lett. 97, 146805 (2006).

Research of field emission properties of single-walled carbon nanotubes modified by annealing and doping with CuCl

Eugene V. Redekop¹, Victor I. Kleshch¹, Alexander A. Tonkikh^{2,3}, Elena D. Obratsova³, and Alexander N. Obratsov^{1,4}

¹Department of Physics, M.V. Lomonosov Moscow State University, 119991, Moscow, Russia

²Faculty of Physics, Southern Federal University, Rostov-on-Don, 344090 Russia

³A.M. Prokhorov General Physics Institute, RAS, 119991, Moscow, Russia

⁴Department of Physics and Mathematics, University of Eastern Finland, 80101, Joensuu, Finland

A significant change in the electronic properties has been recently demonstrated for single-walled carbon nanotubes (SWCNTs), filled with CuCl by the gas phase method. The strong p-type doping induced by encapsulated CuCl crystals provides a possibility of modification of nanotubes work function and correspondingly their field emission (FE) characteristics. Here, we present a comparative study of FE characteristics of flat films composed of pristine, annealed and doped carbon nanotubes performed using a flat phosphor screen technique. A significant increase of the threshold field was observed after annealing or doping of SWCNTs films (Fig. 1). It can be caused by the selective oxidation of the small-diameter nanotubes. This explanation is confirmed by Raman spectroscopy (Fig. 2). Meanwhile FE characteristics of annealed and doped nanotubes coincided with each other, while the Raman spectra substantially changed due to the effective doping of CuCl. These results indicate that CuCl doping does not change the work function of the emitting tip of the carbon nanotubes.

The work was supported by Russian Science Foundation grant 15-12-30041

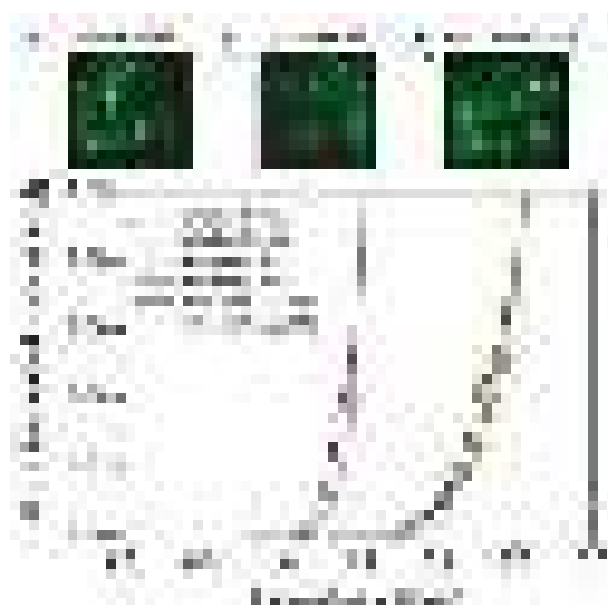
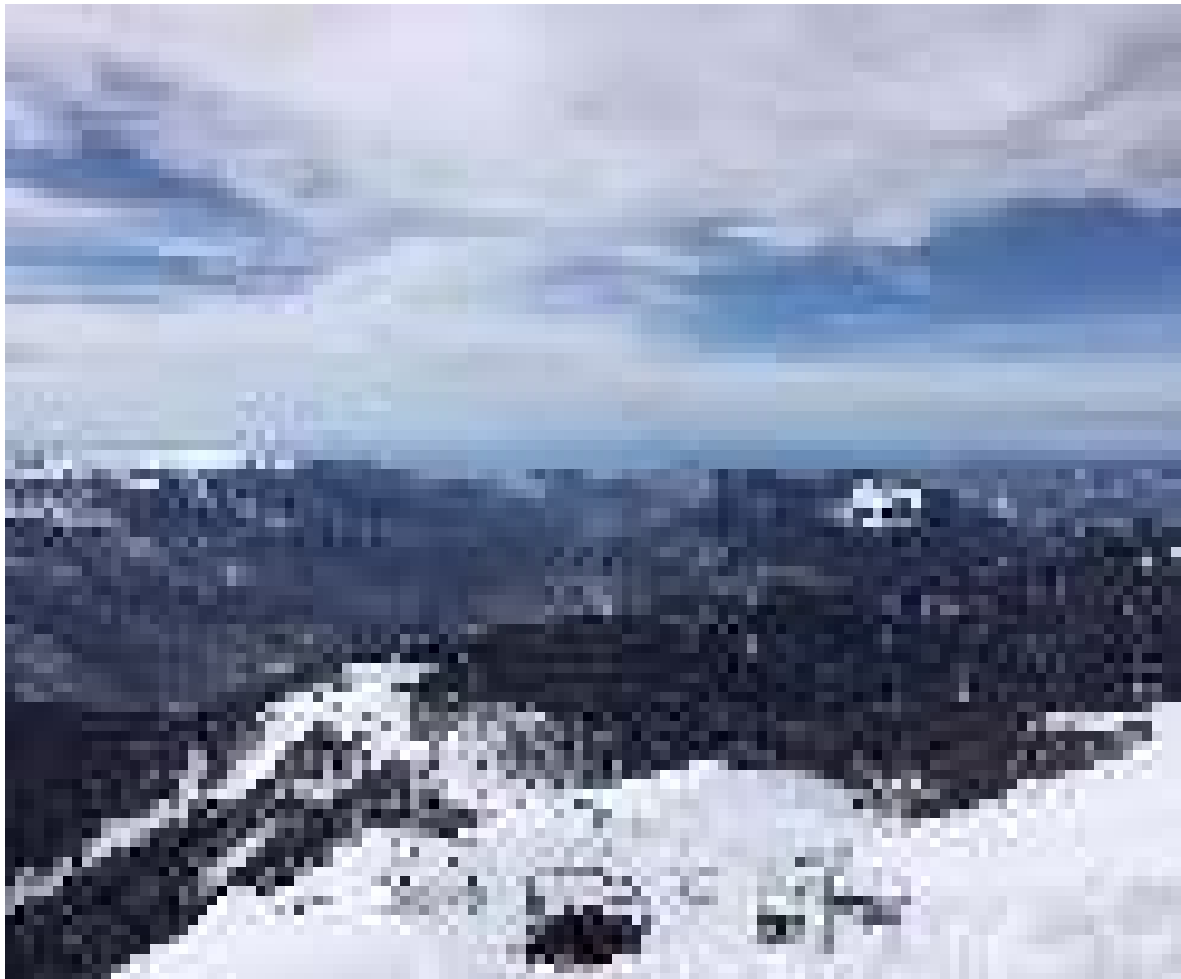


Fig. 1. (a-c) Field emission patterns at the current of 10 μA and cathode-to-anode distance of 500 μm for pristine, annealed and doped SWCNT films. Each pattern size is 1 cm x 1 cm. (d) The dependence of the current normalized on the number of the emission sites versus the electric field for the three types of SWCNT films. For each type of the film two experimental curves obtained for the two different samples are presented.



Fig. 2. The Raman spectra of pristine SWCNT film, annealed at 220 $^{\circ}\text{C}$ for 26 hours and film exposed to CuCl gas at 220 $^{\circ}\text{C}$ for 26 hours. The excitation wavelength is 633 nm.

Thursday, March 23



©A.Chernov

Exciton dynamics in van der Waals materials

Young Hee Lee^{*}

Center for Integrated Nanostructure Physics, Institute for Basic Science, Sungkyunkwan University, Suwon, 440-746, Korea E-mail: leeyoung@skku.edu

In addition to metallic graphene monolayer, insulating hexagonal-BN monolayer and semiconducting layered transition metal dichalcogenides (TMDs) are a new class of transparent and flexible materials, which can be used as essential components of transistors for soft electronics. These materials have known to exhibit exotic physical and chemical phenomena which have never been accessed so far with 3D materials. Among them, excitons in TMD materials is in particular interesting with strong binding energy much larger than thermal energy at room temperature due to weak charge screening effect. This allows much room to play with excitons even including multiexcitons. I will demonstrate some examples of utilizing excitons in optical communication by bridging 2D materials with Ag nanowire. Furthermore the fast exciton dynamics to give rise to efficient carrier multiplications in 2D materials. If time is allowed, I will also discuss robust phase engineering of MoTe_2 via various engineering variables.

Charge dynamics in SWNT-polymer blends for photovoltaics: from charge generation to extraction

LarryrLüer

IMDEA Nanoscience, C/Faraday 9, 28049 Cantoblanco (Spain)

Larry.luer@imdea.org

Single-walled carbon nanotubes (SWNT) present high aspect ratios, charge carrier mobilities and mechanical and chemical stability. Considering also their ability to absorb light in the near infrared optical region, they seem ideally suited for the improvement of the performance and stability of organic solar cells (OSC). However, so far OSC devices comprising SWNT did not fulfil this promise, with power conversion efficiencies remaining far below the expectations. This has been ascribed in part to limitations in sample definition leading for example to the presence of metallic nanotubes, SWNT bundles, charge trapping on low bandgap SWNT or defect sites [1].

But even in ideal samples, the very nature of SWNT might induce additional loss channels that counterbalance the desired electrical performance increase: on one hand, the low optical bandgaps in SWNT might lead to energy transfer towards the SWNT in competition with the desired charged transfer, causing charge generation losses. On the other hand, also charge extraction might be hampered in the presence of SWNT because the working principle of OSC relies on the "bulk heterojunction" (BHJ) concept, where positive and negative charge carriers dwell in the bulk of separate phases, thus limiting recombination to the interface between these phases. The absence of a bulk in SWNT thus breaks the BHJ concept which might lead to increased recombination.

Here, we distinguish and quantify these loss processes in OSC devices comprising SWNT, highly enriched in a single chirality and blended with typical conjugated polymers used for OSC. We perform transient absorption spectroscopy across the femtosecond to millisecond time scales in combination with transient electrical methods such as time-resolved photovoltage and time-resolved photocurrent (TPV/TPC).

We first introduce the optical probes for neutral and charged photoexcitations in SWNT and their electronic interpretation [2]. Then, we use these optical probes to analyze chirality resolved charge transfer in SWNT-polymer blends of different morphologies. Finally, we use transient electrical studies to quantify charge recombination in OSC made from SWNT/polymer blends. We find a significant increase of the recombination coefficient in the presence of SWNT, which is confirmed by reconstruction of current-voltage curves using the parameters obtained from the TPV/TPC studies.

We use these results to estimate maximum achievable benefits of the use of SWNT in OSC devices as function of architecture and material combination.

[1] M. Gong, T. A. Shastry, Y. Xie, M. Bernardi, D. Jasion, K. A. Luck, T. J. Marks, J. C. Grossman, S. Ren, and M. C. Hersam, *Nano Lett.* **14**, 5308–531 (2014)

[2] A. Abudulimu, F. Spaeth, I. Namal, T. Hertel, L. Lüer, *J. Phys. Chem. C*, **120** (35), 19778–19784 (2016).

Ultrafast Exciton and Phonon Dynamics in Two-dimensional van der Waals Materials

Ji-Hee Kim

Center for Integrated Nanostructure Physics, Institute for Basic Science(IBS), 2066 Seobu-ro, Jangsan-gu, Sungkyunkwan University, Suwon 440-746, South Korea
kimj@skku.edu

Two-dimensional (2D) van der Waals materials have attracted great interest due to their unique optical, electrical and structural properties [1,2,3], and have great potential for optoelectronic devices, such as light emitting diodes, photodetectors, and photovoltaics with efficient power conversion. The reduced dimensionality in 2D materials allows strong Coulomb coupling with large exciton binding energy and efficient light-matter interaction. These result in the enhanced excitonic absorption due to the confinement and the reduced screening.

By using femtosecond transient absorption spectroscopy, we study the detailed exciton dynamics of TMdCs in two excitonic bands at K-point and in indirect band, shown in Fig. 1(a) and (b). Formation mechanism of excitons which arises in < 1 ps time scale [4,5], including the exciton absorption strength, will be further discussed. In addition, we will discuss the structural phases via coherent lattice motions in 2D materials.

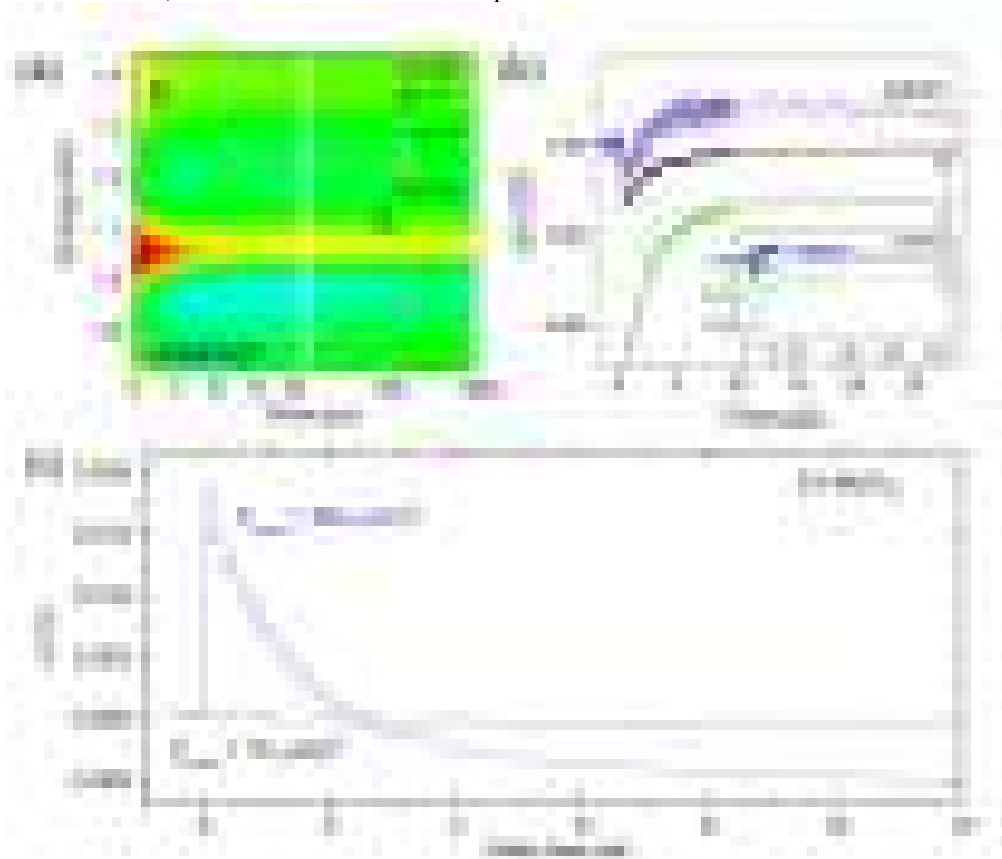


Fig.1. (a) Spectrally- and temporally-resolved ultrafast response after resonant excitation at the B exciton in molybdenum ditellurides. (b) The corresponding temporal dynamics at different transition energies. (c) Coherent phonon oscillations with different pump fluence.

- [1] K. Novoselov, D. Jiang, F. Schedin, T. Booth, V. Khotkevich, S. Morozov, and A. Geim, *Proc. Natl. Acad. Sci.* 102, 10451 (2005)
- [2] A. Splendiani, L. Sun, Y. Zhang, T. Li, J. Kim, C.-Y. Chim, G. Galli, and F. Wang, *Nano Lett.* 10, 1271–1275 (2010)
- [3] Dong Hoon Keum, Suyeon Cho, Jung Ho Kim, Duk-Hyun Choe, Ha-Jun Sung, Min Kan, Haeyong Kang, Jae-Yeol Hwang, Sung Wng Kim, Heejun Yang, K. J. Chang & Young Hee Lee, *Nat. Physics* 11, 482 (2015).
- [4] Akshay Singh, Galan Moody, Kha Tran, Marie E. Scott, Vincent Overbeck, Gunnar Berghäuser, John Schaibley, Edward J. Seifert, Dennis Pleskot, Nathaniel M. Gabor, Jiaqiang Yan, David G. Mandrus, Marten Richter, Ermin Malic, Xiaodong Xu, and Xiaoqin Li, *Phys. Rev. B* 93, 041401 (2016)
- [5] Frank Ceballos, Qiannan Cui, Matthew Z. Bellusa and Hui Zhao, *Nanoscale* 8, 11681 (2016)

Nonlinear optical effects in organic microstructures

T.V. Murzina

*Physics Department, Moscow State university, Leninskie Gory, 119991 Moscow, Russia
murzina@mail.ru*

Microstructures of various design are perspective for photonic applications, including sensing, switching, amplification of the optical effects and lasing. Here an important task is to manipulate the parameters of the microstructures in order to introduce the required properties of a medium. Organic microstructures provide such a possibility in a reasonably easy way, by changing the chemical composition of a medium. Furthermore, additional functional possibilities arise when applying the self-organization technique, which leads to the formation of microstructures of the same shape and reasonable low size dispersion.

It has been shown in a number of papers that organic microstructures can provide substantial amplification of optical effects due to a strong confinement of optical radiation [1,2]. In that case, microstructures operate as optical microcavities with large local field factors, which attain the maximal values under the resonant excitation of whispering gallery modes (WGMs) [3,4]. The latter effect was demonstrated for organic microstructures with the shape of spheres, hemispheres, disks and rods. Very recently the first results on the amplification of the second-order nonlinear optical effects in frustum-shaped microstructures were reported as well [5].

In this talk we discuss the recent results on the composition, linear and nonlinear optical properties of various types of organic microstructures randomly distributed on a solid substrate. Most of these structures are composed of nonlinear dyes and thus are perspective for the nonlinear optical applications. The structures with the shape of a sphere, hemisphere, microrod, inverted frustum or a hollow fiber, reveal the WGMs excitation appearing as a set of narrow spectral peaks in the photoluminescence spectra of a single particle. When analyzing both the arrays of such microstructures and an individual particle, we confirm that the second-harmonic generation (SHG) and two-photon luminescence (TPL) and absorption (TPA) are enhanced as compared to a homogeneous film of the same chemical composition. This is a manifestation of a strong local field enhancement at the fundamental or SHG wavelengths achieved in optical organic microcavities.

The SHG microscopy studies show that the second harmonic radiation and TPL distribution within a single microstructure is rather inhomogeneous and consistent with the WGMs excitation, showing an increase of the intensity closer to the outer diameter of the microresonators. At the same time, SHG and TPL for an array of microparticles is enhanced as well due to the same effect, while individual resonant modes are not distinguished. In that case, amplification of the local field effects is averaged over the array of structures each of them having slightly different set of WGMs. The incident power dependencies of the intensity of these signals show that the SHG reveals the second-order one, while the TPL increases much slower. The underlying mechanism are considered as an interplay of the two strong effects, that are the second order nonlinearity of the noncentrosymmetric dye accompanied by the linear and nonlinear absorption. The perspectives of such structures as lasing systems are discussed.

Acknowledgements. This work was supported by RSCF, grant No. 16-42-02024.

[1] J. Yang, M.B.J. Diemeer, C. Grivas, G. Sengo, A. Driessen, M. Pollnau, *Laser Phys. Lett.*, **7** (9), 650 (2010).

[2] H. Yu, L. Qi, *Langmuir*, **25** (12), 6781 (2009).

[3] D. Venkatakrishnarao and R. Chandrasekar, *Adv. Opt. Mater.*, **4**(1) 112 (2016).

[4] Y. Lei, Q. Liao, H. Fu, J. Yao, *J. Am. Chem. Soc.* **132** (6) 1742 (2010).

[5] D. Venkatakrishnarao, Y.S.L.V. Narayana, M.A. Mohaiddon, E.A. Mamonov, I.A. Kolmychek, A.I. Maydykovskiy, V.B. Novikov, T.V. Murzina, R. Chandrasekar, *Adv. Mater.*, **12**, 1-5 (2016).

Optical Excitation of Semiconducting Field Emission Cathodes

A. Derouet¹, M. Choueib¹, S. C. Cojocaru², A. Ayari¹, P. Vincent¹, N. Blanchard¹, P. Poncharal¹, S. Perisanu¹, R. Martel^{3*} and S. T. Purcell^{1*}

¹ *Institute Lumière Matière, UMR5306 CNRS, Université de Lyon 1, Villeurbanne, France*

² *Laboratoire PICM, École polytechnique, Palaiseau, France*

³ *Département de chimie, Université de Montréal, Montréal, Canada*
r.martel@umontreal.ca, stephen.purcell@univ-lyon1.fr

There has recently been extensive research on optically modulated and optically pulsed tip electron sources for new high field physics in the ultrafast laser community [1], electron microscopy [2] and ultrafast electron diffraction [3]. This is mostly the excitation of metallic tips or surfaces for which the quantum efficiency is extremely low eg. 10^{-3} - 10^{-4} . This means that the high current emission will be limited by temperature effects. Another route is to exploit the photo-excitation of p-type semiconductor tips for which very high photon-electron conversion rates can be obtained (>10%), though at the expense of much slower time responses.

In contrast to the exponentially increasing current as a function of applied voltage common for metal emitters, semiconducting emitters can reveal strong current saturation related to a field-induced depletion zone originating at the emitter apex. The saturation current is highly sensitive to light and temperature. The basic behavior [4] and theory [5] was worked out many years ago followed by many experimental results with cursory analysis. However there is a dearth of in-depth measurements and concomitant understanding of the phenomenon in terms of semiconductor physics. Here we show that SiNWs can serve as an excellent platform for exploring FE from semiconductors with the added advantage for future applications that they are mass produced. Our principal present goal is to understand the time response and eventually apply this knowledge to higher current, faster, cone-like Si emitters.

In-depth FE studies will be presented of individual high quality SiNWs batch-grown by vapor-liquid-solid using Au catalysts with no intentional doping [7]. I-V, FE microscopy, FE energy spectroscopy and in constant and time modulated photo-assisted FE measurements were performed in UHV. Quasi-ideal saturation was found which allowed us to reveal several original FE phenomena such as the ability to vary the degree of saturation by *in situ* cycles of hydrogen passivation and thermal de-passivation. The data is analysed in terms of a simple pin diode allowing us to estimate semiconductor parameters which in general is difficult for individual nanowires. A method was developed to measure the photo time response in the pA range with MHz band pass. The time response is in the 5 μ sec range and is controlled by surface traps.

Some remarks on the potential of this work being extended to carbon emitters will be made.

- [1] P. Hommelhoff and coworkers - PRL **97**, 247402 (2006), Nature **475**, 78 (2011), C. Ropers and coworkers - PRL **98**, 043907 (2007), PRL **105**, 147601 (2010), Nature **483**, 190 (2012), Yanagisawa and coworkers - PRL **103**, 257603 (2009), PRL **107**, 087601 (2011).
- [2] A.H. Zewail, Science **328**, 187 (2010), C. Ropers and coworkers, Nature **52**, 200 (2015).
- [3] C. Ropers and coworkers Science **345**, 200 (2014).
- [4] J.R. Arthur, Applied Physics **36**, 3221 (1965).
- [5] L.M. Baskin, O.E. Lvov and G.N. Fursey Phys. Stat. Solid. B **47**, 49 (1971).
- [6] Lefevre E. et al. Thin Solid Films, **519**, 4603 (2011).

SERS of linear carbon chains synthesized by laser ablation in liquids.

N.R.Arutyunyan^{1,2}, V.V. Kononenko^{1,2}, V.M. Gololobov¹, E.D. Obraztsova^{1,2}

¹A.M. Prokhorov General Physics Institute RAS, Vavilova 38, Moscow 119991, Russia

²National Research Nuclear University MEPhI (Moscow Engineering Physics Institute), Kashirskoye shosse 31, Moscow, 115409, Russia

Corresponding author e-mail: natalia.arutyunyan@gmail.com

Linear carbon chains (LCC) are the one-dimensional structures, consisting of carbon atoms linked with alternating triple and single bonds. Due to the non-resonant character of the Raman scattering the Raman bands from the samples are not detectable. However, it is possible to increase the intensity of scattered light by increasing the local field near the metallic nanoparticles (NP), and thus to perform SERS measurements.

The SERS spectra were registered from mixture of silver NP suspension in water and LCC in ethanol (fig.1). It is seen that the band in the range $1800 - 2200 \text{ cm}^{-1}$ appears in the spectra, and the intensity gain is $> 10^5$. The fine structure of the band consists of few relatively thin well-resolved lines. Each of these lines corresponds to the polyynic chain of certain length. The shorter is the chain, the larger is Raman frequency.

Different visible laser wavelengths from 473 to 647 nm (Ar-Kr and He-Ne lasers) were used for the excitation of SERS spectra (fig.2). Comparing the spectra, one may notice that the shape of the spectra depend on the excitation wavelength. The re-distribution of the lines takes place. It may be explained in frames of two-phonon excitation of LCC. The positions of the LCC absorption bands are defined by the length of the chains [1]. The shorter chains could be excited by the green laser line 514.5 nm, and the longer chains – by the red laser line 632 nm. That's why the lines with larger frequencies are more intense in case of excitation with green laser line, and the lines with smaller frequencies – with red one.



Fig.1. Raman and SERS spectra of LCC in ethanol.

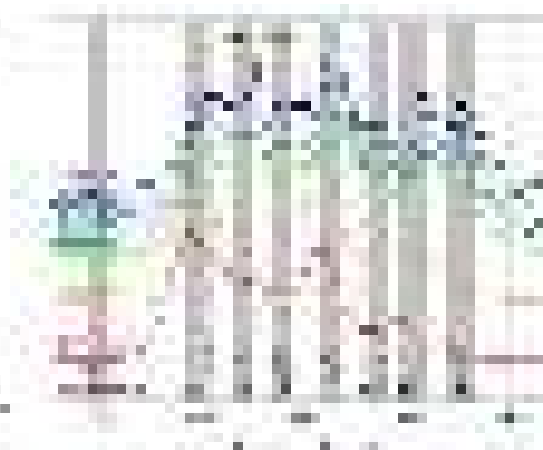


Fig.2. SERS spectra of LCC in ethanol with laser excitation wavelengths from 473 to 647 nm (Ar-Kr and He-Ne lasers).

Acknowledgements The work was supported by project RFBR 15-02-08199.

[1] N.R. Arutyunyan, P.V. Fedotov, V.V. Kononenko, Journal of Nanophotonics 10, 012519 (2016).

Electron Energy Spectroscopy of Field-Emission Coulomb Blockade from Carbon Nanostructures

V.I. Kleshch^{1,*}, V. Porshyn², D. Lützenkirchen-Hecht², and A.N. Obraztsov^{1,3}

¹*Department of Physics, M.V. Lomonosov Moscow State University, Moscow, Russia*

²*Faculty of Mathematics and Natural Sciences, Physics Department, University of Wuppertal, Wuppertal, Germany*

³*Department of Physics and Mathematics, University of Eastern Finland, Joensuu, Finland*

**Corresponding author e-mail: klesch@phys.msu.ru*

A study of field-emission (FE) Coulomb blockade from carbon nanostructures via electron energy spectroscopy is reported. Carbon nanostructures were formed on the apexes of single crystal diamond needles produced by selective oxidation of polycrystalline CVD diamond films [1]. The needles revealed a shape close to a square-based pyramid with a height of $\sim 100\ \mu\text{m}$, a thickness at the base of $\sim 1\ \mu\text{m}$ and a tip apex radius of $\sim 50\ \text{nm}$. FE was observed from the apex of a needle using an UHV system equipped with an electron energy spectrometer [2].

For FE currents below 100 nA, the needles demonstrated a strong saturation in the Fowler-Nordheim (FN) plots usually observed for highly resistive emitters. At higher currents, the needles underwent an abrupt decrease of the resistance and consequently their FN plots became much less saturated. After this transformation the FE current increased in a step-like fashion during the voltage ramp. Such staircase behavior was previously predicted theoretically for nanoscale field emitters and explained by the Coulomb blockade effect [3]. Energy spectra of the emitted electrons consisted of several field-sensitive peaks corresponding to Coulomb energy levels. Performed electron energy spectroscopy permitted direct measurement of charging energy and other parameters of the system.

Transmission electron microscopy (TEM) and Raman spectroscopy were used to characterize structural changes after the FE experiment. It was found that the diamond needle is covered by a layer of amorphous carbon which is responsible for the resistance decrease. Furthermore, TEM revealed a nanoscale protrusion on the apex of the needle which can explain Coulomb blockade behavior. The analysis of the obtained data and the discussion of the results will be presented.

This work was supported by RFBR and Moscow City Government (Grant No. 15-32-70019).

[1] A. N. Obraztsov, P. G. Kopylov, A. L. Chuvilin, N. V. Savenko, *Diamond and Related Materials*, **18**, 1289 (2009).

[2] S. Mingels, V. Porshyn, B. Bornmann, D. Lützenkirchen-Hecht, G. Müller, *Rev. Sci. Instrum.*, **86**, 043307 (2015).

[3] O. E. Raichev, *Physical Review B*, **73**, 195328 (2006).

Oxide matrix composites containing carbon nanotubes.

Kuznetsov V.L.

Boriskov Institute of Catalysis, Novosibirsk 630090, Lavrentieva5

Due to the unique physical and mechanical properties of carbon nanotubes (CNTs), they are considered one of the most promising modifiers for composite structural materials. In the case of inorganic matrix composites, researchers have particularly focused on CNTs as toughening components to overcome the brittleness inherent to ceramic material. At the same time, new functional materials can also be designed with special electrical, optical and thermal conductivity properties. This motivation provoked numerous research attempting to incorporate CNT in brittle ceramics to convert them into tough, strong, electric and thermal conductive materials. This paper reviews the synthesis of oxide composites containing CNT with variable properties (optical, electrical, and chemical). Special attention will be focusing on the formation of interfaces between oxide matrix and CNT surface, which is the most important for the production of materials with uniform and reproducible properties. Several examples of production and properties of different types CNT-oxide composite will be considered; namely: aerogel of SiO_2 for optical applications, Al_2O_3 conductive vacuum-tight ceramic, and foam-glass composite for a radio frequency echoless chambers.

Carbon Related Polymeric Nanomaterials for Photonics and Optoelectronics Applications

Der-Jang Liaw*, Chou-Yi Tsai, Qiang Zhang, Ying-Chi Huang and Yi-Ze Wang

Department of Chemical Engineering, National Taiwan University of Science and Technology, Taipei, 10607 Taiwan,

* liawdj@gmail.com; liawdj@yahoo.com.tw; liawdj@mail.ntust.edu.tw

Carbon-based polymeric nanomaterials including graphene, carbon nanotube, and fullerenes etc. boost as most promising materials for photonics and optoelectronics in the 21st century. Nanographenes prepared through a “bottom-up” chemically synthetic route with extended polycyclic aromatics possess well-defined structures and properties, which have potential applications in nanoelectronics, optoelectronics, and spintronics. Herein, nanographene-containing conjugated polymers and polynorbornenes (PNBs) were prepared *via* the Suzuki Coupling reaction and ring-opening metathesis polymerization (ROMP), respectively. Both polymers showed high thermal stability up to 300°C. The nanographene-containing conjugated polymer and PNB could be highly dispersed in cyclohexylpyrrolidone (CHP) through bath sonication, and exhibited intensive emission (485 and 465 nm) in photoluminescence-excitation (PLE) maps. The intensive and narrow emission of PNB is owing to the unsymmetrical structure of nanographene and donating group covalently bonded to nanographene. In addition, triarylamine-based conjugated polymers were used for high selectivity of semiconducting single-walled carbon nanotubes (SWCNT). The selectivity of (6,5), (7,5), (9,5), or (8,7) nanotubes through polymer wrapping can be controlled by changing the main chain such as polytriarylamine or poly(triarylamine-fluorene), as well as adjusting the aliphatic side-chain length of polymers. Triarylamine-based amphiphilic conjugated polymer was prepared through Suzuki coupling reaction. Micelle and inverse micelle configurations of the same polymer were constituted by adjusting the polarities of the dispersion solution. The two kinds of micelle structures could be used as the anode and cathode buffers for electronic and optoelectronic devices including organic photovoltaics (OPVs), polymer light emitting diodes (PLEDs) and perovskite solar cells (PSCs).

References

- [1] Q. D. Ling, D. J. Liaw, C. X. Zhu, D. S. H. Chan, E. T. Kang, K. G. Neoh, *Prog. Polym. Sci.*, 33, 917 (2008)
- [2] H. Y. Wu, K. L. Wang, D. J. Liaw, K. R. Lee, J. Y. Lai, *J. Polym. Sci. A Polym. Chem.*, 48, 1469 (2010).
- [3] W. H. Chen, K. L. Wang, D. J. Liaw, K. R. Lee, J. Y. Lai, *Macromolecules*, 43, 2236 (2010).
- [4] H. Y. Wu, K. L. Wang, J. C. Jiang, D. J. Liaw, K. R. Lee, J. Y. Lai, C. L. Chen, *J. Polym. Sci. A Polym. Chem.*, 48, 3913 (2010).
- [5] C. H. Chang, K. L. Wang, J. C. Jiang, D. J. Liaw, K. R. Lee, J. Y. Lai, K. H. Lai, *Polymer*, 51, 4493 (2010).
- [6] W. H. Chen, K. L. Wang, W. Y. Hung, J. C. Jiang, D. J. Liaw, K. R. Lee, J. Y. Lai, C. L. Chen, *J. Polym. Sci. A Polym. Chem.*, 48, 4654 (2010)
- [7] C. H. Chang, K. L. Wang, J. C. Jiang, D. J. Liaw, K. R. Lee, J. Y. Lai, K. Y. Chiu, Y. O. Su, *J. Polym. Sci. A Polym. Chem.*, 48, 5659 (2010).
- [8] W. R. Lian, K. L. Wang, J. C. Jiang, D. J. Liaw, K. R. Lee, J. Y. Lai, *J. Mater. Chem.*, 21, 8597 (2011).
- [9] W. R. Lian, C. Ho, Y. C. Huang, Y. A. Liao, K. L. Wang, D. J. Liaw, K. R. Lee, J. Y. Lai, *J. Polym. Sci. A Polym. Chem.*, 49, 5350 (2011).
- [10] W. R. Lian, K. L. Wang, J. C. Jiang, D. J. Liaw, K. R. Lee, J. Y. Lai, *J. Polym. Sci. A Polym. Chem.*, 49, 3248 (2011).
- [11] W. R. Lian, H. Y. Wu, K. L. Wang, D. J. Liaw, K. R. Lee, J. Y. Lai, *J. Polym. Sci. A Polym. Chem.*, 49, 3673 (2011).
- [12] W. R. Lian, Y. C. Huang, Y. A. Liao, K. L. Wang, L. J. Li, C. Y. Su, D. J. Liaw, K. R. Lee, J. Y. Lai, *Macromolecules*, 44, 9550 (2011).
- [13] M. C. Chen, D. J. Liaw, W. H. Chen, Y. C. Huang, J. Sharma, Y. Tai, *Appl. Phys. Lett.* 99, 223305 (2011)
- [14] M. C. Chen, D. J. Liaw, Y. C. Huang, H. Y. Wu, Y. Tai, *Solar Energ. Mat. Sol. Cell*, 95, 2621 (2011)
- [15] C. W. Lin, Y. Tai, D. J. Liaw, M. C. Chen, Y. C. Huang, C. T. Lin, C. W. Huang, Y. J. Yang, Y. F. Chen, *J. Mater. Chem.*, 22, 57 (2012).
- [16] D. J. Liaw, K. L. Wang, Y. C. Huang, K. R. Lee, J. Y. Lai, C. S. Ha, *Prog. Polym. Sci.*, 37, 907 (2012)
- [17] Y. C. Huang, K. L. Wang, C. H. Chang, Y. A. Liao, D. J. Liaw, K. R. Lee, J. Y. Lai, *Macromolecules*, 46, 7443 (2013).
- [18] C. Y. Chi, M. C. Chen, D. J. Liaw, H. Y. Wu, Y. C. Huang, Y. Tai, *ACS Appl. Mater. Interfaces*, 6, 12119 (2014).
- [19] T. Abidin, Q. Zhang, K. L. Wang, D. J. Liaw, *Polymer*, 55, 5293 (2014) (Feature article).
- [20] D. J. Liaw, F. C. Chang, M. K. Leung, M. Y. Chou, K. Muellen, *Macromolecule*, 38, 4024 (2005).
- [21] P. I. Wang, W. R. Shie, J. C. Jiang, L. J. Li, D. J. Liaw, *Polym. Chem.*, 7, 1505 (2016).
- [22] P. I. Wang, W. Pisula, K. Müllen, D. J. Liaw, *Polym. Chem.*, 7, 6211 (2016).
- [23] P. I. Wang; C. Y. Tsai; Y. J. Hsiao; J. C. Jiang; D. J. Liaw, *Macromolecules*, 49, 8520–8529 (2016).

Using solvents for composites and functional inks of 2D materials for optoelectronics and photonics

Guohua Hu, Tawfique Hasan

Cambridge Graphene Centre, University of Cambridge, United Kingdom
th270@cam.ac.uk

Two-dimensional (2D) materials such as graphene, semiconducting transition metal dichalcogenides (s-TMDs) and black phosphorus (BP) have garnered a significant attention because of their diversity and distinct but complementary optoelectronic properties. For example, high nonlinear susceptibility, ultrafast carrier dynamics and wide operation wavelength have enabled graphene and semiconducting TMDs to work as broadband saturable absorbers [1-3], albeit *via* different mechanisms [3,4]. While graphene exhibits broadband behaviour due to its linear dispersion of Dirac electrons, edge-mediated absorption in the TMDs explain their sub-band gap, broadband saturable absorption. BP is another a two-dimensional material of great interest, in part because of its strong saturable absorption, high carrier mobility, thickness dependent direct bandgap bridging TMDs and zero-gap graphene. In addition to being saturable absorbers for photonics, these 2D materials can also be used for a wide range of optoelectronic devices, including as photodetectors.

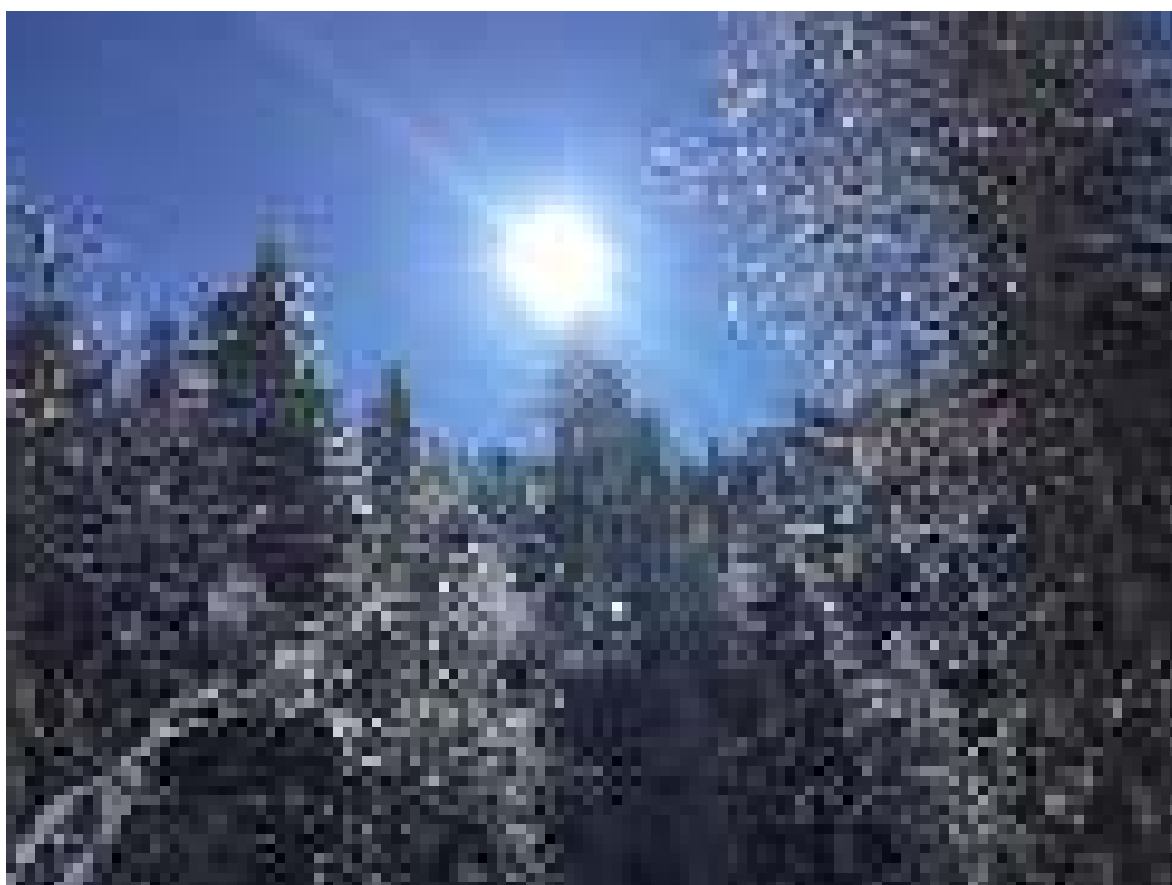
In the majority of the cases, solvents play a critical role in the fabrication of these abovementioned devices. This is applicable to both large area CVD grown as well as ultrasonic assisted liquid phase exfoliated 2D material flakes. In the first example, I will demonstrate, through device fabrication, the choice of solvents can have important consequences for resulting device uniformity, structures or even performance. I will show that solvents can be used to 'soft-pattern' fluorine functionalized graphene, enabling the fabrication of graphene based lateral heterostructures down to few tens of nm resolution. I will show that unlike traditional hard patterning, this soft patterning strategy to form the seamless structure offer opportunities for scalable fabrication of photodetectors [5].

With regards to solution processing, I will demonstrate inkjet printable ink formulation of s-TMDs and BP [6]. I will show that the choice of solvents enable reliable inkjet printing for scalable development of printed saturable absorbers and photodetectors. With regards to BP, I will show that the printed BP working as a saturable absorber for ultrafast lasers without significant oxidative degradation, and can continue to operate for a prolonged period as a nonlinear saturable absorber under encapsulation. In combination with Silicon-graphene schottky junction, I will also demonstrate that our BP ink can be used to fabricate visible to near-infrared photodetectors with high responsivities.

References

- [1] R I Woodward, EJR Kelleher, RCT Howe, G Hu, F Torrisi, T Hasan, SV Popov, JR Taylor, *Tunable Q-switched fiber laser based on saturable edge-state absorption in few-layer molybdenum disulfide (MoS₂)*, Optics Express **22**, 31113 (2015).
- [2] M Zhang, RCT Howe, R I Woodward, EJR Kelleher, F Torrisi, G Hu, SV Popov, JR Taylor, T Hasan, *Solution processed MoS₂-PVA composite for sub-bandgap mode-locking of a wideband tunable ultrafast er: fiber laser*, Nano Research **8**, 1522 (2015).
- [3] RCT Howe, R I Woodward, G Hu, Z Yang, EJR Kelleher, T Hasan, *Surfactant-aided exfoliation of molybdenum disulfide for ultrafast pulse generation through edge-states saturable absorption*, phys stat. sol. (b), **253**, 911 (2016).
- [4] M Trushin, E. J. R. Kelleher, T. Hasan, *Theory of edge-state optical absorption in two-dimensional transition metal dichalcogenide flakes*, Physical Review B **94**, 155301 (2016).
- [5] Y. Xu, A Ali, K Shehzad, N Meng, M Xu, Y Zhang, X Wang, C Jin, H Wang, Y Guo, Z Yang, B Yu, Y Liu, Q He, X Duan, X Wang, PH Tan, WHu, H Lu, T Hasan, *Solvent-Based Soft-Patterning of Graphene Lateral Heterostructures for Broadband High-Speed Metal-Semiconductor-Metal Photodetectors*, Advanced Materials Technologies, Accepted article (2016).
- [6] G Hu, T Albrow-Owen, X Jin, A Ali, Y Hu, R C T Howe, K Shehzad, Z Yang, X Zhu, R I Woodward, T-C Wu, H Jussila, J-B Wu, P Peng, PH Tan, Z Sun, E J R Kelleher, M Zhang, Y Xu, T Hasan, *Black phosphorus ink formulation for inkjet printing of optoelectronics and photonics*, Under review (2016).

Friday, March 24



©E.Obraztsova

Gas sensors and micro-supercapacitors based on fluorinated graphene films

A.V. Okotrub^{1,2}, V.I. Sysoev, A.V. Gusel'nikov, D.V. Gorodetskii, L.G. Bulusheva

Nikolaev Institute of Inorganic Chemistry SB RAS, Novosibirsk, 630090, Russia

spectrum@niic.nsc.ru

Graphene is a remarkable material with the best surface to volume ratio as a result of its 2D nature, which implies that every atom can be considered as a surface one. These features make graphene attractive for use as a sensing material; however, the limiting factor is the chemical inertness of pristine graphene. We propose a method to create reactive centers by removal of fluorine atoms from the outer surface of fluorinated graphene while preserving the backside fluorination. The fluorinated graphite with composition C_2F was synthesized using low temperature fluorination by BrF_3 from natural graphite. Such partially recovered graphene layers were produced by the action of hydrazine-hydrate vapor on initially non-conducting fluorinated graphite. The reduction degree of the material and its electrical response revealed upon ammonia exposure were controlled by measuring the surface conductivity. We showed experimentally that the sensing properties depend on the reduction degree and found the correlation of the adsorption energy of ammonia with the number of residual fluorine atoms by the use of quantum-chemical calculations [1]. Conductive films of few-layered fluorinated graphene have been produced using a one-step process of the exfoliation and partial reduction of the graphite derivatives. The films showed a similar sensitivity on exposure to gaseous ammonia and nitrogen dioxide, while the fluorinated graphene-based sensor had the better recovery by simple argon purging at room temperature [2]. DFT calculations revealed that NO_2 and NH_3 molecules like fluorine and oxygen from hydroxyl group as well as bare carbon atoms located near the functionalized carbon. The highest adsorption energy was obtained for a system oxyfluorinated graphene- NH_3 due to short $H\cdots O$ contacts.

The rapid development of electronic devices has increased necessity of micro supercapacitors. Wafer-scalable routes of fabricating nanostructure materials could significantly enhance the performance of micro-supercapacitors. Graphene materials have been ideal material platform for constructing electronic flexible devices. Its 2D structure, high specific area and good conductivity are attractive for energy storage devices. Exploring a new method to fabricate graphene films with is a key for flexible electronic devices to achieve higher performance. Suspension of fluorinated graphite in toluene was used to produce films having a thickness of 0.1 - 1 μm . The C_2F films were prepared on polymeric substrates and in free standing forms. These films were characterized by XPS and NEXAFS. They had a high resistance and became conductive after UV irradiation. The changes in the microstructure and conductivity were found to depend on the radiation dose. Pattern of microelectrodes was drawing by UV laser and supercapacitors properties of these elements were measured (Fig. 1).

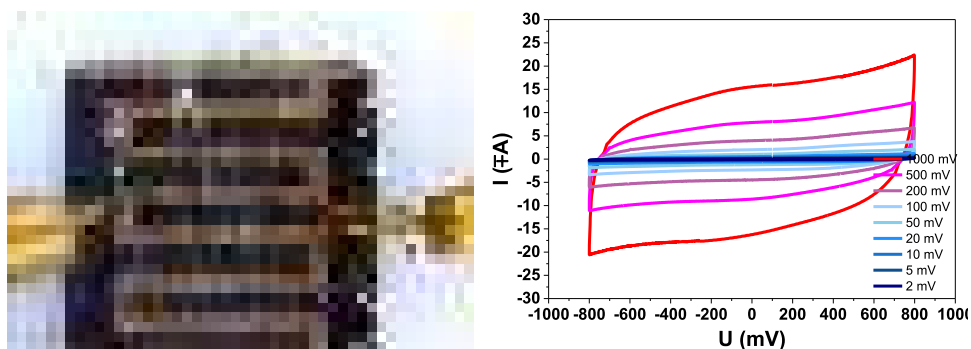


Fig. 1. Optical photo of fluorinated graphene supercapacitor with size $5 \times 5 \text{ mm}^2$ and CVs of supercapacitors for different charge-discharge rates.

[1] M. V. Katkov, V. I. Sysoev, A. V. Gusel'nikov, I. P. Asanov, L. G. Bulusheva, *Phys. Chem. Chem. Phys.*, **17**, 444 (2015).

[2] V. I. Sysoev, L. G. Bulusheva, I. P. Asanov, Yu. V. Shubin and A. V. Okotrub, *Phys. Status Solidi B*, (DOI: 10.1002/pssb.201600270) (2016).

Graphene based field effect transistor for various applications: approaches for engineering

I.V.Antonova^{1,2,3}

¹Rzhanov Institute of Semiconductor Physics SB RAS, Novosibirsk, Russia

²Novosibirsk State Technical University, Novosibirsk, Russia

³Novosibirsk State University, Novosibirsk, Russia

*antonova@isp.nsc.ru

Graphene based field effect transistor (GFET) is the basis element for wide spectrum of electronics, optoelectronics and photonics applications: For instant, quantum dots formed on open channel of bottom gated GFET allows creating the effective photodetectors [1]. Problems of the transistor structure fabrication and various engineering approaches to solve these problems are discussed in the report. Three types of transistors are suspension by means of printing and (c) hybrid variant of GFET when channel of printed transistor was fabricated from exfoliated graphene. Functionalization of domain boundaries of graphene allows us to provide the strong current modulation by gate voltage with ON/OFF relation $\sim 10^4 - 10^5$ dependently on functionalization agents (fluorine, hydrogen, N-methylpyrrolidone) [2]. Negative differential resistance (NDR) and a step-like increase in the current are found for channel created from the partially fluorinated graphene suspension. NDR resulted from formation of the potential barrier system in the film is observed for a relatively low fluorination degree [3]. The observation of NDR in graphene-based heterostructures is known to significantly widen the range of GFET possible applications including resonant terahertz detectors and resonant terahertz emitters [4]. Different ways to improve the carrier mobility in the GFET are also considered in the report. Among them interface engineering, and creation of quasi - suspended graphene channels in hybrid GFET [5]. The main parameter of graphene suspension which provides the increase in carrier mobility in the 2D ink-jet printed GFET is also considered. It was found that the thickness of graphene flakes is determined the carrier mobility in printed layer. This thickness has to be 1-2 monolayer even the thickness of printed layer is tens of nanometers [6]. Increase in flake thickness up to 2-3 nm leads to decrease in carrier mobility down to 2-3 orders of magnitude. As a result, the 2D ink-jet printed GFET on rigid and flexible substrates with relatively high carrier mobility was created. One more approach of GFET with nanostructured graphene channel is discussed. Structuring was performed with use of high energy heavy ions. Two different types of structures were found in this case dependently of the ion energy: these are structures with and without edge defects. Reconstruction of edge binding is suggested for high energy ion structuring.

This study was supported by the Russian Science Foundation (grant No. 15-12-00008).

[1] . Chang-Hua Liu et al. Graphene photodetectors with ultra-broadband and high responsivity at room temperature, *Nature Nanotechnology*, 9 (2014) 273–278.

[2]. I. V. Antonova, I. A. Kotin, N. A. Nebogatikova, V. Ya. Prinz, Modulation of Current in Self-Forming Lateral Graphene-Based Heterostructures, *Technical Physics Letters*, 41, (2015) 950–953.

[3]. I.V. Antonova, I.I. Kurkina, N.A. Nebogatikova, A.I. Komonov, S.A. Smagulova, Films fabricated from partially fluorinated graphene suspension: structural, electronic properties and negative differential resistance, *Nanotechnology*, in press

[4]. V. Ryzhii, et al. Double – graphene – layer terahertz laser: concept, characteristics, and comparison, *Opt. Exp.* 21, (2013), 31569.

[5]. I.A. Kotin, I.V. Antonova, A.I. Komonov, V.A. Seleznev, R.A. Soots, and V.Ya. Prinz, High carrier mobility in graphene on atomically flat high-resistivity layer, *J Phys.D: Appl.Phys.*, 46, (2013) 285303

[6] R. A. Soots, E. A. Yakimchuk, N. A. Nebogatikova, I. A. Kotin, I. V. Antonova, Graphene Suspensions for 2D Printing, *Technical Physics Letters*, 2016, Vol. 42, No. 4, pp. 438–441

Fully carbon microwave absorbers: thin vs light

Polina Kuzhir

*Institute for Nuclear problems of belarusian State University, Minsk 220030, Belarus
polina.kuzhir@gmail.com*

Three classes of carbon-based materials that could possess high absorption ability of electromagnetic (EM) radiation and resonance behavior in microwave-THz frequency ranges are discussed.

- (i) The ability of graphene [1] and other nm-thin carbon films including pyrolytic carbon [2] and pyrolyzed photoresist to absorb microwave radiation is analyzed. We show that being deposited on a properly chosen optically transparent dielectric substrate these nm-thin films can provide more than 20 dB electromagnetic interference shielding efficiency [3].
- (ii) It is also possible to develop an easy to use, cheap, 3D printing process [4] for producing 3D structures of sophisticated geometries made from a nanocarbon-polymer composite fibre and a pure polystyrene fibre. The 3D printing process makes it possible to fabricate devices with predefined electromagnetic response and almost 0-reflection.
- (iii) Another option is to use carbon porous structures, 0.02-0.2 g/cm³ (true foams [5], hollow carbon spheres [6] organized in metamaterial-like surface, 3D printed [7] or polymer-templated [8] carbon lattices).

The peculiarities of EM response of all these carbonaceous materials are investigated; the advantages of each type of carbon structures depending on particular application are emphasized.

[1] K. Batrakov, P. Kuzhir, S. Maksimenko, A. Paddubskaya, S. Voronovich, Ph Lambin, T. Kaplas and Yu Svirko, Scientific Reports, **4**, Article number:7191 (2014)

[2] K. Batrakov, P. Kuzhir, S. Maksimenko, A. Paddubskaya, S. Voronovich, T. Kaplas, and Yu. Svirko, Applied Physics Letters, **103**, 073117 (2013)

[3] K. Batrakov, P. Kuzhir, S. Maksimenko, N. Volynets, S. Voronovich, A. Paddubskaya, G. Valusis, T. Kaplas, Yu. Svirko, and Ph. Lambin, Applied Physics Letters, **108**, 123101 (2016)

[4] A. Paddubskaya, N. Valynets, P. Kuzhir, K. Batrakov, S. Maksimenko, R. Kotsilkova, H. Velichkova, I. Petrova, I. Biró, K. Kertész, G. I. Márk, Z. E. Horváth, L. P. Biró, Journal of Applied Physics, **119**, 135102 (2016)

[5] M. Letellier, J. Macutkevicius, A. Paddubskaya, A. Plyushch, P. Kuzhir, M. Ivanov, J. Banyas, A. Pizzi, V. Fierro, A. Celzard, IEEE EMC, **57**(5), 989 (2015)

[6] D. Bychanok, S. Li, A. Sanchez-Sanchez, G. Gorokhov, P. Kuzhir, F.Y. Ogrin, A. Pasc, T. Ballweg, K. Mandel, A. Szczurek, V. Fierro, and A. Celzard, Applied Physics Letters, **108**, 013701 (2016)

[7] A. Szczurek; A. Ortona; L. Ferrari; E. Rezaei; G. Medjahdi; V. Fierro; D. Bychanok; P. Kuzhir; A. Celzard, Carbon, **88**, 70 (2015)

[8] D. Bychanok, A. Plyushch, K. Piasotski, A. Paddubskaya, S. Varanovich, P. Kuzhir, S. Baturkin, A. Klochkov, E. Korovin, M. Letellier, S. Schaefer, A. Szczurek, V. Fierro and A. Celzard, Phys. Scr., **90**, 094019 (2015)

Production and Application of Multifunctional Carbon Nanotube Electronic Ink

Huaping Liu

*Beijing National Laboratory for Condensed Matter Physics, Institute of Physics, Chinese Academy of Sciences, Beijing 100190, China
Collaborative Innovation Center of Quantum Matter, Beijing 100190, China*

Corresponding author: liuhuaping@iphy.ac.cn (H. Liu)

Abstract:

As one-dimensional structure, single-wall carbon nanotubes (SWCNTs) possess extremely high carrier mobility and structure-tunable bandgaps, and have great potential applications in micro-nano photonic, electronic and optoelectronic devices. The ink-printing technique is a recently developed method for the fabrication of SWCNT-based devices and logic circuits, which could be used to efficiently deposit various SWCNT pattern films by printing SWCNT ink at the desired position on a device substrate. Compared with traditional semiconducting technologies, the ink printing technique has the advantages of simplicity, low cost, high efficiency without involving any complicated lithography and pattern process and is also compatible with various substrates. In order to fabricate high-performance SWCNT-based devices, the production of single-structure SWCNTs ink with identical property is critical. Nevertheless, the synthetic control of SWCNTs with well-defined structures still remains a challenge. Recently, the gel chromatography technique has been developed for the separation of the synthetic SWCNT mixture. With this technique, we achieved the separation of metallic and semiconducting SWCNTs, and even the production of single-chirality SWCNTs with identical properties [1-5]. However, the types of the separated nanotubes currently are very limited, and their diameters are less than 1.1 nm. In this presentation, we will report the recent progress on the structure separation of the SWCNTs for producing different electronic SWCNT inks and their applications in the printed devices.

Acknowledgement.

This work was supported by the National Natural Science Foundation of China (Grant No. 51472264, 11634014, 51361022), and Key research projects of Frontier Science of Chinese Academy of Sciences (Grant No. QYZDB-SSW-SYS028).

References

- [1] H. Liu, Y. Feng, T. Tanaka, Y. Urabe, H. Kataura, Diameter-Selective Metal/Semiconductor Separation of Single-Wall Carbon Nanotubes by Agarose Gel, *J. Phys. Chem. C* 114, 9270-9276(2010).
- [2] H. Liu, D. Nishide, T. Tanaka, H. Kataura, Large-scale single-chirality separation of single-wall carbon nanotubes by simple gel chromatography, *Nat. Commun.* 2, 309(2011)
- [3] H. Liu., T. Tanaka., Y. Urabe, H. Kataura, High-efficiency single-chirality separation of carbon nanotubes using temperature-controlled gel chromatography, *Nano. Lett.* 13, 1996-2003(2013)
- [4] H. P. Liu., T. Tanaka., H. Kataura, Optical isomer separation of single-chirality carbon nanotubes using gel column chromatography. *Nano. Lett.* 14, 6237-6243(2014)
- [5] X. Zeng, Jinwen Hu, Xiao Zhang, Naigen Zhou, Weiya Zhou, Huaping Liu, and Sishen Xie, Ethanol-assisted gel chromatography for single-chirality separation of carbon nanotubes. *Nanoscale* 7, 16273-16281(2015)

Graphene based nanostructures for detecting terahertz radiation.

G. Fedorov, I. Gayduchenko, N. Titova, M. Moskotin, E. Obraztsova, M. Rybin and G. Goltzman

Recently there has been increased interest in the so-called terahertz electromagnetic radiation (from 10^{11} to 10^{13} Hz). This is primarily due to the emergence of new approaches to the creation of sources and detectors of radiation in this range. Efficient detection of THz radiation is still a challengeable task. Increase in the sensitivity of the THz radiation detectors range can be achieved by reducing the size of the sensor element. Graphene is an almost ideal material for creating nanoscale structures that are suitable for this purpose. One of the major advantages of graphene is its high carrier mobility and the associated large coherence length, so that the band structure is determined by the size quantization and can be controlled via the geometry of the structure. Several more or less successful configurations of detectors of THz radiation on the basis of graphene and nanotubes have been proposed recently [1-5]. Further improvement of this type of device is not possible without better understanding of the mechanisms that determine the magnitude of the response to radiation.

In this talk I will present the results of our systematic studies of different configurations of detectors with sensor elements based on graphene as well as its derivatives – CNTs and GNRs. The asymmetry that is crucial for the observation of the DC voltage response to the radiation has been implemented in our devices in two different ways. In the first case different metals are used to contact the channel. In the second the gate electrode is coupled to the radiation.

The data allow us to determine the most promising directions of development of the technology of nanocarbon structures for the detection of THz radiation.

This work was supported by the RFBR under project N 15-02-07787

- [1] L. Vicarelli, M. S., D. Coquillat, A. Lombardo, A. C. Ferrari, W. Knap, M. Polini, V. Pellegrini, and A. Tredicucci, *Nat. Mater.* 11, 865 (2012).
- [2] X. Cai, A. B. Sushkov, R. J. Suess, M. M. Jadidi, G. S. Jenkins, L. O. Nyakiti, R. L. Myers-Ward, S. Li, J. Yan, D. K. Gaskill, T. E. Murphy, H. D. Drew, and M. S. Fuhrer, *Nat. Nanotechnol.* 9, 814 (2014).
- [3] X. He, N. Fujimura, J. M. Lloyd, K. J. Erickson, A. A. Talin, Q. Zhang, W. Gao, Q. Jiang, Y. Kawano, R. H. Hauge, F. Leonard, and J. Kono, *Nano Lett.* 14(7), 3953 (2014).
- [4] G. Fedorov, A. Kardakova, I. Gayduchenko, I. Charayev, B. M. Voronov, M. Finkel, T. M. Klapwijk, S. Morozov, M. Presniakov, I. Bobrinetskiy, R. Ibragimov, and G. Goltzman, *Appl. Phys. Lett.* 103, 585 181121 (2013).
- [5] I. Gayduchenko, A. Kardakova, G. Fedorov, B. Voronov, M. Finkel, D. Jimenez, S. Morozov, M. Presniakov, and G. Goltzman, *J. Appl. Phys.* 118, 194303 (2015).

Hybrid structures from carbon nanotubes and CdS nanoparticles

Yu.V. Fedoseeva, L.G. Bulusheva, A.V. Okotrub, A.G. Kurennya, S.V. Larionov

Nikolaev Institute of Inorganic Chemistry SB RAS, 630090 Novosibirsk, Russia

Corresponding author e-mail fedoseeva@niic.nsc.ru

The hybrid materials consisting of multi-walled carbon nanotube and cadmium sulphide nanoparticles (CNT-CdS) have attractive attention due to their potential application in photovoltaic and optoelectronic devices. Optical properties of the CNT-CdS material mainly depend on size and structure of CdS nanoparticles and interface between CdS and CNTs. Oriented arrays and powder of multi-walled and single-walled CNTs were produced by CVD method. Modification of CNTs were performed using fluorination and oxidation techniques, as well as covering by dielectric layers. CdS nanoparticles have been grown on surface of CNTs from aqueous chemical bath containing thiourea, cadmium chloride, and ammonia. To modify morphology, structure, composition and properties of CNT/CdS hybrid material the key parameters of synthesis were changes. Dynamic light scattering method we applied for characterization of CdS particle size in the solution. Scanning electron microscopy and transmission electron microscopy were used to study the morphology of CdS nanoparticles grown on CNTs and a silica substrate as reference. Raman spectroscopy, X-ray photoelectron spectroscopy and near-edge X-ray absorption fine structure spectroscopy were used for characterization of electronic structure and composition of CNT-CdS hybrid material. It is shown that enhance of duration and temperature of CdS synthesis result in increasing of particle size. Polycrystalline agglomerates of CdS locate on top and side walls of CNT. Addition of polar organic solvent in the aqua solution reduces growth of particles and enhances stability of suspension. Morphology of CdS particles changes when a part of water was replaced by organic solvent. Deposition of CdS on fluorinated CNTs result to formation of CdS particles smaller size, than CdS deposited on as-grown CNTs. Defluorination of CNT occurs after cadmium sulfide growth. CdS nanoparticles of different morphology were growth on single- and multi-walled CNT. Photoluminescence and electroluminescence properties of CNT-CdS hybrid materials have been studied. We demonstrated that optical properties of CNT-CdS depend on concentration, size, crystallinity and composition of CdS nanoparticles and functionalized surface of CNTs.

The work was partially supported by Russian Federation President Grant (No. MK-3277.2017.2).

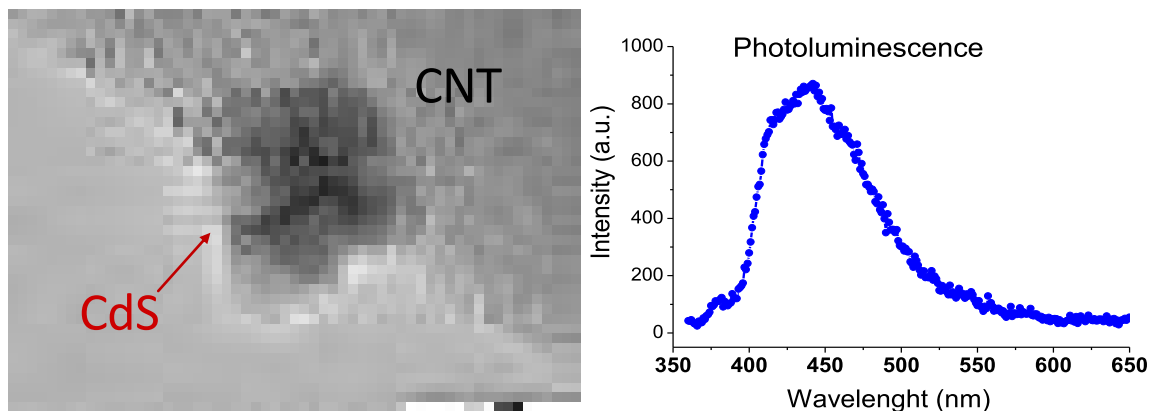


Fig. 1. HR TEM image and photoluminescence spectrum of CNT-CdS hybrid material

Author index

- I.V. Antonova 10, 50, 54, 88
N.R. Arutyunyan 80
M.V. Avramenko 41
K.A. Bagdasarova 46
D.A. Bandurin 29
V.V. Bel'kov 30
S.N. Bokova-Sirosh 43
L.G. Bulusheva 18, 34, 42, 45, 51, 53, 87
D. Bychanok 25, 63
A. Chernov 17, 47, 48
L.A. Chernozatonskii 9
A. Eliseev 7
K.N. Eltsov 8, 12, 55
T.V. Eremin 44
V.A. Eremina 46, 47, 65
G. Fedorov 91
E.O. Fedorovskaya 42
Y.V. Fedoseeva 18, 45
P.V. Fedotov 17, 48
D. Ghazaryan 70
M.M. Glazov 20
B. Gorshunov 22
A. Gruneis 21
O.A. Gurova 49
T. Hasan 84
M. He 6
Y. Hee Lee 75
A.I. Ivanov 50
M.A. Kanygin 51
M.A. Kazakova 52
A. Khlobystov 15
J. Kim 77
V.I. Kleshch 71, 81
M. Kolesnik-Gray 32, 53
I.I. Kondrashov 65
K. Konishi 24, 31
V.O. Koroteev 34
I.A. Kotin 54
S.L. Kovalenko 12, 55
D.V. Krasnikov 4
R.Y. Krivenkov 56, 57
V. Krstic 32, 53
P.P. Kuzhir 25, 89
V.L. Kuznetsov 52, 58, 82
Y. Li 5
D. Liaw 83
H. Liu 90
L. Luer 76
D. Meisak 25, 63
K.G. Mikheev 56, 57
E.D. Mishina 33
S.I. Moseenkov 58
P. Mulbagal Rajanna 23
T.V. Murzina 78
A.Г. Nasibulin 19, 22, 23
N.A. Nebogatikova 10, 50
I. Nefedova 59
N. Nemoto 31
A.N. Obraztsov 71, 81
P.A. Obraztsov 31
E.D. Obraztsova 16, 17, 22, 46, 43, 44, 47,
48, 61, 62, 65, 71, 80
E. Obraztsova 16, 46, 43, 60
A. Okotrub 18, 34, 42, 45, 49, 51, 53, 87
A.S. Orekhov 61
A.V. Osadchy 62
T.V. Pavlova 12, 55
K. Piasotski 25, 63
S. Purcell 79
E.V. Redekop 71
D.V. Rybkovskiy 16, 22, 61
V.V. Savin 62, 69
S.A. Smagulova 11, 64, 67
S. Tarasenko 36
O.E. Tereshchenko 35
A.E. Tomskaya 64
A.A. Tonkikh 16, 22, 61, 65, 71
D.Y. Usachov 3
F.D. Vasileva 66
P.V. Vinokurov 67
R.D. Yamaletdinov 68
L. Yashina 7, 37